*Coordination Chemistry Reviews*, 77 (1987) 89–163
Elsevier Science Publishers B.V., Amsterdam – Printed in The Netherlands



# THE VARIABLE COORDINATION CHEMISTRY OF A POTENTIALLY HEPTADENTATE LIGAND WITH A SERIES OF 3*d* TRANSITION METAL IONS. THE CHEMISTRY AND STRUCTURES OF $[M(py_3tren)]^{2+}$, WHERE M(II) = Mn, Fe, Co, Ni, Cu, AND Zn AND $(py_3tren) = N\{CH_2CH_2N{=}C(H)(C_5H_4N)\}_3$

RICHARD M. KIRCHNER

*Department of Chemistry, Manhattan College, Bronx, NY 10471 (U.S.A.)*

CARLO MEALLI

*C.N.R. Istituto per lo Studio della Stereochimica ed Energetica dei Composti di Coordinazione, via Guerrazzi 27, 50132 Firenze (Italy)*

M. BAILEY

*Department of Chemistry, Central Michigan University, Mt. Pleasant, MI 48859 (U.S.A.)*

N. HOWE

*Everett Community College, Everett, WA 98208 (U.S.A.)*

L.P. TORRE

*M&T Chemicals Inc., Rahway, NJ 07065 (U.S.A.)*

LON J. WILSON

*Department of Chemistry, Rice University, P.O. Box 1892, Houston, TX 77251 (U.S.A.)*

L.C. ANDREWS, N.J. ROSE and E.C. LINGAFELTER

*Department of Chemistry, University of Washington, Seattle, WA 98195 (U.S.A.)*

(Received 22 July 1986)

CONTENTS

A. Introduction . . . . . 90
B. Results and discussion . . . . . 94
(i) Description of the $[M(py_3tren)]^{2+}$ complexes . . . . . 94
(a) Conformation of the $[M(py_3tren)]^{2+}$ coordination polyhedron . . . . . 94
(b) Deviations from the symmetry of a trigonal antiprism . . . . . 98
(ii) Trends within the coordination polyhedra . . . . . 99
(a) MO model for the $[ML]^{2+}$ complexes . . . . . 99
(b) Variation in the metal–nitrogen distances . . . . . 103
(c) Effect of metal ion size on coordination polyhedron conformation . . . . 106

(iii) Special features of the $[M(py_3tren)]^{2+}$ compounds . . . . . 107
(a) $[Mn(py_3tren)](BF_4)_2$ . . . . . 107
(b) $[Fe(py_3tren)](BF_4)_2$ . . . . . 108
(c) $[Co(py_3tren)](BF_4)_2$, an anomalous Co–N(7) distance . . . . . 109
(d) $[Ni(py_3tren)](BF_4)_2$ and $[Ni(py_3tren)](PF_6)_2$ . . . . . 112
(e) Jahn–Teller distortion in $[Cu(py_3tren)](BF_4)_2$ . . . . . 112
(f) $[Cu(py \cdot tren)]^{2+}$, the hydrolysis product of $[Cu(py_3tren)]^{2+}$ . . . . . 113
(g) $[Zn(py_3tren)](BF_4)_2$ . . . . . 114
(iv) Structure of the $py_3tren$ ligand . . . . . 114
(a) The tren bridgehead . . . . . 114
(b) The α-diimine moiety . . . . . 117
(c) Trends within the pyridine rings . . . . . 119
(d) Hydrogen atoms: bond lengths and angles, contact distances . . . . . 120
(e) Overall conformation of the $py_3tren$ ligand . . . . . 122
C. Experimental . . . . . 125
(i) Syntheses . . . . . 125
(ii) Physical measurements . . . . . 128
(iii) X-ray experimental techniques . . . . . 129
(iv) Assessment of the accuracy of the structures: half normal probability plots . 133
Acknowledgments . . . . . 157
References . . . . . 157

## A. INTRODUCTION

Transition metal complexes with a multidentate chelating ligand can exhibit "special" physical, chemical or structural properties such as (1) unusual conformation, (2) extremely high thermodynamic stability, and (3) virtual kinetic inertness. A premeditative design by N.J. Rose of a potentially heptadentate ligand suggested that the geometric specificity of the $py_3tren$ ligand (Fig. 1) with its threefold symmetry and unique placement of its seventh donor atom would result in transition metal complexes exhibiting mono-capped trigonal antiprismatic coordination polyhedra. This paper describes some chemical and physical properties of this potentially heptadentate $py_3tren$ ligand coordinated to $3d^{5-10}$ transition metal ions M = $Mn^{2+}$, $Fe^{2+}$, $Co^{2+}$, $Ni^{2+}$, $Cu^{2+}$ and $Zn^{2+}$ to give a series of $[M(py_3tren)]^{2+}$ $BF_4^-$ and $PF_6^-$ salts. All compounds are high-spin at room temperature except for $[Fe(py_3tren)](BF_4)_2$, which is low-spin. In addition, $[Cu(py \cdot tren)]^{2+}$, the hydrolysis product of $[Cu(py_3tren)]^{2+}$, is described. Related compounds such as $[M(6Me \cdot py_3tren)]^{2+}$ with M = $Fe^{2+}$ and $Ni^{2+}$, where the $6Me \cdot py_3tren$ ligand has a methyl group substituted for a hydrogen atom in position 6 of one, two, or all three of the pyridine rings in $py_3tren$, were subsequently shown by L.J. Wilson et al., to display a range of high/low spin equilibrium effects in the methyl-substituted iron(II) compounds. The study of an extensive series of complexes with the same or related ligands, allows a detailed assessment of the influence of ligand structure in determining the metal ion coordination polyhedron, and permits trends to be understood in

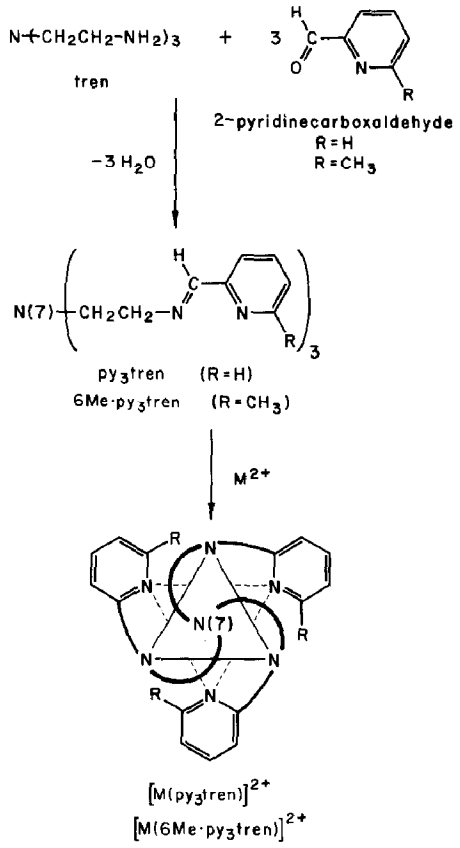


Fig. 1. Preparation of the ligands and representation of the coordination polyhedron for complexes of $py_3tren$ and $6Me \cdot py_3tren$.

terms of changes in metal ion size or electronic configuration.

The $py_3tren$ ligand is the condensation product of tren, $N(CH_2CH_2NH_2)_3$, and 2-pyridinecarboxaldehyde to form three $\alpha$-diimine linkages held together through the bridging tertiary amine atom, N(7). There was great interest as to (1) how much character of tren, a well-characterized tetradentate tripod-like ligand [1], would be present in the $[M(py_3tren)]^{2+}$ complexes; (2) how would the unique tertiary amine N(7) behave toward a metal center; and (3) how would the N(7) bridgehead structure perturb the binding of the three strong-field $\alpha$-diimine linkages.

Representative examples of $\alpha$-diimine ligands are shown below.

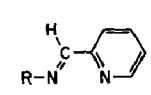

PMI (R=$CH_3$)
PEI (R=$CH_2CH_3$)
PiPI (R=$CH(CH_3)_2$)
PAI (R=$C_6H_5$)

[2]

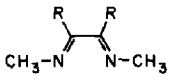

GMI (R=H)
BMI (R=$CH_3$)

[3]

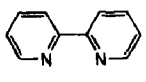

Bipy

[4,5]

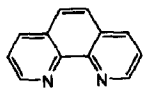

Phen

[4,6,7]

Numerous tris($\alpha$-diimine) complexes are known [4–7]. The conformations adopted by three independent $\alpha$-diimine ligands about a transition metal ion span a range of idealized geometries [8–11].

The $py_3tren$ Schiff base has its three $\alpha$-diimine chelates tied together through the unique bridging tertiary nitrogen atom, N(7). Inspection of space-filling molecular models suggested that the most likely mode of chelation would have the three imine, the three pyridine and the unique tertiary nitrogen donor atoms arranged at or near the apices of a capped trigonal antiprism, whose idealized structure is shown in Fig. 1. Since this arrangement forces the tertiary amine N(7) atom into a capping position with its lone pair of electrons directed toward the metal ion, an intriguing question concerns the nature of the metal–N(7) interaction. Is it bonding, non-bonding or anti-bonding?

Since 1966, when the present work was begun, structures of other complexes containing a single ligand with three $\alpha$-diimine linkages have been reported, but none of these have a potential seventh donor atom. Illustrative sketches of these ligands are shown below in contrast to $py_3tren$.

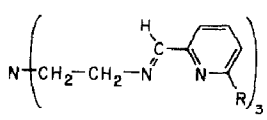

$py_3tren$ (R = H)
6Me-$py_3tren$ (R = $CH_3$)

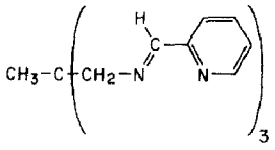

$py_3tame$

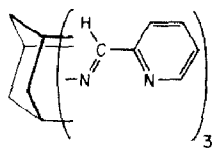

$py_3tach$

X-ray structures of $[M(py_3tame)]^{2+}$ with M(II) = Mn, Fe, Co, Ni and Zn [12,13] and $[M(py_3tach)]^{2+}$ with M(II) = Co, Ni and Zn [12b,14–16] have revealed coordination polyhedra that are between trigonal antiprismatic (TAP) and trigonal prismatic (TP).

Three related ligands, $(pyrol)_3tren$, $(sal)_3tren$ and $(sal)_3tach$, are known and are illustrated below.

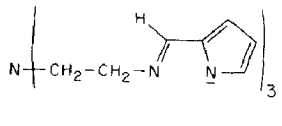

$(pyrol)_3tren$

[17]

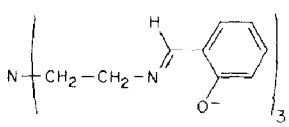

$(sal)_3tren$

[18]

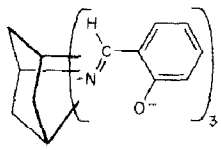

$(sal)_3tach$

[19]

These ligands do not consist of three $\alpha$-diimine chelates. In the last two not all donor atoms are nitrogen and an additional carbon atom is present in each chelate ring. These ligands with formally-charged oxygen or nitrogen

atoms form neutral complexes with trivalent metal ions. The six reported structures of complexes with the $(pyrol)_3tren$, $(sal)_3tren$ and $(sal)_3tach$ ligands all have coordination polyhedra close to TAP. The five structures with a tren bridgehead in the ligand all have long, non-bonding M–N(7) distances.

Also not directly comparable to the $py_3tren$ ligand, but nonetheless interesting, are the tris($\alpha$-diimine) linkages with two bridgeheads (or two bridging groups), which are shown below.

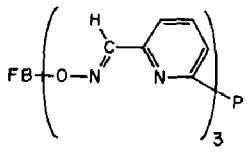


$PccBF^-$

[20,21]

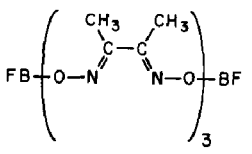


$(Dmg)_3(BF)_2^{2-}$

[22,23]

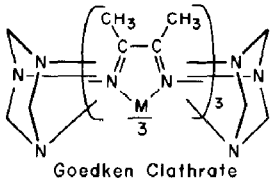


Goedken Clathrate

[24]

The conformations of these complexes must be influenced by the balance between a number of factors including (a) the electronic configuration and "size" of the metal ion, (b) the geometric and electronic properties of the ligand, and (c) the repulsions between atoms in different ligand arms. The tendency of the $py_3tren$, $py_3tame$ and $py_3tach$ ligands to approach TP coordination geometry has been suggested to be a direct consequence of the nature of the bridgehead or bridging group [10,12b,13,25]. However, recent calculations [26] applying the Kepert ligand repulsion model [9] to the conformations of all reported $py_3tren$, $py_3tame$, $py_3tach$, $(pyrol)_3tren$, $(sal)_3tren$, and $(sal)_3tach$ complexes seem to suggest that the relative twist from TAP to TP conformation can be predicted based on minimization of coulombic repulsion between ligating atoms. The calculation requires two types of distances (the metal to ligating-atom distances and the bite distances) to be specified and fixed. Factors (a) and (b) determine the metal ion to ligand donor–atom distances and the ligand bite distances. Once these are specified, then factor (c) determines the relative twist from TAP to TP conformation. To gain further insight into the nature of the metal to ligating-atom interactions, especially the intriguing M–N(7) interaction, we performed and report in this paper some extended Hückel molecular orbital calculations on the $py_3tren$ complexes.

Individual papers cited above describe the geometric and other features of their compounds. In addition, there are some more general reviews and comparisons of complexes within and between the various series of complexes described above [10,12b,13,25]. Also, Hoffmann et al. have done a systematic molecular orbital analysis of geometric alternatives in six- and seven-coordinate molecules [27,28]. Finally, there are reviews of six-coordination [29] and seven-coordination [30,31], with particular emphasis on the

stereochemical effect of introducing various ligands into the coordination polyhedron.

Part of this work has already been published. The chemistry of the $[Ni(py_3tren)]^{2+}$ complex [32], a brief description of the structure of $[Fe(py_3tren)](BF_4)_2$ [33], a mention of the hydrolysis of $[Cu(py_3tren)]^{2+}$ to give $[Cu(py \cdot tren)]^{2+}$ [34], and a comprehensive series of papers particularly describing spin-equilibrium effects observed for iron(II) complexes with ($py_3tren$) and methyl-substituted ligands [35–39] have appeared. The X-ray structures of $[Fe(6Me \cdot py_3tren)](PF_6)_2$ at 295 and 100 K have also been determined [35,40]. Some of the salient features of the $[M(py_3tren)]^{2+}$ series are now described in textbooks [41,42] where particular attention is given to the relationship between the M–N bond distances and the electronic configuration of the metal ion. However, these textbook discussions presume only ligand field theory and regular octahedral coordination, which are insufficient for the description of some of the most interesting features, including the determination of the correct ground state electron configurations of the $[M(py_3tren)]^{2+}$ complexes.

## B. RESULTS AND DISCUSSION

### *(i) Description of the $[M(py_3tren)]^{2+}$ complexes*

#### *(a) Conformation of the $[M(py_3tren)]^{2+}$ coordination polyhedra*

The crystal structures of the $BF_4^-$ salts of $[M(py_3tren)]^{2+}$, where M(II) = Mn, Fe, Co, Ni($BF_4^-$ and $PF_6^-$ salts), Cu and Zn, reveal that the potentially heptadentate $py_3tren$ ligand coordinates to the metal through the three imine and the three pyridine nitrogen atoms. Distances from the metal to the seventh potentially ligating atom, the tertiary amine N(7), are long (greater than 2.79 Å). The direct interaction between N(7) and the metal ion is small compared to the interactions of the other six nitrogen atoms. Interesting features of this M–N(7) interaction will be discussed later in Section B(ii)(b). In general, the coordination polyhedra of the $[M(py_3tren)]^{2+}$ complexes are best described as trigonal antiprisms (TAP) that are considerably distorted toward trigonal prisms (TP).

A geometrical model [43] useful in describing the structures of $[M(py_3tren)]^{2+}$ complexes is illustrated in Figs. 2, 3 and 4. The model assumes the imine nitrogen atoms, N(1), to be located at the vertices of equilateral triangle A and the pyridine nitrogen atoms, N(2), to be located at the vertices of equilateral triangle C. The model allows a description of the distortions and interconnections of the idealized coordination geometries found in six-coordinate complexes, namely octahedral or trigonal antiprismatic (TAP) geometry and trigonal prismatic (TP) geometry. Triangles A

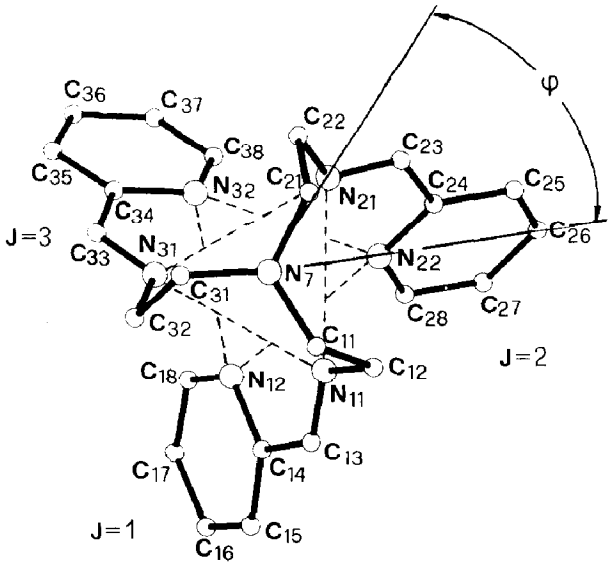


Fig. 2. Coordination polyhedron model and atom numbering scheme. Particular atoms, for example C($J1$), are designated in terms of $J$ (the arm number) and $I$ (the atom number), except for the tertiary amine which is designated N(7). When a general type of atom is referred to, only the single digit ($I$) is used. For example, N(21) refers to the amine nitrogen in arm two, whereas N(1) refers to amine atoms in general. General pyridine atoms are thus N(2). The numbering scheme for general hydrogen atoms is given in Fig. 9. The coordination polyhedron is given by dashed lines (- - - - - -) showing the top triangle, A, defined by the positions of the imine nitrogen atome N(1), and the bottom triangle, C, defined by the positions of the pyridine nitrogen atoms N(2). The twist angle, $\phi$, is the projected angle between triangles A and C (i.e. angle N(1)–N(7)–N(2) in projection).

and C have side lengths designated as $a$ and $c$, respectively. The ratio $a/c$ is a measure of the size difference between the two triangles. Figure 2 shows a view of the model with triangle A over triangle C, and illustrates how the ligand fits the model. The "bridging" tertiary amine atom, N(7), is above triangle A. The metal ion, M, is located directly below N(7) and between triangles A and C, such that the M–N(7) line is the $C_3$ axis of the model. When the metal atom is not located midway between the two triangles but is displaced toward triangle A the magnitude of the displacement is given as $\delta M$. The twist angle, $\phi$, is a projected angle between triangles A and C [44].

The conformation described by this model is trigonal prismatic when $\phi = 0°$ and trigonal antiprismatic when $\phi = 60°$. The (regular) octahedral conformation has $\phi = 60°$ and $a = b = c$, where $b$ is defined as the chelate "bite" distance. There are other parameters defined and illustrated in Figs. 3 and 4 that are useful in describing the coordination polyhedra. One parameter is the height-to-bite ratio, $h/b$, which is 1.0 for a trigonal prism and 0.816 for an octahedron. Another parameter is the polar angle of the ligating

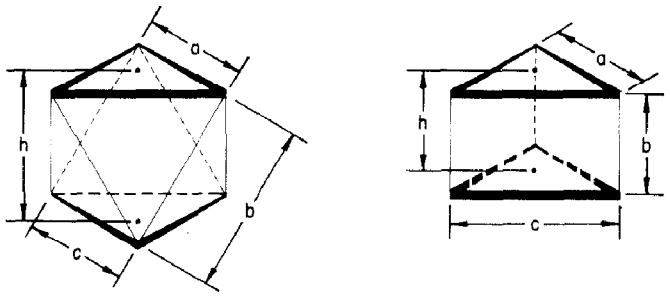


Fig. 3. Coordination polyhedron model. Triangle A and C have side lengths of $a_i$ and $c_i$ ($i = 1$, 2, or 3 respectively). The metal ion, M, lies between the two triangles. The displacement of the metal ion from the midpoint between the two triangles in the direction of triangle A is given by $\delta$M. The distance between centroids of triangles A and C, measured along the M–N(7) axis, is the height, $h$. The non-bonding distance between chelating imine N(1) and pyridine N(2) atoms in the same ligand arm is the bite distance, $b$.

nitrogen atoms, $\theta$. The angle $\theta$ has a value of 54.7° in an octahedron. Another parameter is the rotation angle $\alpha$ which describes the orientation of the planar chelate rings with respect to the $C_2$ axes of the model. The value of $\alpha$ is calculated as the angle between the threefold axis and the plane of the M–N–C–C–N chelate ring (ignoring the inherent lack of twofold symmetry within the chelate ring). The angle $\alpha$ is 0° for TP and 35.3° for TAP. This latter value for $\alpha$ is obtained when the three chelate planes are mutually orthogonal, as in an idealized octahedral conformation. The

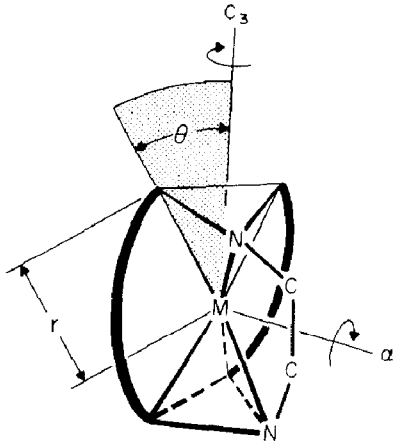


Fig. 4. Coordination polyhedron model. The polar angle $\Theta$ is defined as the angle between the M–N(7) line and the M–N($JI$) line. The polar coordinate $r$ is the M–N($JI$) distance. The rotation angle $\alpha$ is defined as the angle between the planar M–($\alpha$-diimine) chelate ring and the M–N(7) or $C_3$ axis of the model.

TABLE 1

Summary of Coordination Polyhedron Model Values

| Parameter, weighted mean value [a] | $MnL(BF_4)_2$ | $FeL(BF_4)_2$ | $CoL(BF_4)_2$ | $NiL(BF_4)_2$ | $NiL(PF_6)_2$ | $CuL(BF_4)_2$ [b] | $ZnL(BF_4)_2$ | $Cu(py\cdot tren)(BF_4)$ |
|---|---|---|---|---|---|---|---|---|
| $\bar{\phi}$, twist angle | 42.96(*R*11) [a] | 53.97 (*R*4.0) | 48.67 (*R*5.7) | 49.14 (*R*4.8) | 50.88 (*R*2.2) | 47.69 (*R*23) | 45.9 (*R*14) | |
| M–N(7) [c] | 2.794 (2) [c] | 3.439 (4) | 2.870 (2) | 3.227 (4) | 3.235 (4) | 3.110 (2) | 3.013 (2) | 2.032 (7) |
| $\overline{M\text{–}N(J1)}$ | 2.201 (*R*1.7) | 1.942 (*R*2.3) | 2.093 (*R*2.1) | 2.087 (*R*3.0) | 2.081 (*R*6.4) | 2.102 (*R*58) | 2.128 (*R*68) | 2.04 |
| $\overline{M\text{–}N(J2)}$ | 2.317 (*R*32) | 1.967 (*R*1.7) | 2.200 (*R*30) | 2.100 (*R*9.2) | 2.105 (*R*2.3) | 2.143 (*R*93) | 2.226 (*R*36) | 2.00 (7) [c] |
| $\overline{M\text{–}N_6}$ | 2.262 (*R*63) | 1.955 (*R*10) | 2.149 (*R*56) | 2.094 (*R*9.1) | 2.093 (*R*11) | 2.122 (*R*92) | 2.180 (*R*57) | |
| $\bar{a}$ | 3.495 (*R*45) | 2.885 (*R*4.0) | 3.292 (*R*32) | 3.122 (*R*13) | 3.134 (*R*3.7) | 3.209 (*R*72) | 3.293 (*R*35) | |
| $\bar{c}$ | 3.237 (*R*50) | 2.881 (*R*5.4) | 3.095 (*R*33) | 3.040 (*R*20) | 3.094 (*R*4.8) | 3.104 (*R*72) | 3.137 (*R*42) | |
| $\bar{a}/\bar{c}$ | 1.080 | 1.001 | 1.064 | 1.027 | 1.013 | 1.034 | 1.050 | |
| $\delta M$ | 0.2491 (9) | 0.025 (1) | 0.205 (1) | 0.050 (2) | 0.045 (2) | 0.111 (1) | 0.1752 (9) | |
| $\bar{b}$, "bite" | 2.672 (*R*6.8) | 2.544 (*R*4.3) | 2.642 (*R*7.6) | 2.654 (*R*2.3) | 2.639(*R*3.7) | 2.664(*R*12) | 2.684(*R*7.3) | 2.56(1) [c] |
| $h$, "height" | 2.256 (2) | 2.047 (3) | 2.156 (2) | 2.202 (3) | 2.138 (3) | 2.222 (2) | 2.257 (2) | |
| $h/\bar{b}$ | 0.844 | 0.805 | 0.816 | 0.830 | 0.810 | 0.834 | 0.841 | |
| $\bar{\Theta}$[N(*J*1)] | 66.47 (*R*6.6) | 59.05 (*R*0.5) | 65.36 (*R*8.1) | 59.77 (*R*4.8) | 60.53 (*R*4.2) | 61.60 (*R*27) | 63.39(*R*4.5) | |
| $\bar{\theta}$[N(*J*2)] | 53.66 (*R*30) | 57.80 (*R*10) | 54.44 (*R*20) | 56.80 (*R*11) | 58.09 (*R*8.3) | 55.62 (*R*48) | 54.33 (*R*26) | |
| $\alpha$ [d] | 31.5 (1.9) | 36.7 (0.6) | 34.2 (1.5) | 33.6 (1.1) | 36.1 (0.2) | 32.9 (1.8) | 32.1 (1.6) | |

[a] Distances are given in Å, angles are given in degrees. Parameters with weighted mean values have a bar over the symbol of the parameter. The weighted mean value is calculated as $\mu = \Sigma(x_i/\sigma_i^2)/\Sigma(1/\sigma_i^2)$, where $x_i$ is the individual value and $\sigma_i$ is its estimated standard deviation (e.s.d.). $R$ is the normalized range limit, $|((x_i-\mu)/\sigma_i)_{max} - ((x_j-\mu)/\sigma_j)_{min}|$, for the values used to calculate the mean. The values averaged are of the same population at the 99.5% confidence level if $R \leqslant 4.4$ for a sample size of 3; and if $R \leqslant 5.1$ for a sample size of 6. For a complete table of "Probability Integrals of the Range" see pp. 273–281 in the "Handbook of Tables for Probability and Statistics", W.H. Beyer (ed.), The Chemical Rubber Co., Cleveland, OH, 1966. [b] $CuL(BF_4)_2$ shows a Jahn–Teller distortion. The values used to calculate the mean show the largest significant differences from each other within the $ML^{2+}$ series. [c] Only one value. The number in parentheses is the estimated standard deviation in the least significant figure. [d] Defined in Fig. 4.

parameters $\phi$ and $\theta$ describe a coordination polyhedron of $L_6M$ points, whereas $\alpha$ describes how three rigid bidentate donor groups within a flexible multidentate ligand define the coordination polyhedron.

The compound which is most nearly octahedral is $[Fe(py_3tren)](BF_4)_2$, which has $\phi = 54°$, $a/c = 1.001$, $\theta[N(1)] = 59.05°$, $\theta[N(2)] = 57.78°$ and $\alpha = 36.7°$, followed closely by $[Ni(py_3tren)](PF_6)_2$. All other compounds show larger deviations from the ideal values for an octahedron. The compound that is the most distorted from octahedral conformation (in terms of the weighted mean values) is $[Mn(py_3tren)](BF_4)_2$, followed closely by $[Zn(py_3tren)](BF_4)_2$. Since the bite distance, $b$, is so much smaller than either $a$ or $c$ in all compounds, the trigonal antiprism (i.e., a compressed octahedron) is better than the octahedron (where $a = b = c$) as a reference polyhedron to describe the coordination polyhedra.

*(b) Deviations from the symmetry of a trigonal antiprism*

A summary of the weighted mean values that describe the coordination polyhedron of all $[M(py_3tren)]^{2+}$ salts is given in Table 1. There are several types of distortions observed from the $D_3$ symmetry of an ideal trigonal antiprism (TAP) attainable for the $py_3tren$ ligand in which the inherent difference between amine and pyridine nitrogen atoms, as well as the bridgehead, are ignored. A trigonal distortion (i.e. toward a TP coordination polyhedron) is revealed by the twist angle, $\phi$, which ranges from 54 to 43°, less in all cases than the ideal value of $\phi = 60°$ for TAP coordination polyhedron. A second distortion from ideal TAP is that the size of triangle A is larger than triangle C ($a/c > 1$). This limits the highest molecular symmetry to $C_3$ (whether or not the imine N(1) and pyridine N(2) nitrogen atoms are considered equivalent). A third distortion is that all metal ions are displaced toward the imine nitrogen triangle A. Thus, the mean M–N(1) distances are always smaller than M–N(2) distances, and the weighted mean polar angle of the imine nitrogen atoms, $\Theta[N(1)]$, is always larger than that for the pyridine nitrogen atoms, $\Theta[N(2)]$.

In actuality the $[M(py_3tren)]^{2+}$ cations in the crystal do not even possess $C_3$ symmetry because the three arms of the $py_3tren$ ligand are not equivalent. The values given in Table 1 are, for the most part, weighted mean values. The three twist angles, $\phi(J)$ (where $J = 1$, 2, or 3), that make up the mean $\phi$ are not all equal, the triangles A and C are not equilateral, the individual $\Theta[N(J1)]$ and $\Theta[N(J2)]$ values are not all equal, and finally, the individual M–N($J1$) and M–N($J2$) distances are not all equal. A discussion of these individual parameters is given in a later section. A pictorial view of the deviations from $C_3$ symmetry for representative $[M(py_3tren)]^{2+}$ cations is presented in Fig. 5, where each cation is projected onto the plane defined by its imine nitrogen triangle A.

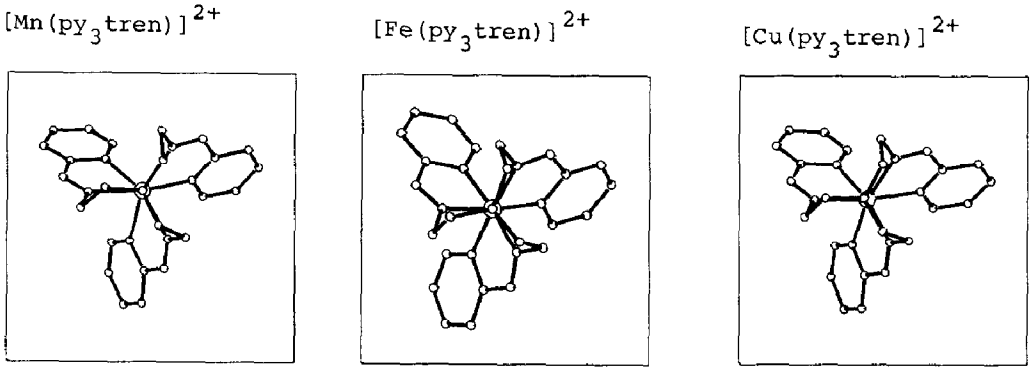


Fig. 5. Projections of representative $[M(py_3tren)]^{2+}$ cations (M(II) = Mn, Fe, and Cu) on to the plane defined by the imine nitrogen triangle A. This view reveals deviations from the near threefold molecular symmetry axis M–N(7). $[Fe(py_3tren)]^{2+}$ has the most nearly octahedral coordination polyhedron, while $[Mn(py_3tren)]^{2+}$ is the most distorted from an octahedral coordination polyhedron. All other cations in the series except copper(II) exhibit intermediate structures between the iron(II) and manganese(II) extremes. Note particularly that in $[Cu(py_3tren)]^{2+}$, which displays a Jahn–Teller distortion, there is a unique shift of the M–N(7) vector (represented by the displacement of the two central circles representing the Cu and N(7) atoms) away from the threefold molecular symmetry axis. Operations associated with space groups $C2/c - C_{2h}^6$ and $P2_1/c - C_{2h}^5$ generate an equal number of cations with the $py_3tren$ ligand attached as either a left- or right-handed screw.

### *(ii) Trends within the coordination polyhedra*

The relative distortion from TAP coordination and the variation in the metal–nitrogen distances from metal to metal can be explained in terms of two main factors: the nuclear charge of the metal ion, and the 3*d* electron configuration of the metal. These factors have been discussed by other authors [41,45,46]. Essentially, as the atomic number increases for atoms within a *d* shell there is a general increase in the effective nuclear charge and a general decrease of the metal ion radius which results in shorter metal–ligand distances.

The 3*d* electronic configuration of the metal is very important because changes in electronic configuration or spin state have been shown to affect metal–ligand distances to a greater extent than changes in the electrostatic charge of the metal ion [46]. To explore how these factors affect not only the metal–nitrogen distances but also some conformational trends in the $[M(py_3tren)]^{2+}$ series, we have carried out some extended Hückel molecular orbital (EHMO) calculations [47].

#### *(a) MO model for the $[ML]^{2+}$ complexes*

Only those aspects of the calculation which are relevant to the evaluation

of geometrical trends within the $[M(py_3tren)]^{2+}$ series of molecules are discussed. Our simplified model uses three independent symmetric α-diimine bidentate ligands, shown as **1**, in place of the more realistic pyridine-2-carboxaldimino chelate, shown as **2**. The bridgehead part of the $py_3tren$ ligand is not included in the tris(α-diimine)metal(II) model, but perturbations by a flexible amine atom (N(7)) located along the molecular threefold axis will be considered at a later stage.

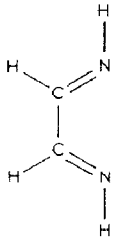

1

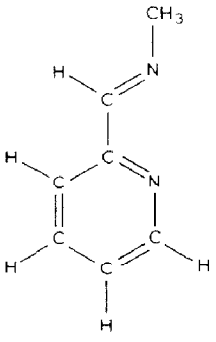

2

The above simplification does not dramatically alter the bonding capabilities of the chelate to the metal atom. These are mainly provided by the symmetric (S) and antisymmetric (A) combinations of lone pairs at the nitrogen atoms, shown as **3**, and, to a lesser extent, by empty $\pi$ orbitals of the conjugated system, shown as **4**. The corresponding $\pi$ MO, shown as **5**, calculated for the more realistic molecule **2** is not intrinsically different from **4**, although its energy is higher (ca. 0.5 eV) and the $p_\pi$ orbital is more developed at the imine than at the pyridine nitrogen.

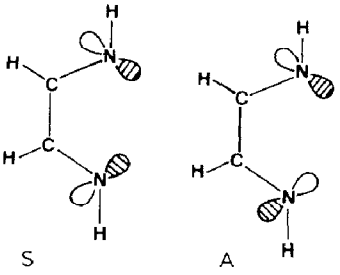


3

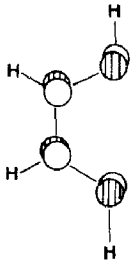

4

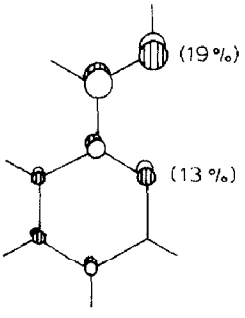


5

(The percent contribution of the nitrogen $p_\pi$ to the MOs in question are reported in parentheses above in **5**.)

An EHMO calculation, performed by using the quasi-experimental trigonal antiprismatic structural parameters (TAP) for a tris($\alpha$-diimine)iron(II) model [48], produces the order, shown as **6**, for the frontier MOs.

$3e$ —— "metal-like" orbitals

$2e$ ——
$a_2$ — "ligand-like" orbitals

$1e$ ——
$a_1$ — "metal-like" orbitals

**6**

The order of metal $d$ orbitals in Scheme **6** is similar to that found in complexes with pseudo-octahedral structure, namely a set of three lower levels, $a_1$, and the doubly degenerate $1e$ (these are equivalent to the $t_{2g}$ set in $O_h$), and a higher destabilized degenerate $3e$ level (the equivalent of $e_g$ in $O_h$). Although $a_1$ is calculated to lie below $1e$, the presence of a $\sigma$ lone pair on the bridgehead amine N(7) may invert this order by pushing the $a_1$ (i.e. $d_{z^2}$ orbital) level up in energy.

What is peculiar to this tris($\alpha$-diimine)metal(II) system is that between the well-separated two groups of metal levels there are three combinations of the individual $\alpha$-diimine ligand $\pi$ orbitals, individually shown as **4**. The combination ligand orbitals are close in energy and are labeled by symmetry as $a_2$ and $2e$, and are shown below in **7** and **8**, respectively. The presence of these ligand orbitals at energies comparable to that of metal $d$ levels [49] very likely is an electronic cause of deformations from TAP coordination. In particular, the observed deformations are consistent with the avoidance of transfer of metal electrons to ligand orbitals [50].

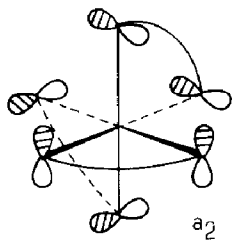


**7**

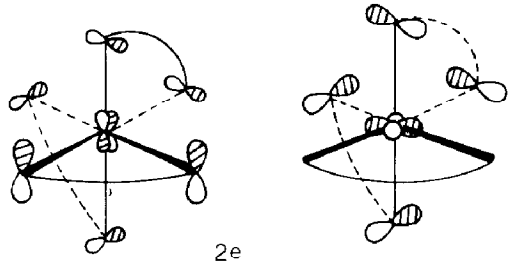


**8**

Additional information about deformations from ideal TAP coordination can be obtained from studying a possible pathway for the interconversion of the coordination polyhedron of our tris($\alpha$-diimine)metal(II) model from a trigonal antiprism (TAP) to a trigonal prism (TP). Previous theoretical studies performed for hexacoordinated complexes used models with six

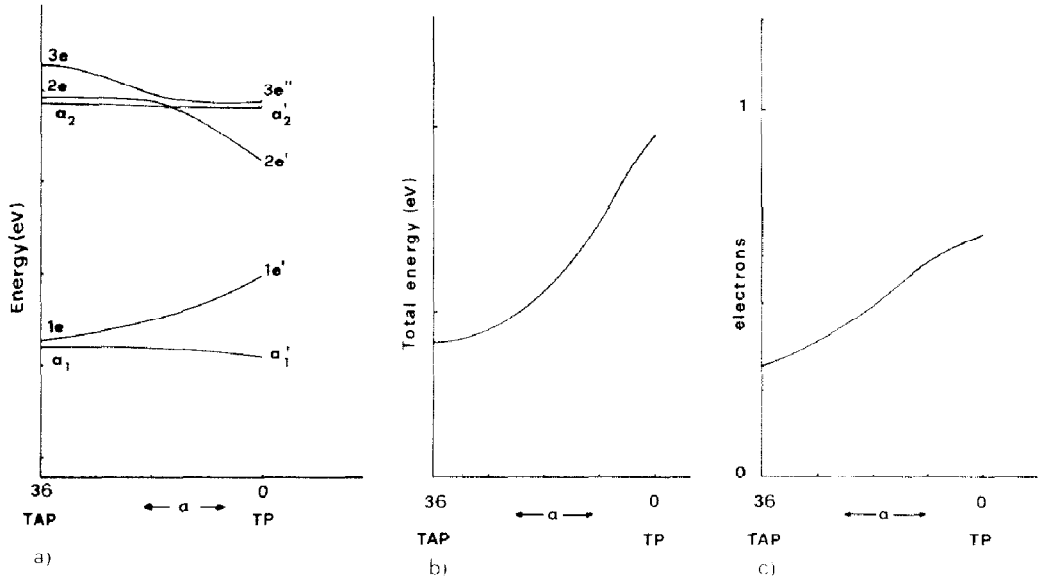


Fig. 6. Trigonal antiprismatic (TAP) to trigonal prismatic (TP) interconversion pathway.
(a) Evolution of the frontier orbitals in the model compound, tris(α-diimine) metal(II) for the TAP–TP interconversion governed by the parameter $\alpha$ defined in Fig. 4. The levels are labeled according to $D_3$ and $D_{3h}$ symmetry at the TAP and TP ends, respectively, in this Figure. Note that the TAP end level $2e$ is "ligand-like" but at the TP end this level is "metal-like". The atomic parameters of cobalt were used to construct the diagram.
(b) Total energy variation along the same pathway for a low-spin $d^6$ electron configuration.
(c) Variation of the fraction of electrons occupying the ligand $\pi$ orbitals, shown as in **4**, as a result of increasing $\pi$-backdonation along the TAP–TP pathway. The latter plot was calculated using iron(II) parameters.

independent ligands [25,27], where the interconversion TAP to TP could be easily governed by the twist angle, $\phi$, defined in Fig. 2. However, the nitrogen donor atoms in $[M(py_3tren)]^{2+}$ are not isolated points but belong to three planar, conjugated (rigid) α-diimine ligands. In order to account for the bonding capabilities (especially those of the $\pi$ type) of the α-diimine chelates, we regulate our description of the TAP to TP interconversion by the parameter $\alpha$ (defined in Fig. 4 and described in Section (i)(a), which allows simultaneous rotations of the chelate planes about the twofold axes of the $D_3$ model compound.

Figure 6(a) shows a typical Walsh-type diagram for the evolution of the frontier MOs between TP and TAP coordination. If the presence of the ligand $a_2$ and $2e$ levels is for the moment disregarded, the Figure shows the features pointed out by others who studied the TAP–TP interconversion of six-coordinate complexes [25,27]. Thus the level $3e$ stabilizes toward TP because the $\sigma^*$ interaction of metal and ligand orbitals becomes less directional. Also, in the interconversion direction toward TP, a combination

of nitrogen lone pairs having $e$ symmetry destabilizes the metal $1e$ level. Actually, $1e$ destabilizes in spite of the increasing $\pi$ bonding interaction in which **8** represents the antibonding counterpart. As shown in Fig. 6(c), the metal to ligand $\pi$ back-donation is maximized at TP at least for low spin $d^6$ species. Further discussion of $\pi$ interactions appears in Sections B(iii)(b), B(iv)(b) and B(iv)(e).

Figure 6(b) indicates that the tris($\alpha$-diimine)iron(II) model has a minimum total energy toward TAP. This is mainly a consequence of the stabilization of the level $1e$ which carries a total of four electrons.

The most interesting information which can be derived from the Walsh diagram given in Fig. 6(a) is that, on approaching TP, a switch (technically an "avoided crossing") occurs in the order of ligand and metal higher levels. Note that level $2e$ is "ligand-like" at the TAP end, and "metal-like" at the TP end of Fig. 6(a), respectively. Away from TAP, the typical three below two split of metal orbitals is attainable with no intermediate ligand levels. The precise point at which the inverted level order occurs is strongly parameter dependent [51]. The diagram of Fig. 6(a) provides valuable qualitative, but not quantitative, information.

In summary, the presence of the ligand $\pi$ orbitals at an energy comparable with that of the M–N $\sigma^*$ levels may impose some geometrical constraints in the different complexes, such as a deformation toward TP coordination geometry to maintain metal orbital levels below ligand orbital levels [51]. However, the energy of two of the three lower metal $d$ orbitals minimizes at TAP, and thus in general this coordination polyhedron is favored [52]. Our MO investigation has been limited to a highly symmetrical ($D_3$ symmetry) TAP–TP interconversion pathway, whereas the actual $[ML]^{2+}$ complexes often have only $C_1$ symmetry. Nevertheless, we are confident that the arguments still apply and that they help rationalize most of the major trends found within this series of compounds.

*(b) Variation in the metal–nitrogen distances*

The metal–nitrogen distances in $[M(py_3tren)]^{2+}$ are plotted vs. the atomic number of the metal in Fig. 7. A well known pattern is apparent and it is related to the splitting of the metal $d$ orbitals into three non-bonding and two metal–ligand antibonding levels, typical for six-coordinate complexes, and to the different electron configurations of the metal atoms. Ignoring overlap of orbitals and all $\pi$-bonding effects (the Crystal Field model), this pattern is described in the older literature as due to a Crystal Field Stabilization Energy (CFSE). What is emphasized in Fig. 7 is that the metal nitrogen distances are an almost exactly linear function of the atomic number for a given electron population of the $3e$ or $a_1$ orbitals. The dashed lines (- - - - -) show that for a constant number of electrons in the upper $3e$

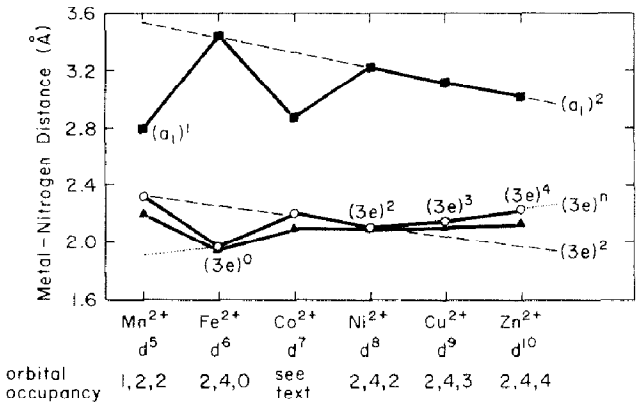


Fig. 7. Effect of orbital occupancy on metal–nitrogen distances. Upper part of diagram gives the M–N(7) non-bonding distances (shown as ■). The lone pair of the tertiary amine atom is directed at the $a_1$ orbital on the metal ion. The lower part of the diagram gives the M–N(1) and M–N(2) weighted mean bond distances. The imine and pyridine nitrogen atoms are directed at the $3e$ orbitals on the metal ion. The values (shown as ▲) for imine nitrogen atoms, N(1), are slightly shorter and thus are located just below the values (shown as ○) for pyridine nitrogen atoms, N(2). Dashed lines (- - - - - -) represent a constant number, while the dotted line (· · · · · ·) represents an increasing number of electrons in a given type of orbital on the metal ion. The orbital occupancy, $(a_1)^x(1e)^y(3e)^z$, is given under each metal ion as $x$, $y$, $z$.

orbitals there is a linear decrease in the weighted mean M–N(1) and M–N(2) distances as the atomic number and effective nuclear charge on the metal increases. This same relationship holds for the M–N(7) distances. When there is a constant number of electrons in the $a_1$ orbital, the M–N(7) distances linearly decrease as the atomic number and effective nuclear charge on the metal ion increases. The slopes of the dashed lines are not exactly the same, and there is a slightly greater effect on the distances in the order: M–N(7) > M–N(2) > M–N(1). The dotted line (· · · · · ·) in Fig. 7 shows that for an increasing number of electrons in the metal $3e$ orbitals that project in an antibonding fashion toward the imine and pyridine nitrogen lone pairs there is a linear increase in the M–N(1) and M–N(2) bond distances. There is a similar but much more dramatic increase in the M–N(7) distances when another electron is added to the $a_1$ orbital (substantially the metal $d_{z^2}$ orbital) which is directed toward the bridging amine nitrogen lone pair.

As the atomic number increases, the increase in M–N(2) distances is greater than the increase in M–N(1) distances partly because the ligand $\pi$ MO has a better developed $p_\pi$ orbital on the imine than the pyridine nitrogen, as shown in **5**. Also, as $\phi$ decreases (i.e. increasing distortion toward TP coordination polyhedron) the steric crowding increases between pyridine rings (namely, close contacts between atom H(*J*9) attached at

position 6 of a given pyridine ring with an adjacent pyridine ring) [15a,15b]. This crowding forces the pyridine nitrogen donor atoms to spread apart (as the atomic number increases the size of triangle C increases faster than the size of triangle A), resulting in longer M–N(2) distances [12a]. Thus, $[FeL]^{2+}$ and $[NiL]^{2+}$, the complexes that are most nearly TAP and have the largest values of $\phi$, have values for M–N(1) and M–N(2) that are nearly the same; whereas $[MnL]^{2+}$ and $[ZnL]^{2+}$, the complexes that are most distorted toward a TP coordination polyhedron and that have the smallest values of $\phi$, have values for M–N(2) that are longer than for M–N(1).

The M–N(7) distances in the $[M(py_3tren)]^{2+}$ series of complexes indicate that the interaction between the metal ion and the bridging amine nitrogen atom, N(7), is directly determined by the repulsive forces between the electrons in the metal $a_1$ orbital and the lone pair on N(7). The M–N(7) distances are approximately 0.1 Å larger than the value for the sum of the van der Waals radii of nitrogen and the metals for which radii are reported in the literature [53], except for Mn(II) and Co(II), for which there is less *d* electron density projecting from the metal toward the lone pair on N(7). Although the M–N(7) distances in the Mn(II) and Co(II) complexes are shorter than the sum of the van der Waals radii (the generally accepted criterion for an attractive interaction between a metal and a ligand donor atom), they are nevertheless very much longer than the M–N(1) and M–N(2) bonding distances. Thus we conclude that the N(7) is weakly bonded to Co(II) and Mn(II) due to having less than a 4-electron totally repulsive interaction with the metal ion, as is the case in all the other complexes in the $[ML]^{2+}$ series. The N(7) atom in the bridgehead of all complexes in the series is forced into this type of interaction because it is tied through the three arms of the $py_3tren$ ligand to three strong-field $\alpha$-diimine groups which bind tightly to the metal through imine and pyridine nitrogen donor atoms. Although the bridgehead appears somewhat flexible, the ligand restricts the movement of N(7) away from the metal [41]. The bond angles about the bridging amine atom (C(*J*1)–N(7)–C(*J*'1)) vary linearly with the M–N(7) distance, from 112° (approximately $sp^3$ hybridization as expected for an unconstrained tertiary amine nitrogen atom) in Mn(II) (where the repulsion is least) up to a maximum value of 120° (approximately $sp^2$ hybridization) in the Fe(II) complex (where the repulsion is greatest), as shown below in **9**.

9

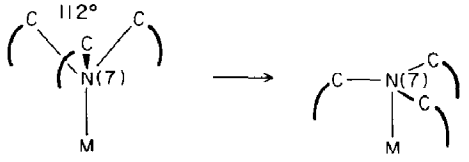

As the repulsion increases, the change in hybridization from $sp^3$ to $sp^2$ in N(7) minimizes the projection of the lone pair of electrons in N(7) toward the metal ion. The geometrical variation in the structure of the bridgehead is discussed in detail in Section B(iv)(a).

*(c) Effect of metal ion size on coordination polyhedron conformation*

Instead of arbitrarily chosen metal ion radii, we use the size of the coordination polyhedron, which is given by $M-N_6$, the weighted mean of all M–N bond distances, not including M–N(7), as the parameter to discuss further trends within the coordination polyhedra. The value of $M-N_6$ for each individual compound is given in Table 1. These experimentally determined values are most appropriate for describing features of the $[M(py_3tren)]^{2+}$ compounds, and are a linear function of the atomic number and electron configuration of the particular metal atom [54].

The twist angle, $\phi$, is often used to help describe the relative position of a compound along the TAP–TP interconversion pathway. As can be seen in Fig. 8, the mean twist angle, $\phi$, is a function of the size of the coordination polyhedron ($M-N_6$). As the coordination polyhedron size increases, the ligand arms twist away from a TAP toward a TP configuration, as shown by a linear decrease in the values for $\phi$. Figure 8 shows that $[Ni(py_3tren)](PF_6)_2$ and $[Co(py_3tren)](BF_4)_2$ are not part of the "smooth" trend that includes all other $BF_4^-$ salts. The difference of 1.8° in mean values of $\phi$ for $[NiL](BF_4)_2$ and $[NiL](PF_6)_2$ can be attributed to differences in packing forces between $BF_4^-$ and $PF_6^-$ counter ions, and provides an estimate of the variation possible in $\phi$ values that does not derive from properties of the metal ions. An analysis of twist angle values from the perspective of minimizing ligand atom–ligand atom repulsions between arms with given restrictions (e.g. bite distances) [9] is given elsewhere [26].

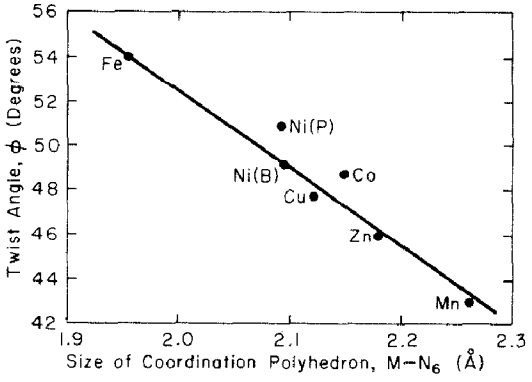


Fig. 8. Size of coordination polyhedron, $M-N_6$ (Å) vs. twist angle, $\phi$.

Note that the mean polar angles, $\theta$, also reported in Table 1, show a larger range of values for imine than pyridine nitrogen atoms ($\theta$(N(1)) = 59 to 66° while $\theta$(N(2)) = 54 to 58°) indicating that as the coordination polyhedron size increases and the ligand arms twist away from TAP geometry, a different rearrangement occurs in the imine triangle A than in the pyridine triangle C of the metal coordination sphere. It has already been noted that within each complex the differences between M–N(1) and M–N(2) bond distance values increase as the complexes distort toward TP geometry. Thus, increasing $M-N_6$ increases $\theta$(N(1)) relative to $\theta$(N(2)) while increasing triangle size c (N(2)) relative to triangle size a (N(1)).

Although $[Fe(py_3tren)]^{2+}$ is included in the "smooth" part of the plot of $M-N_6$ vs. $\phi$ discussed above, it is shown elsewhere [26] that the observed $\phi$ for $[FeL]^{2+}$ must also correlate with, in part, the chelate bite distance, *b*. An explanation of why the bite distance in $[FeL]^{2+}$ is shorter than the relatively constant bite distances in all other $[ML]^{2+}$ compounds is given in Section B(iii)(b).

Finally, as the coordination polyhedron size increases (increasing $M-N_6$ values) there is a linear increase in $\delta M$, the height ($h$), and triangle sizes a and c, except that c for $[Fe(py_3tren)]^{2+}$ may be low. As expected, the non-chelate (inter-arm) distance (N($J$1)–N($J'$2)) also increases with increasing $M-N_6$.

Crystal packing forces may affect some of the parameters closely associated with ligand conformation in the coordination polyhedron. Thus, the isomorphous set of high spin $[M(L)]^{2+}$ complexes with anion $BF_4^-$ (space group = $C2/c$, $Z = 8$, M(II) = Mn, Co, Ni, Cu and Zn) are directly comparable but may differ slightly from $[Ni(py_3tren)](PF_6)_2$ (space group $P2_1/c$, $Z = 4$) or the low spin $[Fe(py_3tren)](BF_4)_2$ (space group $P2_1/c$, $Z = 4$) due to different crystal packing forces arising from packing arrangements in different space groups ($C2/c$ vs. $P2_1/c$) or different counter ions. Nevertheless, various correlations of parameters (taken pairwise) for the $BF_4^-$ salts are most often monotonic and "smooth", but when this is not the case it is generally $[Fe(py_3tren)]^{2+}$ and/or $[Co(py_3tren)]^{2+}$ that stand out. The atypical nature of $[Fe(py_3tren)]^{2+}$ (in the sense of trends) is primarily due to electronic effects which result in short Fe–N(1) and Fe–N(2) bonds (see Section B(iii)(b)). Why the $[Co(py_3tren)]^{2+}$ complex is anomalous is not so clear (see Section B(iii)(c)).

*(iii) Special features of the $[M(py_3tren)]^{2+}$ compounds*

*(a) $[Mn(py_3tren)](BF_4)_2$*

Within the $[M(py_3tren)]^{2+}$ series, the Mn(II) compound is the most distorted from a regular octahedral coordination polyhedron. It also has the

largest difference between mean M–N(1) and M–N(2) distances. The Mn to N(7) distance is less than the sum of the van der Waals radii (see Section B(ii)(b)), and $[Mn(py_3tren)](BF_4)_2$ is described as more than six-coordinate.

*(b) $[Fe(py_3tren)](BF_4)_2$*

The effects of orbital occupation on M–N distances is particularly striking in the $[Fe(py_3tren)]^{2+}$ complex, the only low spin compound in the series. The electron configuration of Fe(II) is $(a_1)^2(1e)^4$ which maximizes electron density toward the bridging amine (giving the longest M–N(7) distance in the series) while minimizing the electron density toward the imine and pyridine nitrogen atoms (giving the shortest M–N(1) and M–N(2) distances in the series). The short M–N distances make the Fe(II) complex unique in this series due to an enhanced interaction between filled $1e$ orbitals on the metal and empty $\pi^*$ orbitals on the $\alpha$-diimine moiety of the ligand. A more detailed explanation of this interaction is given in Section B(iv)(b) which describes the $\alpha$-diimine moiety.

The chelate bite distance, $b$, remains almost the same (2.639($R$3.7)–2.684-($R$7.4) Å) for all complexes except $[Fe(py_3tren)]^{2+}$, where it is shorter at $b = 2.544(R4.3)$ Å. The relatively constant bite distances are not surprising in view of the limited flexibility expected in the $\alpha$-diimine moiety due to $sp^2$ hybridization of all non-hydrogen atoms. A simple electronic argument justifies the shorter bite found in the iron complex. In this almost octahedral complex the 18 electron rule is observed in the sense that the ligands donate six lone pairs to a low spin $d^6$ Fe(II) ion which accepts them in empty orbitals. Four of the metal orbitals are the high lying $s$ and $p$ AOs, whereas the other two are $d$ orbitals, canonically represented as $d_{z^2}$ and $d_{x^2-y^2}$ (which have $e_g$ symmetry in the $O_h$ group) [55]. This donation from the ligands transfers a certain amount of electron density to the metal. In all of the other $[ML]^{2+}$ complexes the metal $e_g(3e)$ levels are half or totally filled with the consequence that not only the average M–N bond order, but also the ligand-to-metal charge transfer, is significantly reduced. We presume that the size of the N $\cdots$ N bite is regulated by the extent of the repulsion between the lone pairs on the nitrogen atoms within each $\alpha$-diimine moiety. As negative charge is depleted from these lone pairs, the repulsion decreases, and the bite distance decreases, as observed for $[FeL]^{2+}$. However, for the other complexes that have electrons in the metal $e_g$ orbitals, the $\sigma$ M–N bonding is reduced, more charge accumulates in the lone pairs of the nitrogen atoms, and the bite distance is larger. A similar trend was also observed in the comparison between $[Fe(phen)_3]^{2+}$ and $[Ni(phen)_3]^{2+}$, even though the bite distance in the N–C–C–N chelate in phen has much less flexibility for opening or closing than in $py_3$tren [56].

As already noted in the MO discussion and illustrated in Fig. 6, the $1e$

level stabilizes toward TAP coordination geometry, and a filled $1e$ level helps make the coordination polyhedron of the iron compound the most nearly TAP within the $[M(py_3tren)]^{2+}$ series.

*(c) $[Co(py_3tren)](BF_4)_2$; an anomalous Co–N(7) distance*

To our knowledge $[Co(py_3tren)](BF_4)_2$ is the only Co(II) compound that can be considered to be heptacoordinate. However, as described in Section B(ii)(b), we consider the metal(II)–N(7) interaction to be only weakly bonding. The lone pair on N(7) seems to "float" on the van der Waals surface of the metal ion, being attracted closer by the overall positive charge on the metal ion only when there are fewer than four electrons in the region between the metal ion and the donor atom.

The M–N(7) distance in the Co(II) compound is anomalous. The interaction between Co(II) and N(7), although much smaller than the interaction between Co and the strong-field $\alpha$-diimine nitrogen atoms, raises the energy level of the $a_1$ orbital and may, in the case of Co(II), interchange the $a_1$ and $1e$ energy levels. The actual point symmetry of $[CoL]^{2+}$ is $C_1$, in which the degeneracy of the $e$ levels is removed. But since mean values for parameters in each arm are used in this discussion (increasing the symmetry to $C_3$) the higher symmetry $C_3$ model is still appropriate. The two possible ground state electron configurations for high-spin $d^7$ Co(II) in $C_3$ symmetry (but with levels labeled as in the MO discussion) are shown in **10**.

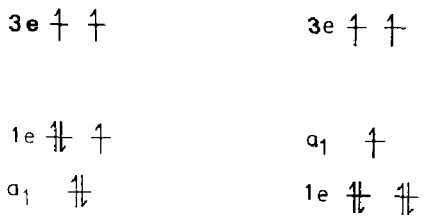


10

Note that a small, perhaps not observable, Jahn–Teller effect is predicted for the configuration on the left. Also, the energetics associated with spin–orbit coupling for this configuration are larger than those expected to result from a Jahn–Teller effect [57]. A ground state with the configuration given on the right is more reasonable, on the basis of the Co–N(7) distance which is much shorter than expected for two electrons in $a_1$. However, the Co–N(7) distance is not as short as would be predicted from Fig. 7 for only one electron in the $a_1$ orbital, but lies between values expected for one or two electrons in the $a_1$ orbital. A comparable Co–N distance has been observed in an analogous $d^7$ Co(II) six-coordinate, distorted octahedral complex, $[Co(terpy)_2](ClO_4)_2 \cdot 0.5\ H_2O$, which is described as 70% high-spin

TABLE 2

Solid state magnetic data for the $[M(py_3tren)](X)_2$ (A), $[M(6\ Me\cdot py_3tren)](X)_2$ (B), $[M(py\cdot tren)](X)_2$ (C) salts

| | M | $X^-$ | Temperature (K) | $\chi_M(corr)\times10^{-6}$ (c.g.s.) [a] | $\mu_{eff}$ (BM) |
|---|---|---|---|---|---|
| (A) | Mn | $PF_6$ | 296 | 14,578 | 5.88 |
| | | $BF_4$ | 296 | 14,441 | 5.85 |
| | | I | 297 | 14,329 | 5.84 |
| | Fe | $PF_6$ | 297 | 119 | 0.53 |
| | | $BF_4$ | 298 | 151 | 0.60 |
| | | I | 298 | 132 | 0.56 |
| | Co | $PF_6$ | 296 | 8,319 | 4.44 |
| | | $BF_4$ | 296 | 8,558 | 4.50 |
| | | I | 296 | 8,391 | 4.46 |
| | Ni | $PF_6$ | 300 | 3,872 | 3.05 |
| | | $BF_4$ | 301 | 3,880 | 3.06 |
| | | I | 301 | 3,816 | 3.03 |
| | Cu | $PF_6$ | 297 | 1,423 | 1.84 |
| | | $BF_4$ | 297 | 1,439 | 1.85 |
| | | I | 297 | 1,438 | 1.85 |
| (B) | Fe | $PF_6$ | 297.5 | 11,937 | 5.33 |
| | Ni | $PF_6$ | 300 | 3,779 | 3.01 |
| (C) | Cu | $BF_4$ | 300 | 1,424 | 1.85 |

[a] Corrected molar susceptibility. Diamagnetic corrections: $[M(py_3tren)](X)_2$: $-297\times10^{-6}$ c.g.s. ($PF_6^-$), $-243\times10^{-6}$ c.g.s. ($BF_4^-$), $-271\times10^{-5}$ c.g.s.(I); $[M(6Me\cdot py_3tren)](PF_6)_2$: $-341\times10^{-6}$ c.g.s.; $[Cu(py\cdot tren)](BF_4)_2$: $-205\times10^{-6}$ c.g.s.

and 30% low-spin Co(II) [58]. The average Co–N bond distance is 2.10 Å in $[Co(terpy)_2]^{2+}$ (compare with 2.149($R$56) Å in $[Co(py_3tren)](BF_4)_2$). No disorder within the cation was detected in the X-ray crystal structure analysis of $[Co(terpy)_2](ClO_4)_2\cdot 0.5\ H_2O$ [59] or $[Co(py_3tren)](BF_4)_2$, which is similar to that reported in other room temperature crystal structure analyses of complexes displaying a high/low-spin equilibrium phenomenon [60,61]. However, an analysis of difference vibrational parameters, $\Delta U$(M–N), following the method of Chandrasekhar and Bürgi [62] reveals no evidence for either a Jahn–Teller distortion or high/low-spin equilibrium in $[Co(py_3tren)](BF_4)_2$.

Magnetic susceptibility data for $[CoL](BF_4)_2$, $[CoL](PF_6)_2$ and $[CoL]I_2$, where L = $py_3tren$, are given in Table 2. Magnetic susceptibility values for $d^7$ Co(II) high-spin octahedral complexes lie in the range $\mu_{eff} = 4.8$ to 5.2 BM at room temperature [63], whereas the $[CoL]^{2+}$ values are lower. For

$[CoL](BF_4)_2$ the magnetic susceptibility dependence upon temperature is linear in the region from 32 K ($\mu_{eff} = 4.40$ BM) to 296 K ($\mu_{eff} = 4.45$ BM), again indicating no high/low-spin equilibrium.

Finally, it is interesting to compare $[Co(py_3tren)]^{2+}$ with two cobalt complexes that have no spin-equilibrium properties but have a non-bonded interaction between Co and a bridging tertiary amine atom that is exactly similar to our Co–N(7) interaction, where N(7) is located directly above the $a_1$ metal orbital that projects along the molecular three-fold axis. The two tetrahedral cobalt complexes have the flexible tripodal ligand $np_3$, tris-(2-diphenylphosphinoethyl)amine, which maintains $C_{3v}$ symmetry with the bridging amine atom located directly above the $d_{z^2}$ orbital of the cobalt atom (see **11**).

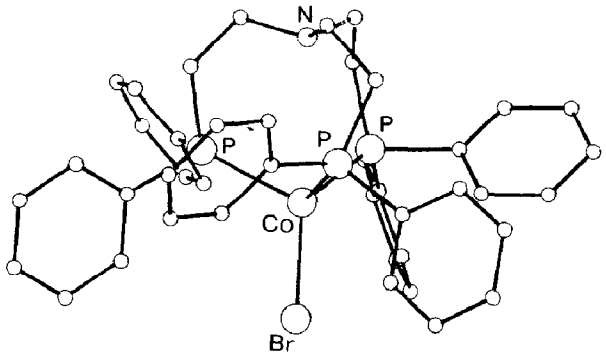


**11**

In $[(np_3)CoBr]^+$ the $d^7$ Co(II) metal ion has one electron in the metal $d_{z^2}$ orbital projecting toward the bridging amine nitrogen atom in $np_3$ and the Co–N non-bonding distance is 2.73(1) Å [64]. In $[(np_3)CoBr]$ the $d^8$ Co(I) has two electrons in the $d_{z^2}$ orbital and the Co–N non-bonding distance increases to 3.34(1) Å, exactly as expected for an increase of one electron in an orbital that projects from cobalt toward the bridging amine nitrogen atom [65]. These two values for the distances, 2.73(1) and 3.34(1) Å, when plotted in Fig. 7, fall where expected for one electron, $(a_1)^1$, or two electrons, $(a_1)^2$, for a non-bonding Co–N(7) distance. This is remarkable and seems to indicate that the direct repulsive interaction between electrons in metal orbitals projecting toward donor atoms dominates the determination of non-bonding distances, making less influential other factors that differ in the comparison between these $np_3$ and $py_3tren$ complexes, such as six-coordinate octahedral vs. four-coordinate tetrahedral coordination polyhedra, or Co(I) vs. Co(II) formal oxidation states.

*(d) [Ni(py$_3$tren)](BF$_4$)$_2$ and [Ni(py$_3$tren)](PF$_6$)$_2$*

Two structures, each with a different anion ($BF_4^-$ or $PF_6^-$), were determined with the $[Ni(py_3tren)]^{2+}$ cation in order to assess crystal packing forces (vida infra). The coordination polyhedra of both $[NiL](BF_4)_2$ and $[NiL](PF_6)_2$ follow closely after iron in approaching a TAP conformation. The nickel compounds have the smallest differences between mean M–N(1) and M–N(2) bonds (about the same as that found in the iron compound) but there is a more pronounced twisting of the coordination polyhedron toward a TP conformation in nickel ($\phi = 49.1$ and 50.9° in the $BF_4^-$ and $PF_6^-$ salts, respectively) than in the iron compound ($\phi = 54.0°$) due to the larger ionic radius of high spin Ni(II) compared to low spin Fe(II) (see Section B(ii)(c) and ref. 51).

*(e) Jahn–Teller distortion in [Cu(py$_3$tren)](BF$_4$)$_2$*

The Cu(II) compound is unique in the series in that it shows considerable distortion from $C_3$ symmetry. The distortion from $C_3$ symmetry is clearly visible in Fig. 5, where the central double circles representing the N(7) and M atoms (which usually lie on a pseudo three-fold symmetry axis) are shifted relative to those in all the other complexes.

The individual values used to calculate the weighted mean parameters given in Table 1 for $[Cu(py_3tren)]^{2+}$ are sometimes as much as 100 standard deviations different from each other. The distortion is dramatically reflected in the individual metal–nitrogen bond distances (Table 3). The ranges shown in Table 3 are highly significant compared with the corresponding ranges exhibited by the other complexes. The latter ranges are ~ 3 sigma for M–N(1) distances and ~ 36 sigma for M–N(2) distances. Thus, a large part of the magnitude of the distortion in $[Cu(py_3tren)](BF_4)_2$ clearly arises from an electronic effect of the Jahn–Teller type, as expected for a $d^9$ hexacoordinate complex, and not from packing effects. An estimation of the amplitude of the Jahn–Teller distortion can be obtained from the differences, $\Delta U$(M–N), in atomic mean-square displacements $U$(M) and $U$(N) along M–N bonds [66a]. The Jahn–Teller radius calculated [66b] for the

TABLE 3

| Cu–N($IJ$) bond distance (Å) | Weighted mean | Range |
|---|---|---|
| Cu–N(11) 2.089 (3)<br>Cu–N(21) 2.184 (3)<br>Cu–N(31) 2.047 (2) | 2.102($R$58) | ~ 65 sigma |
| Cu–N(12) 2.305 (3)<br>Cu–N(22) 2.052 (2)<br>Cu–N(32) 2.160(2) | 2.143($R$93) | ~ 100 sigma |

copper compound is 0.197 Å, which is smaller than values found in compounds displaying only a static Jahn–Teller distortion. Even the short Cu–N bonds have an appreciable value for $\Delta$(Cu–N), which indicates the presence of a dynamic as well as a static Jahn–Teller distortion in $[Cu(py_3tren)]^{2+}$.

The gross character of the distortion is best described as orthorhombic i.e., the imine nitrogen with the shortest Cu–N distance is "*trans*" to the pyridine nitrogen atom with the shortest Cu–N distance. Similarly, the imine and pyridine nitrogen atoms with the longest Cu–N distances are mutually "*trans*". Other Cu(II) complexes with similar tris($\alpha$-diimine) ligands such as bipy and phen also show a Jahn–Teller effect [67]. In both $[Cu(bipy)_3]^{2+}$ and $[Cu(phen)_3]^{2+}$ elongated tetragonal $CuN_6$ chromophores with approximate $C_2$ symmetry are observed [68]. The nature of the Jahn–Teller distortion in $[Cu(py_3tren)]^{2+}$ is different from the very similar $[Cu(bipy)_3]^{2+}$ and $[Cu(phen)_3]^{2+}$ complexes. The structure of the $py_3tren$ ligand affects the nature of the Jahn–Teller distortion. The site symmetry of $[Cu(py_3tren)]^{2+}$ is reduced to $C_1$, with a ligand conformation similar, but much exaggerated in the magnitude of the distortion, to that found for the other $[M(py_3tren)]^{2+}$ cations which have pseudo-$C_2$ site symmetry (see Section B(iv)(e)).

Despite the variation between individual Cu–N bond distances and the resultant distortions found in $[Cu(py_3tren)]^{2+}$, the weighted mean parameters for this complex fit smoothly, and are used without further qualification, in the description of the overall trends within the series of $[M(py_3tren)]^{2+}$ complexes.

*(f) $[Cu(py \cdot tren)]^{2+}$, the hydrolysis product of $[Cu(py_3tren)]^{2+}$*

The $[Cu(py_3tren)]^{2+}$ complex is unstable with respect to hydrolysis compared with the other $[M(py_3tren)]^{2+}$ complexes. It is conceivable that the ready reactivity of the copper complex is in part a consequence of the one particularly long bond (Cu–N(12) = 2.305(3) Å) in $[Cu(py_3tren)]^{2+}$. The product of the hydrolysis of $[Cu(py_3tren)]^{2+}$ corresponds to the parent chelate with two of the three possible 2-pyridinecarboxyldehyde fragments removed, giving the new species, $[Cu(py \cdot tren)]^{2+}$.

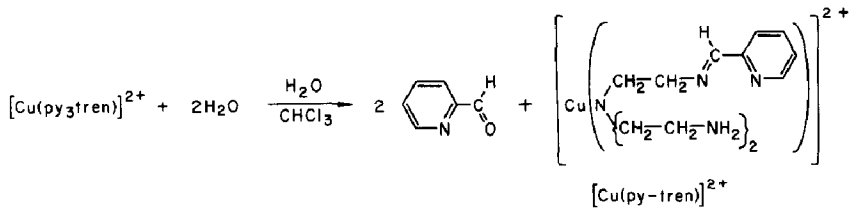


The crystal structure of the hydrolysis product, $[Cu(py \cdot tren)](BF_4)_2$,

shows that the Cu(II) ion coordinates to the five nitrogen atoms of the py · tren ligand resulting in a distorted trigonal bipyramidal coordination polyhedron. This is in agreement with the known disposition of copper to form five-coordinate complexes and the shape is similar to that found in $[M(tren)(NCS)]^+$ (M(II) = Cu and Zn) [69–71] and $[M(Me_6tren)X]^+$ (M(II) = Mn, Fe, Co, Ni, Cu and Zn; $Me_6tren = N(CH_2CH_2N(CH_3)_2)_3$) [72–74] where a tren moiety is functioning as a tripodal ligand with the unique tertiary nitrogen atom occupying the axial site and the remaining nitrogen atoms the three equatorial sites. In $[Cu(py \cdot tren)]^{2+}$, all five coordination sites are occupied by the donor atoms of the pentadentate py · tren ligand. The crystal structure analysis of the hydrolysis product suffers from anion disorder and a space group ambiguity, and will not be further discussed. Structural parameters and atomic coordinates are given in Section C(iii).

*(g) $[Zn(py_3tren)](BF_4)_2$*

The $3e$ level is filled in the $d^{10}$ Zn(II) ion. As shown in Fig. 6(a), the $3e$ level stabilizes toward TP coordination conformation. Thus it is not surprising to find that the zinc and manganese compounds, both of which have a large fraction of their "$d$" electron density in the $3e$ level, are the most distorted toward TP coordination conformation within the $[M(py_3tren)]^{2+}$ series.

*(iv) Structure of the $py_3tren$ ligand*

For convenience, the $py_3tren$ ligand will be discussed in terms of (a) the tren bridgehead, (b) the $\alpha$-diimine moiety, and (c) the pyridine ring. The overall conformation of the ligand will then be described.

Weighted mean values for some distances and angles within the $py_3tren$ ligand are given in Figs. 9 and 10, respectively. For those distances and angles that are statistically of the same population throughout the $[M(py_3tren)]^{2+}$ series, an estimated standard deviation (e.s.d.) serves as a measure of the range of values. For those parameters which are not statistically of the same population, a normalized range of the individual values used in calculating the mean is given. The use of a normalized range value is indicated by the letter $R$ in the parentheses following the mean value. A summary of weighted mean values for the various types of carbon–hydrogen bond angles and distances has also been made [75].

*(a) The tren bridgehead*

The M–N(7) distance is directly determined by the size of the metal ion and the orbital population of the metal $a_1$ orbital, as previously discussed in Section B(ii)(b). The tren ligand appears to be flexible in accommodating

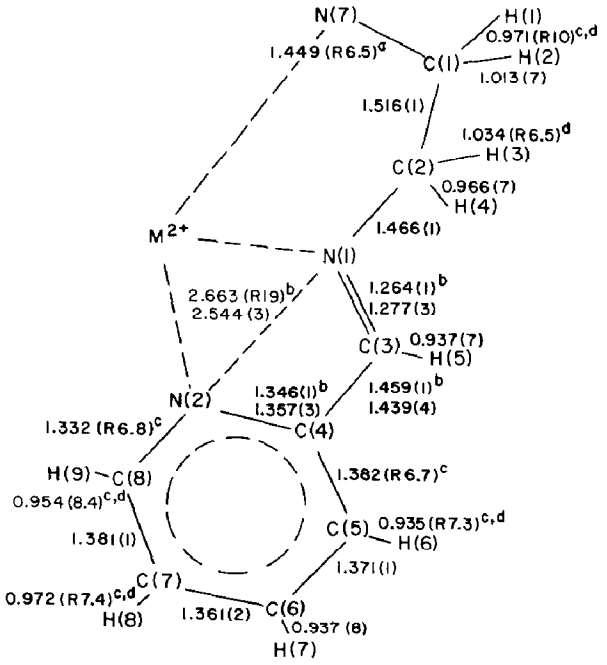


Fig. 9. Weighted mean values for bond distances (Å) within the $py_3tren$ ligand. The numbers within the parentheses represent estimated standard deviations (e.s.d.) in the least significant figure, for those means with $R \leqslant 5.9$; the cut off value signifying the values averaged are from the same population at a 99.5% confidence level for a sample size of 21. ($R$ is defined in footnote a of Table 1.) For $R > 5.9$ the e.s.d. is undefined since the individual values are significantly different at the 99.5% confidence level. (a) The N(7)–C(1) distance varies as a function of the metal–nitrogen repulsion within the constraints of the bridgehead geometry, see text. (b) Upper values do not include $[FeL](BF_4)_2$ values in the calculation of the mean. Weighted mean values for $[FeL](BF_4)_2$ are given as the lower figure. (c) These values seem to show a variation due to effects from packing or from the metal to pyridine–nitrogen binding, see text. (d) Weighted mean values involving hydrogen atoms are determined from a sample size of 18 (99.5% confidence level obtained when $R \leqslant 5.8$). The hydrogen atoms in $[NiL](PF_6)_2$ are in calculated positions and were not refined.

increases in M–N(7) distances through rearrangements of the bridgehead conformation about N(7) from tetrahedral to planar, as can be seen in the values given in Table 4. There is a linear relationship between the M–N(7) distance and the ligand conformation about N(7), except in $[CoL](BF_4)_2$ where the bridgehead structure is more tetrahedral than expected due to a short Co–N(7) interaction, and in $[NiL](PF_6)_2$ which has a different anion and consequently different packing forces than the other compounds in the $[ML]^{2+}$ series. Also, as the N(7) goes from an approximately $sp^3$ (Mn–N(7)–C(1) = 112.6(2)°) to a $sp^2$ (Fe–N(7)–C(1) = 120.0(3)°) hybridized state the N(7)–C(1) bond distance decreases by 0.031 Å in a linear relationship.

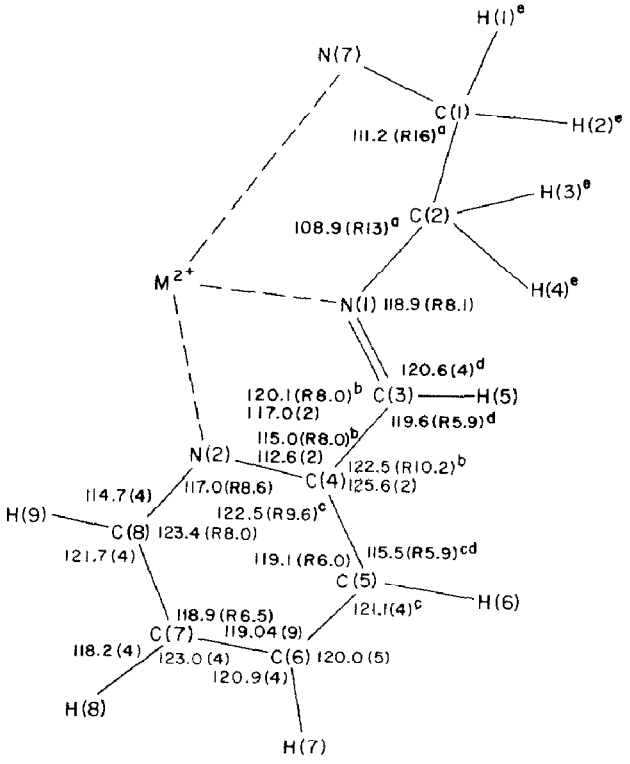


Fig. 10. Weighted mean bond angles (degrees) within the $py_3tren$ ligand. See caption of Fig. 9 for explanations of range values ($R$). (a) These values vary with changes in the bridgehead geometry, see text. (b) See note (b) Fig. 9. (c) See note (c) Fig. 9. (d) See note (d) Fig. 9. (e) Weighted mean values involving atoms H(1) through H(4) are as follows:
H(1)–C(1)–H(2), 106.9($R$7.3)(c,d);
H(3)–C(2)–H(4), 109.2(6); N(7)–C(1)–H(1), 111.3(4);
N(7)–C(1)–H(2), 109.1(4); H(1)–C(1)–C(2), 109.4(4);
H(2)–C(1)–C(2), 108.7(4); C(1)–C(2)–H(3), 112.1(4);
C(1)–C(2)–H(4), 110.4(4); H(3)–C(2)–N(1), 106.5(4);
H(4)–C(2)–N(1), 109.6(4).

TABLE 4

Weighted mean values describing the $py_3tren$ bridgehead geometry

| | C(1)–N(7) –C(1) | M–N(7) –C(1) | N(7)–C(1) –C(2) | C(1)–C(2) –N(1) | N(7) –C(1) |
|---|---|---|---|---|---|
| $MnL(BF_4)_2$ | 112.6 (2) | 106.2 (1) | 110.5 (2) | 107.3 (2) | 1.467 (3) |
| $FeL(BF_4)_2$ | 120.0 (3) | 90.0 (2) | 116.1 (3) | 111.2 (2) | 1.436 (4) |
| $CoL(BF_4)_2$ | 114.2 ($R$4.8) [a] | 104.2 ($R$5.6) | 110.1 (2) | 107.8 (2) | 1.457 (3) |
| $NiL(BF_4)_2$ | 117.5 (3) | 99.2 (2) | 111.4 (3) | 109.7 (3) | 1.435 (5) |
| $NiL(PF_6)_2$ | 118.2 (2) | 97.8 (1) | 112.1 (2) | 109.8 (2) | 1.449 (4) |
| $CuL(BF_4)_2$ | 116.5 ($R$4.7) | 101.1 ($R$23) | 110.9 (2) | 109.5 (2) | 1.441 (3) |
| $ZnL(BF_4)_2$ | 115.3 (2) | 102.7 (1) | 110.6 (2) | 108.7 (2) | 1.448 (3) |

[a] See footnote [a] in Table 1 for explanation of $R$ values. The 99.5% confidence level that the three measurements averaged are of the same population is given by $R \leqslant 4.4$.

Within the ethylene diamine part of the tren moiety (N(7)–C(1)–C(2)–N(1)), the arms have the "*gauche*" configuration, as in similar complexes containing a R · tren ligand [76]. However, only the $[M(py_3tren)]^{2+}$ complexes reveal extensive changes in bridgehead geometry, from tetrahedral to trigonal planar, about the bridging tertiary amine (N(7)) atom.

*(b) The α-diimine moiety*

For iron, α-diimine molecules are strong-field ligands. From spectroscopic evidence it is shown that in some cases these molecules are able to activate $d_\pi$–$p_\pi$ interactions with the metals to which they are coordinated [78]. This is also a well known feature of other conjugated π-chelate ligands. Some of us have recently discussed this feature in related ligands such as *N*,*N'*-ethylenebis(thioacetylacetoneiminato), sacacen [79], and in the tetraimine macrocyclic ligand, TIM [80,81], which contains α-diimine moieties.

It is apparent that the possibility of π-bonding interactions with the metal also improves the σ-bonding capabilities of the ligand. In other words, as the metal-atom to donor-atom distance becomes smaller, a strong field character of the ligand develops due to synergistic σ- and π-bonding effects.

In the present series of compounds the bond distances within the α-diimine moiety of the $py_3tren$ ligand are practically constant except for $[FeL](BF_4)_2$ which shows "special character". Figure 9 shows that for $[FeL](BF_4)_2$ there is a statistically significant lengthening (by ~ 4 e.s.d.) of the C(3)–N(1) and C(4)–N(2) multiple bond lengths, concomitant with a statistically significant shortening (by ~ 5 e.s.d.) of the C(3)–C(4) bond length. Using the bond length to bond order relationship given by Bayer and Hafelinger [82] for C=N bonds, we estimate the C(3)=N(1) π-bond order to be ~ 0.74 in $[FeL](BF_4)_2$ and 0.86 in the other $[ML]^{2+}$ complexes. A similar analysis using Pauling's relationship between bond length and bond order [83] indicates that the magnitudes of the decrements in the pyridine ring C(4)–N(2) π-bond order and the increase in C(3)–C(4) π-bond order are also small (ca. 0.1). It should be noted that the mean value of the C(3)–C(4) bond length [1.459(1) Å] in the $[ML]^{2+}$ complexes (excluding Fe(II)) is already shorter than that expected for a $sp^2$–$sp^2$ C–C single bond. Electron diffraction studies report $sp^2$–$sp^2$ bond lengths of 1.489(8)° in biphenyl [84] and 1.515(15) Å in hexaphenylbenzene [85]. The latter values presumably correspond to a $sp^2$–$sp^2$ C–C interaction free of π-electron delocalization effects since the phenyl rings in these latter compounds are non-planar (dihedral angles between rings are 41.6 and 90°, respectively).

If the crystallographic data themselves suggest a "special character" to the iron complex, much more dramatic evidence is provided by vibrational spectroscopy. In Fig. 11 the IR bands associated with the α-diimine chromophore of the Fe(II) complex ((C) in Figure 11) show that this compound is

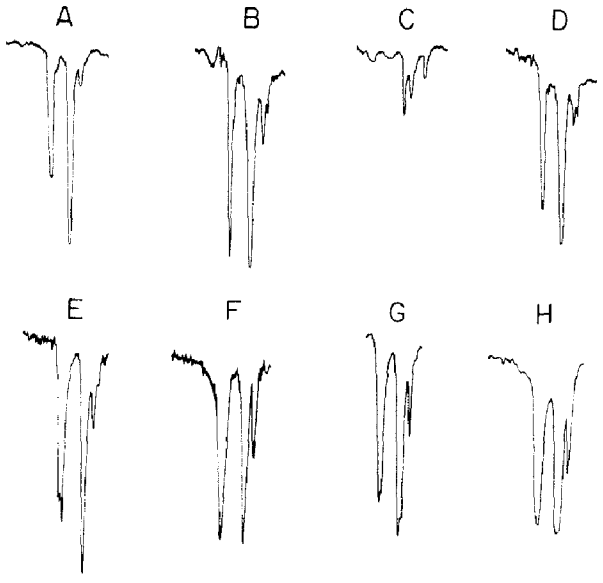


Fig. 11. Infrared spectra in the 1700–1550 $cm^{-1}$ region for the $[ML]^{2+}$ complexes. Infrared spectra (higher energy to the left) for (A) $[Ni(py_3tren)](PF_6)_2$ as a nujol mull; (B) [Ni(6 Me·$py_3$tren)]$(PF_6)_2$ as a nujol mull; (C) $[Fe(py_3tren)](PF_6)_2$ as a nujol mull; (D) [Fe(6 Me·$py_3$tren)]$(PF_6)_2$ as a nujol mull; (E) $[Zn(py_3tren)](BF_4)_2$ as a nujol mull; (F) $[Zn(py_3tren)](BF_4)_2$ in $d_3$-acetonitrile solution; (G) $[Cu(py_3tren)](BF_4)_2$ as a nujol mull, and (H) $[Cu(py_3tren)](BF_4)_2$ in $d_3$-acetonitrile solution. In all cases (except for (C)), the highest energy envelope (to the left) is assigned to C=N stretching modes and the two lower energy envelopes to pyridine vibration modes.

unique within the series. In the spectra for all of the complexes the highest energy envelope is clearly identifiable and assignable to a C=N stretching mode. Similarly the two lower energy envelopes are assigned to pyridine vibration modes [32]. Clearly the situation is different for iron: the intensities of the envelopes are reduced and assignments are speculative. The tendency for the C–N stretching band to have a low intensity for low-spin Fe(II) $\alpha$-diimine complexes has been previously observed [86]. This confirms the "special character" of the Fe(II) complex but Raman spectra are required for unambiguous assignment of the C–N stretching vibration. For the Fe(II) complex this vibration occurs at 1616 $cm^{-1}$ whereas all the other complexes exhibit C–N bands in the 1650–1670 $cm^{-1}$ range [86]. Thus, the proposal that the C–N bond order is smallest for the Fe(II) complex is supported by the Raman spectra.

We now refer back to the MO picture in Section B(ii)(a) to understand more about M–L $\pi$-interactions, clearly evident in $[FeL]^{2+}$, and to rationalize the different behavior of the other complexes. It was mentioned that each

$\alpha$-diimine chelate has $\pi$-acceptor bonding capabilities due to the presence of an empty $\pi^*$ orbital (as shown in either diagram **4** or diagram **5**) at low energy. It was also pointed out that, of their symmetry combinations, only the one having $e$ character matches with metal $d$ orbitals to give rise to bonding and antibonding M–L $\pi$ MOs. The antibonding level ($2e$ in diagram **6**) is not populated in the iron complex. This empty orbital accounts for any M–L $\pi$-backdonation which occurs. The overall effect cannot be expected to be large since each Fe–N bond can have at most only $2/6(=1/3)$ double bond character. Recall that the a-diimine $\pi$-acceptor orbital is shared by the two nitrogen atoms and that one of the three $\pi$ MOs of the ligand ($a_2$) is not involved by symmetry) in any interaction with the metal. Finally, the perturbation theory arguments which are based on overlap and the energy gap, are not optimal for a strong $\pi$-interaction. Nonetheless, the $\pi$ back-donation occurs for low spin Fe(II). It was shown in Fig. 6(c) that, although not as large as at TP, the electron density accepted by the ligand $\pi^*$ orbital is not null at TAP. In addition, the experimental crystallographic evidence of the lengthening of C=N and of the shortening of C–C bonds is in agreement with the nature of the accepting ligand $\pi$-orbital, as the latter has both C–N $\pi^*$ antibonding and C–C $\pi$ bonding character.

We have previously argued that in all of the $py_3tren$ complexes where two or more electrons occupy the higher energy MOs (above $a_1$ and $1e$), the distortions from TAP avoid an electron occupancy of the ligand–metal $\pi^*$ levels (namely $2e$ in **6**, but $a_2$ as well). It can also be argued that in the other complexes of the series a vacancy in these levels can activate M–L $\pi$-backdonation effects similar to those observed in the iron compound. The point to be made is that the presence of electrons in the M–L $\sigma^*$ orbitals induces a dramatic elongation of all the M–N bonds. Even though still allowed by symmetry, the M–L $\pi$ interaction is greatly reduced because the poorer $\sigma$ interaction also limits the possibility of good M–L $d_\pi$–$p_\pi$ overlap.

*(c) Trends within the pyridine rings*

A comparison of the pyridine rings in the $[ML]^{2+}$ complexes with 32 similar pyridine rings in other metal complexes reveals that they have remarkably similar features, differing mainly in parameters associated with the pyridine nitrogen atoms due to the variety of different attached metal ions [87a]. The pyridine rings in the $[ML]^{2+}$ series of complexes differ from the general pattern only in having mean bond lengths for C(6)–C(7) and C(7)–C(8) which are slightly shorter (by 0.013 and 0.016 Å, respectively).

However, within the overall pattern noted above there exist significant systematic trends in the $[ML]^{2+}$ series [87b]. We conclude that differences in the local environment about each arm of the isomorphous compounds are

more important in causing variations in distance and angle values than are differences resulting from changes in metal ions.

The pyridine rings are not exactly planar but deviate from planarity by small significant amounts. There is a slight boat shape to the pyridine ring. Each hydrogen atom deviates from the plane in a direction opposite to that of the carbon atom to which it is attached.

Atoms C(3), N(1) and M are also displaced (up to a maximum of 0.2 Å) from the pyridine ring least-squares plane. These atoms are most nearly co-planar in the $[FeL]^{2+}$ complex, consistent with this complex having the greatest $\pi$-electron delocalization in the ligand. These atoms are the farthest from the pyridine ring least-squares plane in the $[CoL]^{2+}$ complex [88]. The $[CoL]^{2+}$ complex is also unique in that N(7) has the shortest mean distance (1.320(*R*95) Å) from the pyridine ring least-squares plane, shorter than in $[MnL]^{2+}$, which has the shortest M–N(7) distance. This has the effect of forcing the Co(II) ion farthest (0.150(*R*110) Å) from the pyridine ring least-squares plane, in the direction opposite to the displacement of N(7). All metal ion displacements are dependent upon the size of the coordination polyhedron, $M-N_6$. As $M-N_6$ increases, the metal ion displacement from the pyridine plane increases. The metal ion displacement in $[CoL](BF_4)_2$ is larger than expected with respect to $M-N_6$.

*(d) Hydrogen atoms: bond lengths and angles, contact distances*

Hydrogen atom positions and isotropic thermal parameters, *B*, have been refined for all $[ML]^{2+}$ complexes except $[NiL](PF_6)_2$. Weighted mean values for individual bond distances and angles involving hydrogen atoms are given in Figs. 9 and 10, respectively.

An examination of intramolecular contact distances reveals some interesting features about the $py_3tren$ ligand. Atom H(9) projects toward a pyridine ring of a neighboring arm. As the coordination polyhedron size, $M-N_6$, decreases the ligand wraps about the metal in a tighter fashion. This causes H(9) to move closer to the metal, with the shortest contact distance being 3.00(3) Å for H(9)–Fe, and at the same time brings the H(9) atom closer to the N(2) atom in this neighboring pyridine ring, with the shortest distance being 2.52(3) Å for H(29)–N(19) in $[FeL](BF_4)_2$. The latter distance is significantly shorter than the value of 2.7 Å estimated as the sum of the van der Waals radii for these atoms [89]. These contact distances are given in Table 5 where it can be seen that there are considerable variations in values for contact distances within different arms of the ligand. In particular, in arm 2 all $[ML]^{2+}$ cations have H(29) in close contact with a neighboring $BF_4^-$ anion except for $[FeL]^{2+}$ where the H(29) atom has been pulled in toward the central metal ion. Also, only arm 3 of the $[ML]^{2+}$ complexes has a relatively short contact between H(39) and a neighboring pyridine ring

TABLE 5

Selected intramolecular contact distances (Å)

| | | MnL-$(BF_4)_2$ | FeL-$(BF_4)_2$ | CoL-$(BF_4)_2$ | NiL-$(BF_4)_2$ | CuL-$(BF_4)_2$ | ZnL-$(BF_4)_2$ |
|---|---|---|---|---|---|---|---|
| H(*J*9)–M | arm 1 | 3.39 (3) | 3.07 (3) | 3.29 (3) | 3.25 (4) | 3.44 (2) | 3.36 (3) |
| | arm 2 | 3.29 (3) | 3.00 (3) | 3.16 (2) | 3.11 (3) | 3.06 (2) | 3.22 (3) |
| | arm 3 | 3.35 (2) | 3.04 (3) | 3.28 (2) | 3.20 (4) | 3.25 (2) | 3.30 (3) |
| H(*J*9)–N(*J'*2) [a] | arm 1 | 2.70 (3) | 2.55 (3) | 2.66 (3) | 2.71 (4) | 2.91 (3) | 2.69 (3) |
| | arm 2 | 2.80 (3) | 2.52 (3) | 2.67 (3) | 2.72 (4) | 2.72 (2) | 2.74 (3) |
| | arm 3 | 2.61 (3) | 2.57 (3) | 2.58 (3) | 2.66 (4) | 2.67 (2) | 2.66 (3) |
| H(39)–C(28) | | 2.79 (3) | 3.02 (3) | 2.82 (3) | 2.90 (4) | 2.84 (2) | 2.85 (3) |
| H(*J*4)–H(*J*5) [b] | | 2.17 (2) | 2.26 (3) | 2.15 (2) | 2.16 (3) | 2.23 (2) | 2.17 (2) |

[a] $J' = J - 1$, except $J' = 3$ for $J = 1$. [b] Weighted mean value with pooled e.s.d. of the mean given in parentheses.

carbon atom C(28). As the $M-N_6$ size decreases the H(39) atom shifts its position away from C(28) toward N(22). The increase in H(39)–C(28) contact distances from 2.79(3) Å in $[MnL](BF_4)_2$ (comparable to the van der Waals sum of the radii) to 3.02(3) Å in $[FeL](BF_4)_2$ is linear with decreasing $M-N_6$. Also, it was the step-wise substitution of a methyl group for H(9) atoms in the arms of the $py_3$tren ligand that allowed the "fine tuning" of ligand-packing effects where the steric interaction of the methyl group forces Fe–N bond distances to increase, which changes the metal orbital energy levels sufficiently to give rise to a range of observed magnetic behavior (true spin equilibrium) in the $[Fe(6Me \cdot py_n py_{3-n}tren)]^{2+}$ (where $n = 1$, 2 or 3) complexes [35–38].

The remaining intramolecular contact distances given in Table 5 show that there is a close contact between H(4) and H(5). The ligand shows a range of torsional angles about the C(2)–N(1) bond as the ligand twists to relieve strain or to accommodate a preferred conformation (Fig. 12). The twists are presumably constrained by the close H(4)–H(5) contacts, but there is no correlation between the torsional angles about the C(2)–N(1) bonds and the H(4)–H(5) contact distances.

Our hope to elucidate the packing forces arising from the interaction of $[ML]^{2+}$ cations and $BF_4^-$ and $PF_6^-$ anions was frustrated due to anion disorder in crystals of all compounds. Some of the anion disorder models are described in detail [90–93]. Hydrogen atoms H(14, 15, 16, 17, 18, 25, 29, 31, 35, 36, 37 and 38) tend to have close contacts with the anions. Reference to Figs. 9 and 10 shows that the individual values for bond lengths and angles involving hydrogen atoms vary, and it is presumed that this variation is due to packing forces.

*(e) Overall conformation of the $py_3tren$ ligand*

The $py_3tren$ ligand appears to be very flexible in the tren bridgehead moiety containing the tertiary bridging amine atom and the ethylene diammine arms. This flexible bridgehead is connected to the rest of the arm that contains the strongly-ligating nitrogen atoms in the $\alpha$-diimine moiety. The $\alpha$-diimine moiety is relatively rigid and co-planar with the pyridine ring due to $\pi$-electron delocalization. As the coordination polyhedron size ($M-N_6$) decreases the ligand wraps itself more tightly about smaller metal ions to approach the trigonal antiprismatic (TAP) coordination geometry predicted to be most stable. The ligand twists about the C(2)–N(1) bond of each arm to allow optimal metal-to-$\alpha$-diimine bonding, as can be seen in Fig. 12.

The values for the torsional angles correlate smoothly with the $M-N_6$ size; as the coordination polyhedron size decreases the torsional angles about C(2)–N(1) increase. The 18° range of values for the C(2)–N(1) torsional angle is large, and the only restriction to twisting about this bond is minimal, due to close contacts that can occur between H(4) on C(2) and H(5) on C(3), as discussed in Section B(iv)(d). The 3° range of torsional angle values about C(1)–C(2) is typical for an ethylenediamine moiety. The ranges of values about N(1)–C(3) and C(3)–C(4) are small, as expected for an $\alpha$-diimine moiety with delocalized $\pi$-electron density. Bond angles about C(1), C(2) and N(1) also vary as a function of the metal ion size, as shown by the large $R$ values in Fig. 9 and as previously discussed in Section B(iv)(a), providing further flexibility to the "tren" part of the ligand.

The general nature of the deviation from 3-fold symmetry can be described for the isomorphous $[ML](BF_4)_2$ compounds (M = Mn, Co, Ni, Cu

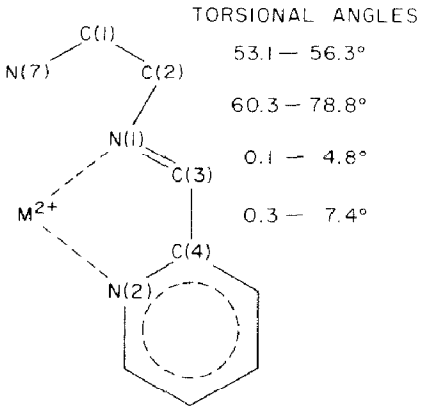


Fig. 12. Range of mean torsional angles within the $py_3tren$ ligand. The torsional angle about C(1)–C(2) is defined as the dihedral angle between the plane defined by N(7)–C(1)–C(2) and the plane defined by C(1)–C(2)–N(1). An analogous definition holds for all the other torsional angles.

and Zn) as a spreading apart of ligand arms 1 and 2 accompanied by other small motions. It was pointed out in Section B(iv) (c) that there are differences in the local environment about each arm, and that these conformational distortions persist in the $[ML]^{2+}$ series regardless of metal ion type. A close inspection of selected parameters (given in Table 6) describing the metal-to-$\alpha$-diimine interaction as a function of arm (rather than a function of metal or metal ion size) is interesting. To eliminate uncertainty due to variable packing forces between anions and cations, we discuss only the isomorphous series of compounds, specifically excluding $[CuL](BF_4)_2$ because of its unique distortion due to Jahn–Teller effects. Thus, in the $[ML](BF_4)_2$ salts (where M(II) = Mn, Co, Ni and Zn), arm 1 is unique by always having the shortest M–N(1) and the longest N(1)=C(3) bond distances; this peculiarity is an indication of a modest metal–ligand $\pi$-bonding enhancement through the imine nitrogen donor atom. However, arm 1 also always has the longest (not shortest) M–N(2) bond distance. It is arm 2 that always has the shortest M–N(2) and longest N(2)–C(4) bond distances, again indicating a modest metal–ligand $\pi$-bonding, but this time to the pyridine nitrogen donor atom. There are only four exceptions (two exceptions that differ by less than 0.001 Å and one each that differ by 0.001 Å and 0.002 Å, respectively) to these trends among 60 values. Arm 3 tends to have intermediate values for M–N bond distances. The two M–N bonds that have been shortened lie in the plane of the chelate ring of arm 3. The longest M–N bonds tend to be in positions above and below this plane. The three chelate rings seem to be related by a "pseudo" two-fold axis, as shown below in **12**.

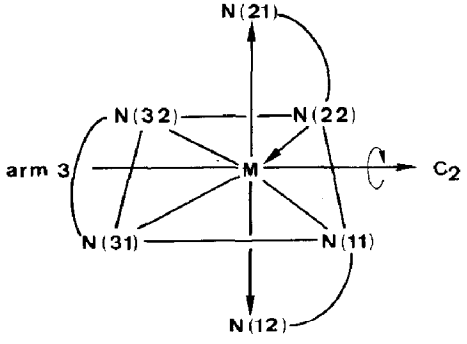


12

Arm 1, which always has the one shortest distance (M–N(1)), also always has the largest displacement of the metal ion from its $\alpha$-diimine least squares plane (N(1)=C(3)–C(4)=N(2)), as shown by values of $\delta M$(diimine) in Table 6. The values of $\delta M$(diimine) in arm 1 range from $-0.171$ to $-0.259$ Å,

TABLE 6

Arm-by-arm analysis of packing and $\pi$-bonding effects within the isomorphous $[ML](BF_4)_2$ compounds [a]

| | arm ($J$) | Mn | Co | Ni | Zn |
|---|---|---|---|---|---|
| $\delta M$(diimine) [b] | 1 | −0.259 | −0.186 | −0.171 | −0.219 |
| | 2 | −0.159 | −0.177 | −0.156 | −0.167 |
| | 3 | −0.054 | −0.022 | −0.023 | −0.006 |
| $\delta N$(diimine) [c] | 1 | −0.002/0.002 | −0.001/0.001 | −0.008/0.007 | −0.005/0.005 |
| N($J$1)/N($J$2) | 2 | −0.015/0.014 | −0.020/0.018 | −0.013/0.012 | −0.014/0.012 |
| | 3 | 0.010/−0.009 | 0.013/−0.012 | 0.007/−0.006 | 0.008/−0.007 |
| M–N($J$1) | 1 | 2.200 (2) | 2.091 (3) | 2.077 (4) | 2.118 (3) |
| | 2 | 2.200 (2) | 2.096 (3) | 2.092 (4) | 2.132 (2) |
| | 3 | 2.204 (2) | 2.091 (2) | 2.091 (4) | 2.134 (2) |
| M–N($J$2) | 1 | 2.348 (2) | 2.227 (3) | 2.113 (4) | 2.260 (3) |
| | 2 | 2.279 (2) | 2.157 (2) | 2.078 (4) | 2.182 (2) |
| | 3 | 2.342 (2) | 2.219 (2) | 2.112 (4) | 2.256 (2) |
| N($J$1)=C($J$3) | 1 | 1.271 (5) | 1.273 (5) | 1.273 (8) | 1.262 (5) |
| | 2 | 1.260 (5) | 1.265 (5) | 1.264 (7) | 1.263 (4) |
| | 3 | 1.260 (4) | 1.261 (4) | 1.270 (7) | 1.260 (4) |
| C($J$3)–C($J$4) | 1 | 1.457 (6) | 1.453 (6) | 1.465 (9) | 1.451 (6) |
| | 2 | 1.459 (5) | 1.454 (6) | 1.450 (7) | 1.466 (5) |
| | 3 | 1.468 (4) | 1.452 (4) | 1.459 (6) | 1.465 (4) |
| N($J$2)=C($J$4) | 1 | 1.348 (4) | 1.347 (4) | 1.342 (7) | 1.344 (4) |
| | 2 | 1.349 (4) | 1.354 (5) | 1.353 (7) | 1.342 (4) |
| | 3 | 1.344 (4) | 1.345 (4) | 1.348 (6) | 1.346 (4) |
| N($J$1)–N($J$2) | 1 | 2.679 | 2.657 | 2.657 | 2.694 |
| | 2 | 2.658 | 2.647 | 2.647 | 2.671 |
| | 3 | 2.677 | 2.658 | 2.658 | 2.687 |

[a] All distances are given in Å. [b] $\delta M$(diimine) is the distance of the metal ion from the $\alpha$-diimine least squares plane defined by atoms N(1)–C(3)–C(4)–N(2). [c] $\delta N$(diimine) is the distance of the nitrogen atom from this same plane. A displacement from the least-squares plane in the direction toward atom N(7) is defined as positive.

where a displacement in the direction toward N(7) is taken as positive. The displacements are smaller in arm 2, and very much smaller in arm 3, where $\delta M$(diimine) ranges from −0.006 to −0.054 Å, indicating that the chelate ring in arm 3 in almost planar. The metal–ligand $\pi$-bonding interaction should be greater for N-imine than N-pyridine (see molecular fragment **5** in Section B(ii)(a), which shows that N(1) has a better developed $\pi$-bonding capacity than N(2)). Consistent with this is the fact that the C(3)–C(4) bonding distance is usually shorter (again indicating metal–ligand $\pi$-elec-

tron delocalization) in arm 1 where the largest $\pi$ interaction occurs. Notice that the chelate bite distance, $b$, is usually longest in arm 1, and usually smallest in arm 2.

The pattern of distortions due to packing forces within the isomorphous series can be summarized as consisting of one nearly planar chelate ring with approximately equal M–N bond distances, and two chelate rings each with a displaced metal ion and one short and one long M–N bond distance, producing a coordination polyhedron with approximate two-fold symmetry. This pattern seems to persist in $[FeL]^{2+}$, not a member of the isomorphous series. $[FeL]^{2+}$ is the most symmetric (coordination polyhedron closest to trigonal antiprismatic, and smallest distortions of the ligand conformation) complex in the $[ML]^{2+}$ series and has very strong metal–ligand $\pi$-bonding interactions with six nitrogen donor atoms. Finally, arm-by-arm distortions are present, but the pattern is different, in $[NiL](PF_6)_2$.

Distortions in the local environment about ligand arms are caused by packing forces between cations and anions. Pseudo $C_2$ symmetry seems to be maintained in the $[ML]^{2+}$ complexes, while the nature of the distortions favors, in part, weak $\pi$-bonding interactions.

## C. EXPERIMENTAL

### *(i) Syntheses*

The reagents used as starting materials were obtained commercially and used without further purification. All solvents were reagent grade. Reactions were carried out at room temperature unless otherwise specified. All products were dried at room temperature over $P_4O_{10}$ for approximately 12 h at 1 Torr. Analytical results for $[M(py_3tren)](X)_2$, $[M(6Me \cdot py_3tren)](PF_6)_2$, and $[Cu(py \cdot tren)](BF_4)_2$ salts are reported in Table 7.

*Isolation of the 2,2′,2″-triaminotriethylamine · trihydrochloride salt, tren · 3 HCl*

Tren · 3 HCl was isolated and purified as previously described [32].

*Preparation of the tris[4-(2-pyridyl)-3-aza-3-butenyl]aminemetal(II) hexafluorophosphate salts, $[M(py_3tren)](PF_6)_2$, M(II) = Mn, Co, Ni and Cu*

The $PF_6^-$ salts were prepared and purified as previously described for the Ni(II) compound [32]. Yields for the $[M(py_3tren)](PF_6)_2$ salts are: Mn (1.36 g, 46%), Co (1.70 g, 57%), Ni (1.43 g, 48%), Cu (1.35 g, 45%).

*Preparation of the tris[4-(2-pyridyl)-3-aza-3-butenyl]amineiron(II) hexafluorophosphate salt, $[Fe(py_3tren)](PF_6)_2$*

$FeCl_2 \cdot 4\ H_2O$ (0.78 g, 3.9 mmol) was refluxed for 1 h in 50 ml of methanol which contained 1.0 g of iron powder. The resulting hot methanolic

TABLE 7

Analytical and conductivity data for the $[M(py_3tren)](X)_2$(A), $[M(6Me\cdot py_3tren)](X)_2$(B) and $[M(py\cdot tren)](X)_2$(C) salts

| | M | X | Color | Calc. (%) | | | | Found (%) | | | | $\Lambda_c$ [a] | |
|---|---|---|---|---|---|---|---|---|---|---|---|---|---|
| | | | | C | H | N | Other | C | H | N | Other | | |
| (A) | Mn | $PF_6$ | yellow | 38.20 | 3.59 | 12.93 | – | 38.58 | 3.67 | 12.81 | – | 369($CH_3CN$); | 343(acetone) |
| | | $BF_4$ | yellow | 44.99 | 4.25 | 15.30 | 23.71 (F) | 45.08 | 4.38 | 15.26 | 23.46 (F) | 363($CH_3CN$); | 252(MeOH) |
| | | I[4] | yellow | 39.90 | 3.77 | 13.56 | 35.14 (I) | 39.75 | 3.86 | 13.53 | 35.36 (I) | 230($H_2O$); | 234(MeOH) |
| | Fe | $PF_6$ | dark red | 38.00 | 3.59 | 12.91 | – | 38.17 | 3.52 | 12.86 | – | 370($CH_3CN$); | 340(acetone) |
| | | $BF_4$ | dark red | 44.92 | 4.24 | 15.27 | 23.69 (F) | 44.67 | 4.35 | 15.10 | 23.32 (F) | 365($CH_3CN$); | 255(MeOH) |
| | | I | dark red | 39.87 | 3.90 | 13.56 | 35.10 (I) | 39.80 | 3.83 | 13.43 | 35.23 (I) | 219($H_2O$); | 230(MeOH) |
| | Co | $PF_6$ | red orange | 37.90 | 3.58 | 12.85 | – | 37.71 | 3.60 | 13.09 | – | 373($CH_3CN$); | 343(acetone) |
| | | $BF_4$ | red orange | 44.71 | 4.22 | 15.20 | 23.58 (F) | 44.82 | 4.33 | 15.07 | 23.73 (F) | 361($CH_3CN$); | 257(MeOH) |
| | | I | red orange | 39.68 | 3.75 | 13.51 | 34.97 (I) | 39.87 | 3.91 | 13.39 | 35.15 (I) | 233($H_2O$); | 231(MeOH) |
| | Ni | $PF_6$ | gold brown | 37.90 | 3.58 | 12.85 | – | 38.06 | 3.81 | 12.81 | – | 370($CH_3CN$); | 344(acetone) |
| | | $BF_4$ | gold brown | 44.72 | 4.22 | 15.21 | 23.58 (F) | 44.56 | 4.30 | 15.06 | 23.32 (F) | 363($CH_3CN$); | 256(MeOH) |
| | | I | gold brown | 39.67 | 3.75 | 13.51 | 34.97 (I) | 39.68 | 3.66 | 13.35 | 35.19 (I) | 234($H_2O$); | 234(MeOH) |
| | Cu | $PF_6$ | apple green | 37.55 | 3.55 | 12.78 | – | 37.68 | 3.70 | 12.98 | – | 374($CH_3CN$); | 358(acetone) |
| | | $BF_4$ | apple green | 44.39 | 4.19 | 15.09 | 23.41 (F) | 44.54 | 4.09 | 14.94 | 23.99 (F) | 366($CH_3CN$); | 250(MeOH) |
| | | I | olive green | 39.44 | 3.72 | 13.41 | 34.72 (I) | 39.30 | 3.61 | 13.24 | 34.63 (I) | – ; | 234(MeOH) |
| | Zn | $PF_6$ | yellow | 37.46 | 3.54 | 12.78 | – | 37.44 | 3.68 | 12.98 | – | 377($CH_3CN$); | 343(acetone) |
| | | $BF_4$ | yellow | 44.27 | 4.18 | 15.05 | 23.34 (F) | 44.38 | 4.29 | 15.08 | 23.10 (F) | 365 ($CH_3CN$); | 260(MeOH) |
| | | I | yellow | 39.34 | 3.77 | 13.56 | 35.14 (I) | 39.75 | 3.86 | 13.53 | 35.36 (I) | 230($H_2O$); | 237(MeOH) |
| (B) | Fe | $PF_6$ | red | 40.44 | 4.15 | 12.24 | 28.45 (F) | 40.36 | 4.29 | 12.23 | 28.41 (F) | 372($CH_3CN$); | 350(acetone) |
| | Ni | $PF_6$ | lime green | 40.29 | 4.11 | 12.19 | 28.36 (F) | 40.32 | 3.75 | 11.82 | 28.40 (F) | 377($CH_3CN$); | 343(acetone) |
| (C) | Cu | $BF_4$ | dark green | 30.50 | 4.48 | 14.83 | 31.17 (F) | 30.45 | 4.24 | 14.97 | 32.46 (F) | 385($CH_3CN$); | 266($H_2O$) |

[a] $Ohm^{-1}$ equiv $^{-1}$ $cm^2$, $1\times10^{-4}$ M solutions at 25°C. References establishing di-univalent electrolyte behavior in acetonitrile and methanol: Leonard V. Interrante, Inorg. Chem., 7 (1968) 943; in acetone and water: L.J. Wilson and Norman J. Rose, J. Am. Chem. Soc., 90 (1968) 6041.

solution was then filtered, under dry nitrogen, into 100 ml of an aqueous solution containing tren · 3HCl (1.00 g, 3.9 mmol), NaOH (0.47 g, 11.7 mmol) and 2-pyridinecarboxaldehyde (1.25 g, 11.7 mmol). After addition of a filtered solution of $NaPF_6$ (1.35 g, 8.0 mmol) in 20 ml of water, the deep red solution was allowed to stand overnight at room temperature. The dark red crystals which volunteered were collected and recrystallized from a 1 : 3 (by volume) acetone–hexane solvent mixture. Yield, 1.18 g (40%).

*Preparation of the tris[4-(2-pyridyl)-3-aza-3-butenyl]aminezinc(II) hexafluorophosphate salt, [Zn(py$_3$tren)](PF$_6$)$_2$*

2-Pyridinecarboxaldehyde (1.25 g, 11.7 mmol) was added to a mixture of tren · 3HCl (1.00 g, 3.9 mmol) and NaOH (0.47 g, 11.7 mmol) dissolved in 100 ml of methanol. After stirring for 1 h, the methanolic solution was filtered to remove the NaCl which had formed. To the resulting clear yellow solution, a filtered solution of anhydrous $ZnCl_2$ (0.53 g, 3.9 mmol) dissolved in 100 ml of methanol was added with stirring. Upon addition of a filtered solution of $NaPF_6$ (1.35 g, 8.0 mmol) in 20 ml of water, a yellow crystalline solid deposited. This solid was recrystallized from a 1 : 1 (by volume) acetone–hexane mixture. Yield, 1.51 g (51%).

*Preparation of the tris[4-(2-(6-methylpyridyl)-3-aza-3-butenyl]aminemetal(II) hexafluorophosphate salts, [M(6Me · py$_3$tren)](PF$_6$)$_2$ M(II = Fe, Ni*

Procedures identical to those given above for the preparation of the Fe and Ni compounds of [M(py$_3$tren)](PF$_6$)$_2$ were followed, except that 6-methyl-2-pyridinecarboxaldehyde (1.42 g, 11.7 mmol) was substituted for 2-pyridinecarboxaldehyde. Yields for the [M(6Me · py$_3$tren)](PF$_6$)$_2$ salts were: Ni (1.70 g, 54%), Fe (1.81 g, 58%).

*Preparation of the tris[4-(2-pyridyl)-3-aza-3-butenyl]aminemetal(II) iodide salts, [M(py$_3$tren)]I$_2$, M(II) = Mn, Fe, Co, Ni, Cu, Zn*

A filtered solution of 50 ml of acetone containing NaI (0.33 g, 2.12 mmol) was added to a 100 ml acetone solution containing 1.06 mmol of the appropriate [M(py$_3$tren)](PF$_6$)$_2$ salt. Solids were immediately obtained in all cases and crystallization was completed by cooling the solutions in an ice bath for approximately 15 min. Yields for the [M(py$_3$tren)]I$_2$ salts were: Mn (0.65 g, 85%); Fe (0.59 g, 77%); Co (0.68 g, 88%); Ni (0.66 g, 87%); Cu (0.66 g, 89%); Zn (0.71 g, 91%).

*Preparation of the tris[4-(2-pyridyl)-3-aza-3-butenyl]aminemetal(II) tetrafluoroborate salts, [M(py$_3$tren)](BF$_4$)$_2$, M(II) = Mn, Fe, Co, Ni, Cu, Zn*

2-Pyridinecarboxaldehyde (1.25 g, 11.7 mmol) was added to a mixture of tren · 3HCl (1.00 g, 3.9 mmol) and NaOH (0.47 g, 11.7 mmol) dissolved in

100 ml of water. To this aqueous ligand solution, a filtered solution of the appropriate $MCl_2 \cdot xH_2O$ salt (3.9 mmol) dissolved in 50 ml of methanol was added with stirring. (Note that for the Fe(II) complex, the methanolic $FeCl_2 \cdot 4H_2O$ solution was first treated with iron powder in the manner described in the synthesis of the $[Fe(py_3tren)](PF_6)_2$ salt; for the Zn(II) complex, anhydrous $ZnCl_2$ was used as the metal ion source.) The solutions remained clear upon the addition of a filtered solution of $NaBF_4$ (88 g, 8.0 mmol) in 50 ml of water. Well-formed crystals of the tetrafluoroborate salts deposited as these solutions were allowed to evaporate at room temperature to a volume of approximately 30 ml. The salts were recrystallized from boiling methanol. Yields for the $[M(py_3tren)](BF_4)_2$ complexes were: Mn (0.95 g, 38%); Fe (0.83 g, 33%); Co (0.96 g, 38%); Ni (0.91 g, 36%); Cu (0.91 g, 36%); Zn (0.79 g, 31%).

*Preparation of [(4-(2-pyridyl)-3-aza-3-butenyl)-bis(2-aminoethyl)]amine-copper(II) tetrafluoroborate salt, $[Cu(py \cdot tren)](BF_4)_2$, via hydrolysis*

$[Cu(py_3tren)](BF_4)_2$ (3.85 g, 8.15 mmol), dissolved in 150 ml of water, was stirred vigorously with 200 ml of chloroform for approximately 5 h. The chloroform layer was then separated from the aqueous phase and the entire procedure was repeated three more times with fresh portions of chloroform, during which the aqueous phase changed in color from apple-green to blue. The resulting blue water phase was then taken to dryness under reduced pressure at 60–65°C and the solid which remained was recrystallized from boiling methanol. Yield, 1.70 g (61%).

*(ii) Physical measurements*

Infrared measurements on the solids were obtained with Beckman IR-10 and Perkin–Elmer Model 21 spectrophotometers as Nujol mulls in the range 4000 to 400 $cm^{-1}$. Solution IR spectra were obtained using IR-Tran windowed cells.

Magnetic susceptibility measurements were obtained on the solids by the Faraday technique using $Hg[Co(NCS)_4]$ as the calibrant [94] and are tabulated in Table 2. Values of $\mu_{eff}$ in Bohr magnetons have been calculated using the equation $\mu_{eff}(BM) = 2.83[X_M(corr)T]^{1/2}$ where $X_M(corr)$ is the corrected molar susceptibility (c.g.s.) and $T$ the absolute temperature (K). The molar diamagnetic corrections used in determining the $X_M(corr)$ values have been calculated from Pascal's constants [95]: $py_3tren$, $-169 \times 10^{-6}$ c.g.s. units; $py \cdot tren$, $-131 \times 10^{-6}$ c.g.s. units; $6Me \cdot py_3tren$, $-213 \times 10^{-6}$ c.g.s. units; $PF_6^-$ anion, $-64 \times 10^{-6}$ c.g.s. units; $BF_4^-$ anion, $-37 \times 10^{-6}$ c.g.s. units; $I^-$ anion, $-51 \times 10^{-6}$ c.g.s. units.

Conductivity measurements were obtained at 25.0°C using a Beckman

Model RC-18A conductivity bridge supplemented with a Heathkit Model IN-27 decade capacitor.

Microanalyses were performed by Alfred Bernhardt, Mikroanalytisches Laboratorium, West Germany; Galbraith Laboratories, Inc., Knoxville, Tennessee; and Chemalytics Inc., Tempe, Arizona.

*(iii) X-ray experimental techniques*

Procedures used for data collection and for solving the structure have been described in detail for the complexes $[MnL](BF_4)_2$ [90], $[NiL](BF_4)_2$ [91], $[CuL](BF_4)_2$ [92], $[ZnL](BF_4)_2$ [93], and $[Cu(py \cdot tren)](BF_4)_2$ [91] where L = $py_3tren$. Only the procedures used in general for all the complexes will be described here. Information specific to each compound is given in Table 8.

The space groups were determined from preliminary Weissenberg and precession photography. Cell parameters were determined at room temperature from a least-squares refinement of more than 20 $2\theta$ values (averages of $+2\theta$ and $-2\theta$) for intense high-order reflections, hand-centered on a Picker four-circle diffractometer. For each compound a density measured by flotation was compared with a calculated density, providing a check of the molecular weight and giving the number of molecules per unit cell, $Z$.

Intensity data were collected at room temperature using MoK$\alpha$ radiation filtered through 0.001 inch niobium foil. The $\theta - 2\theta$ scan method was employed using the formula of Alexander and Smith [96]:

Scan range = $A + 1.0 \tan \theta$

The value of $A$ was determined by measuring the width of some low-order intense reflections. Stationary background measurements were made at the start and finish of each scan. Periodically the intensities of standard reflections were remeasured after each group of about 150 reflections, and these values were used to calculate a scale factor for each group and also a stability constant, $k$, for all of the data collection. Intensity measurements were recorded in truncated dekacounts and the intensities and their estimated standard deviations were calculated from

$$I = S - \frac{t_s}{2t_B}(B_1 + B_2) - 0.45\left(2\frac{t_s}{2t_B} - 1\right)$$

and

$$\sigma_I^2 = \tfrac{1}{10}\left[S + \left(\frac{t_s}{2t_B}\right)^2 (B_1 + B_2)\right] + k^2\left[S + \frac{t_s}{2t_B}(B_1 + B_2)\right]^2 + 0.25$$

where $S$ = dekacounts recorded during scan times $t_s$, $B$ = dekacounts recorded during background time $t_B$, and $k$ = empirical stability constant. The

TABLE 8

Summary of X-ray experimental data (L = $py_3tren$)

| | $MnL(BF_4)_2$ | $FeL(BF_4)_2$ | $CoL(BF_4)_2$ |
|---|---|---|---|
| Crystal dimensions (mm) along *a* | 0.31 | | |
| Crystal dimensions (mm) along *b* | 0.39 | | |
| Crystal dimensions (mm) along *c* | 0.28 | | |
| Space group | $C2/c-C_{2h}^{6}$ [a] | $P2_1/c-C_{2h}^{5}$ [b] | $C2/c$ [a] |
| Cell parameters (with standard deviations) | | | |
| *a* (Å) | 28.077 (1) | 10.599 (2) | 28.064 (7) |
| *b* (Å) | 10.780 (1) | 15.504 (3) | 10.665 (2) |
| *c* (Å) | 19.233 (2) | 17.247 (3) | 18.995 (3) |
| $\beta$ (degrees) | 101.29 (1) | 96.383 (9) | 101.32 (2) |
| Volume (Å$^3$) | 5709 | 2817 | 5575 |
| *Z* | 8 | 4 | 8 |
| Calculated density (g cm$^{-3}$) | 1.489 | 1.516 | 1.540 |
| Experimental density (g cm$^{-3}$) | 1.48 (1) | 1.51 (1) | 1.53 (1) |
| *Data collection* | | | |
| Reflections per data group | 50 | 140 | 150 |
| Scan constant, *A*, degrees | 1.6 | 1.0 | 1.0 |
| Group scale factor variation (%) | | 2.7 | 1.1 |
| Stability factor used | 0.002 | 0.01 | 0.003 |
| Unique reflections measured | 4982 | 4866 | 6326 |
| Type of special reflections | $-I$ [d] | $-I$ [e] | $-I$ [e] |
| Special reflections | 500 | | 779 |
| Type of *R* | $RwF$ [b,g] | $RwI$ [h] | $RwI$ [h] |
| *R* value | 0.058 | 0.067 | 0.067 |
| GOF [j] | | 2.00 | 2.12 |
| Absorption coefficient (cm$^{-1}$) | 5.75 | 6.80 | 7.31 |
| Max–min transmission factors | 0.85–0.72 | 0.92–0.86 | 0.91–0.83 |
| Absorption correction | no | yes [k] | yes |
| Anomalous dispersion correction | yes | yes | yes |

[a] Systematic absences, hk$\ell$ for h + k odd, h0$\ell$ for $\ell$ odd. [b] Systematic absences, h0$\ell$ for $\ell$ odd, 0k0 for k odd. [c] Systematic absences, 0k0 for k odd. [d] All data considered observed. Those with net negative intensity were coded as such to be included as negative $F_o^2$'s in the least-squares refinement. [e] Same as [d] except that coded reflections included as negative $I$'s in the least-squares refinement. [f] Reflections with $I < 2\sigma(I)$ tagged as unobserved and assigned value of $I = I + \sigma(I)$ for special treatment in least-squares refinement. [g] The function minimized was $w(F_o^2 - F_c^2)^2$ where $F_c$ is the calculated structure factor value and $w$ is the statistical weight defined to be $(1/\sigma_{F_o^2})^2$. The weighted residual index, $RwF^2$, is defined as $= [\Sigma w(F_o^2 - F_c^2)^2/\Sigma w(F_o^2)^2]^{1/2}$. [h] Refinement based upon minimizing $[\Sigma w(I_o - I_c)^2]$

terms 0.45 and 0.25 are corrections for the truncation of the counts to dekacounts. Lorenz and polarization factors were applied.

All calculations were carried out on either an IBM 7040-7094 direct coupled system (for $NiL(PF_6)_2$) or its successor, a CDC 6400 system (all

| $NiL(BF_4)_2$ | $NiL(PF_6)_2$ | $CuL(BF_4)_2$ | $ZnL(BF_4)_2$ | $[Cu(py \cdot tren)](BF_4)_2$ |
|---|---|---|---|---|
| | 0.25 | 0.32 | 0.22 | 0.24 |
| | 0.25 | 0.34 | 0.36 | |
| | 0.25 | 0.20 | 0.32 | 0.40 |
| $C2/c$ [a] | $P2_1/c$ [b] | $C2/c$ [a] | $C2/c$ [a] | $P2_1$ or $P2_1/n$ [c] |
| 28.171 (12) | 14.980 (2) | 28.088 (4) | 28.042 (8) | 7.7930 (3) |
| 10.666 (4) | 10.689 (2) | 10.654 (2) | 10.686 (3) | 14.9100 (6) |
| 18.802 (5) | 19.938 (3) | 18.959 (2) | 19.082 (4) | 16.7445 (10) |
| 101.52 (3) | 108.83 (1) | 102.12 (1) | 101.25 (2) | 96.391 (5) |
| 5536 | 3022 | 5547 | 5608 | 1934 |
| 8 | 4 | 8 | 8 | 4 |
| 1.549 | 1.675 | 1.558 | 1.545 | 1.62 |
| 1.54 (1) | 1.66 (1) | 1.55 (1) | 1.57 (1) | 1.59 (1) |
| 200 | | 170 | | |
| 0.95 | 1.6 | 0.9 | 1.0 | 1.3 |
| 3.8 | | 3.4 | 3.9 | 1.0 |
| 0.005 | | 0.01 | | 0.007 |
| 6942 | 5235 | 6294 | 6338 | |
| $-I$ [e] | unobserved [f] | $-I$ | $-I$ [d] | |
| | 1537 | 726 | 598 | |
| $RwI$ [h] | $RwF$ [i] | $RwI$ [h] | $RwF$ [2,g] | $RF$ |
| 0.078 | 0.058 | 0.079 | 0.074 | 0.148 |
| | | 1.62 | 2.16 | |
| | 8.52 | 9.1 | 10.0 | |
| | 0.81 – 0.70 | 0.84 – 0.79 | 0.77 – 0.59 | |
| yes | no | yes | no | no |
| yes | yes | yes | yes | no |

with all reflections ($\pm I$) considered observed. Replace the $F^2$ by $I$ in [g] to get the comparable $I$ functions. [i] The function minimized in the least squares refinement was $[\Sigma w(|F_o| - |F_c|)^2]$ with $w = (1/\sigma_F)^2$ except that any observed reflection with $F_c < F_o$ was given $w = 0$. The function used to calculate the residual was $RwF$. $RwF = [\Sigma w(F_o - F_c)^2/\Sigma wF_o^2]^{1/2}$ and the standard deviation of an observation of unit weight is calculated by $GOF = [\Sigma w(F_o - F_c)^2/n_o - n_v]^{1/2}$. [j] GOF is the "goodness of fit", the standard deviation of an observation of unit weight: $GOF = [\Sigma w(F_o^2 - F_c^2)^2/(n_o - n_v)]^{1/2}$ where $n_o$ = number of observations and $n_v$ = number of variables. [k] Using the Tompa absorption program [97], as modified by D. Cullen and E. Adman at the University of Washington.

other complexes). The sets of programs used were written or adapted by J.M. Stewart; X RAY-63 [98] for the direct coupled system and X RAY-70 [99] for the CDC system. Scattering factors for non-hydrogen neutral atoms were taken from Doyle and Turner [100] except for $[CoL](BF_4)_2$ and

$[NiL](PF_6)_2$ where they were taken from Cromer and Waber [101]. Hydrogen atom scattering factors were taken from Table 2 of Stewart, Davidson and Simpson [102]. When anomalous dispersion effects were included in the calculation of $F_c$ the values tabulated by Templeton [103] for $\Delta f'$ and $\Delta f''$ were used for metal atoms, except that the values used for zinc were calculated by Cromer [104].

For the compounds $[NiL](PF_6)_2$, $[MnL](BF_4)_2$, $[FeL](BF_4)_2$ and $[Cu(py \cdot tren)](BF_4)_2$ a three-dimensional Patterson synthesis revealed the metal atom positions. All other non-hydrogen atoms were located from three-dimensional Fourier syntheses. The remaining M(II)($py_3$tren) tetrafluoroborate salts had space groups and cell parameters that indicated the complexes were isostructural with $[MnL](BF_4)_2$. In general each of these complexes was solved by taking the atomic parameters from the previously solved compound that had the most similar cell parameters and using these atomic parameters as a starting model for the new structure. Refinement was by full-matrix least squares. The function minimized in the least squares program is given in Table 8 for each compound. Hydrogen atom positions were revealed by three-dimensional difference Fourier syntheses when possible; otherwise they were put in calculated positions. The Fourier syntheses also revealed substantial disordering of the $BF_4^-$ groups of the $[ML](BF)_4$ salts that crystallized in space groups $C2/c$. This disorder phenomena has been described in detail [90–93]. Essentially the electron density of the anion region was accounted for by placing fluorine atoms at peaks of electron density until no significant electron density remained. Least squares refinement using anisotropic thermal parameters for non-hydrogen atoms and isotropic thermal parameters for hydrogen atoms, was continued with the matrix divided into three blocks until the shift/error was less than 1.0 for all parameters except those of $[Cu(py \cdot tren)](BF_4)_2$. The intensity data collected for $[Cu(py \cdot tren)](BF_4)_2$ contained some reflections with an almost completely resolved component at a slightly larger value of $2\theta$. There is also a space group ambiguity. Reflections systematically absent in $P2_1/n$ sometimes had measurable intensity if their $2\theta$ setting angle was $< 20°$. The possibility of disorder of the $BF_4^-$ ions was not investigated. Nevertheless the general features of the cation of $[Cu(py \cdot tren)](BF_4)_2$ are clear and the inclusion of these structural results seems warranted. For all other complexes in this series, the refinements converged and there was no evidence of secondary extinction in the data of these compound. Final three-dimensional difference Fourier syntheses revealed no unusual peaks. Analysis of the $R$ factor for various classes of reflections based upon $|F_o|$, Miller indices, and $(\sin \theta)/\lambda$ show no unexpected trends. Final atomic parameters for $[MnL](BF_4)_2$, $[FeL](BF_4)_2$, $[CoL](BF_4)_2$, $[NiL](BF_4)_2$, $[NiL](PF_6)_2$, $[CuL](BF_4)_2$, $[ZnL](BF_4)_2$ and $[Cu(py \cdot tren)](BF_4)_2$ are listed in Tables

9–16, respectively. The anisotropic thermal parameters are of the form $\exp(-\frac{1}{4}\sum_{i=1}^{3}\sum_{j=1}^{3}B_{ij}h_ih_ja_i^*a_j^*)$, while the isotropic thermal parameters are of the form $\exp(-B(\sin^2\theta)/\lambda^2)$. The values of the estimated standard deviations have been corrected for the fact that not all variables were refined simultaneously. Final values of the observed and calculated structure factors for each compound are available [105].

*(iv) Assessment of accuracy of the structures: half normal probability plots*

A comparison of bond lengths of the $[ML]^{2+}$ salts shows large differences in metal–nitrogen bond distances between different metals (see Table 1). $[CuL](BF_4)_2$, in particular, shows large differences in metal–nitrogen distances between different arms. All complexes show some deviations from 3-fold symmetry in the angles $Q$ between corresponding atoms in different arms in projection on the plane normal to the M–N(7) axis. In particular, the isomorphous set, M(II) = Mn, Co, Ni, Cu, and Zn, show a different (and consistent) deviation from $[FeL](BF_4)_2$ and $[NiL](PF_6)_2$ (see Table 17). Therefore we might expect that the bond lengths would be more nearly identical among the set $[MnL](BF_4)_2$, $[CoL](BF_4)_2$, $[NiL](BF_4)_2$, and $[ZnL](BF_4)_2$, with larger deviations for $[FeL](BF_4)_2$, $[CuL](BF_4)_2$, and $[NiL](PF_6)_2$.

Abrahams has pointed out the usefulness of the half normal probability plot for comparison of independent sets of measured (or calculated) quantities [106]. For the case of two sets one calculates for each quantity, $q_i$, (for example a particular bond distance, $d_i$) the difference between the two measurements divided by the calculated standard deviation of the difference

$$x_i = |q_{i1} - q_{i2}|/\left(\sigma_{i1}^2 + \sigma_{i2}^2\right)^{1/2}$$

The $x_i$ values are then ranked according to their magnitudes and plotted against the expected values derived from the normal distribution.

If the two sets are identical and the estimated standard deviations, $\sigma_{ik}$, are valid estimates, the points will fall on a straight line passing through the origin and the slope of the line will be 1. If the two sets are not identical or if the $\sigma$ values have been under-estimated the line will have a slope greater than 1. If the $\sigma$ values have been over-estimated the slope will be less than 1.

For the case of more than two sets, we may use

$$x_i = |q_{ik} - \bar{q}_i|/\left(\sigma_{ik}^2 + \sigma_{i\text{mean}}^2\right)^{1/2}$$

The intra-ligand bond lengths in the $[ML]^{2+}$ series have been examined by half normal probability plots. The result for all complexes analyzing all bonds is that the slope is 1.43. This large slope suggests that either the

TABLE 9

Final atomic parameters for [Mn(py$_3$tren)](BF$_4$)$_2$, tris(4-(2-pyridyl)-3-aza-3-butenyl)amine manganese(II) tetrafluoroborate

| Atom | $x/a$ | $y/b$ | $z/c$ | $B_{11}$ | $B_{22}$ | $B_{33}$ | $B_{12}$ | $B_{13}$ | $B_{23}$ |
|---|---|---|---|---|---|---|---|---|---|
| *Positional parameters ($\times 10^5$) and thermal parameters ($\times 10^2$)* | | | | | | | | | |
| Mn | 13391 (1) | 17280 (4) | 23034 (2) | 360 (2) | 395 (2) | 431 (2) | 22 (2) | 110 (2) | 6 (2) |
| N(11) | 11063 (8) | 36360 (21) | 20062 (11) | 534 (14) | 431 (15) | 542 (14) | 9 (11) | 147 (11) | 27 (11) |
| N(12) | 10886 (8) | 26470 (22) | 32789 (11) | 454 (13) | 513 (15) | 474 (13) | −21 (11) | 126 (11) | −61 (11) |
| N(21) | 17659 (7) | 10146 (22) | 15449 (11) | 454 (13) | 596 (16) | 463 (13) | 80 (12) | 120 (11) | 23 (12) |
| N(22) | 21361 (7) | 21048 (21) | 27717 (11) | 429 (12) | 485 (15) | 512 (13) | −44 (11) | 96 (10) | −27 (11) |
| N(31) | 6520 (8) | 6862 (24) | 20425 (12) | 397 (13) | 446 (15) | 414 (13) | 38 (12) | 56 (11) | 63 (12) |
| N(32) | 14326 (8) | −1084 (22) | 29664 (11) | 370 (13) | 443 (14) | 392 (13) | 10 (12) | 8 (11) | 21 (11) |
| N(7) | 8670 (8) | 19768 (23) | 8903 (11) | 526 (14) | 480 (15) | 468 (13) | 68 (12) | 106 (11) | 87 (12) |
| C(11) | 7426 (16) | 32953 (41) | 7836 (22) | 687 (25) | 588 (24) | 579 (24) | 89 (23) | 55 (20) | 232 (21) |
| C(12) | 10956 (16) | 40948 (39) | 12873 (23) | 656 (25) | 458 (23) | 708 (26) | −3 (20) | 172 (21) | 116 (20) |
| C(13) | 9035 (12) | 42598 (35) | 24282 (23) | 503 (20) | 407 (21) | 738 (26) | 30 (17) | 110 (18) | −14 (20) |
| C(14) | 8802 (11) | 37663 (35) | 31259 (20) | 398 (17) | 498 (21) | 632 (22) | −60 (15) | 162 (16) | −164 (18) |
| C(15) | 6468 (13) | 44120 (41) | 35922 (28) | 494 (21) | 590 (28) | 926 (31) | −84 (20) | 248 (22) | −274 (25) |
| C(16) | 6432 (16) | 38987 (53) | 42463 (28) | 596 (25) | 919 (35) | 804 (32) | −266 (24) | 330 (24) | −461 (31) |
| C(17) | 8613 (16) | 27800 (53) | 44178 (24) | 662 (25) | 936 (33) | 524 (27) | −192 (23) | 198 (21) | −226 (26) |
| C(18) | 10790 (13) | 21913 (40) | 39157 (22) | 573 (21) | 698 (27) | 481 (21) | −49 (19) | 152 (17) | −121 (20) |
| C(21) | 12187 (16) | 15767 (44) | 4646 (20) | 707 (25) | 729 (28) | 416 (20) | 4 (23) | 151 (18) | 22 (21) |
| C(22) | 15360 (16) | 5428 (43) | 8383 (21) | 649 (25) | 745 (28) | 495 (22) | 154 (22) | 201 (19) | −83 (20) |
| C(23) | 22220 (15) | 10769 (37) | 17156 (21) | 581 (23) | 670 (23) | 573 (23) | 106 (20) | 269 (20) | −2 (18) |
| C(24) | 24485 (11) | 16055 (32) | 23987 (19) | 360 (17) | 543 (20) | 648 (21) | 23 (16) | 150 (16) | 118 (18) |
| C(25) | 29474 (15) | 16119 (45) | 26548 (27) | 457 (23) | 831 (30) | 936 (31) | 108 (22) | 185 (23) | 177 (26) |
| C(26) | 31335 (17) | 21112 (45) | 33087 (29) | 443 (25) | 814 (32) | 1059 (37) | −31 (23) | −62 (25) | 212 (27) |
| C(27) | 28203 (17) | 26157 (40) | 36910 (25) | 584 (26) | 656 (26) | 807 (31) | −100 (21) | −62 (23) | 91 (22) |
| C(28) | 23249 (15) | 25955 (34) | 34006 (23) | 489 (22) | 480 (21) | 753 (27) | 47 (17) | 99 (20) | 35 (19) |
| C(31) | 4389 (14) | 11691 (39) | 7997 (20) | 546 (22) | 634 (25) | 448 (20) | −1 (19) | −36 (17) | 76 (18) |
| C(32) | 2473 (12) | 10955 (38) | 14820 (20) | 398 (18) | 579 (23) | 510 (20) | −16 (17) | −12 (16) | 96 (18) |
| C(33) | 6266 (11) | −3658 (33) | 23179 (16) | 312 (16) | 538 (21) | 402 (17) | −24 (16) | 93 (13) | −15 (16) |

| | | | | | | | | | |
|---|---|---|---|---|---|---|---|---|---|
| C(34) | 10362 (11) | −8351 (29) | 28463 (15) | 427 (17) | 427 (18) | 310 (15) | 11 (15) | 115 (13) | 20 (13) |
| C(35) | 10000 (14) | −19405 (33) | 31952 (17) | 516 (20) | 509 (22) | 397 (17) | −57 (18) | 96 (15) | 51 (16) |
| C(36) | 13909 (16) | −23324 (35) | 36992 (19) | 784 (26) | 486 (22) | 421 (20) | −15 (20) | 146 (18) | 116 (17) |
| C(37) | 18004 (14) | −16101 (37) | 38322 (17) | 591 (21) | 542 (22) | 403 (18) | 77 (19) | −26 (16) | 77 (17) |
| C(38) | 18091 (12) | −5128 (33) | 34566 (18) | 519 (20) | 466 (21) | 467 (19) | −43 (17) | 18 (16) | 17 (16) |
| B(1) | 29198 (36) | 317 (89) | 1240 (47) | 828 (58) | 719 (56) | 670 (57) | −22 (47) | 241 (39) | −105 (39) |
| B(2) | 47537 (17) | 21782 (44) | 38794 (22) | 554 (25) | 591 (27) | 405 (22) | −43 (21) | −13 (19) | 47 (20) |
| F(11) | 30963 (12) | 117 (32) | 8524 (21) | 1019 (24) | 1083 (27) | 798 (28) | −159 (19) | 147 (18) | −28 (20) |
| F(12) | 24840 (17) | −5491 (40) | −477 (18) | 892 (31) | 1312 (34) | 1110 (25) | −255 (23) | 137 (19) | 22 (21) |
| F(13) | 29398 (71) | 12118 (160) | −1493 (124) | 870 (115) | 671 (94) | 814 (128) | −190 (68) | 83 (75) | 143 (67) |
| F(14) | 32574 (73) | −6158 (385) | −1916 (125) | 758 (96) | 1152 (251) | 758 (116) | 324 (93) | 247 (64) | −277 (98) |
| F(15) | 30776 (125) | −11844 (211) | 1476 (158) | 1537 (136) | 1168 (120) | 1057 (103) | 293 (89) | 364 (108) | 133 (88) |
| F(16) | 26814 (73) | 10995 (168) | 2336 (112) | 1107 (82) | 1146 (80) | 1107 (87) | 252 (64) | 15 (70) | −382 (64) |
| F(17) | 33372 (114) | 3362 (586) | −288 (235) | 1174 (144) | 1588 (257) | 1594 (170) | 14 (141) | 823 (126) | −32 (187) |
| F(18) | 29263 (115) | 3293 (437) | −5521 (178) | 1171 (150) | 2393 (228) | 1239 (143) | −344 (142) | 544 (111) | −64 (166) |
| F(21) | 48381 (7) | 12016 (20) | 43324 (10) | 1082 (15) | 800 (14) | 691 (12) | 139 (12) | 99 (11) | 246 (11) |
| F(22) | 47646 (8) | 18110 (21) | 32055 (9) | 1794 (21) | 826 (14) | 464 (11) | 70 (15) | 113 (12) | −86 (11) |
| F(23) | 43260 (8) | 27102 (23) | 39039 (12) | 699 (13) | 1429 (21) | 1432 (19) | 378 (14) | 476 (13) | 650 (16) |
| F(24) | 51004 (7) | 30549 (23) | 40433 (10) | 839 (14) | 1131 (17) | 960 (15) | −378 (14) | 40 (11) | −80 (14) |

*Positional parameters ($\times 10^4$) and thermal parameters ($\times 10$)*

| | | | | |
|---|---|---|---|---|
| H(11) | 744 (11) | 3522 (29) | 284 (15) | 82 (10) |
| H(12) | 408 (10) | 3424 (28) | 897 (14) | 67 (9) |
| H(13) | 1447 (10) | 4005 (26) | 1204 (14) | 67 (9) |
| H(14) | 1020 (11) | 5007 (29) | 1282 (15) | 80 (10) |
| H(15) | 764 (10) | 5076 (27) | 2269 (14) | 66 (9) |
| H(16) | 497 (11) | 5220 (29) | 3410 (16) | 80 (12) |
| H(17) | 491 (11) | 4377 (30) | 4583 (17) | 97 (12) |
| H(18) | 878 (11) | 2420 (30) | 4890 (16) | 85 (12) |
| H(19) | 1223 (11) | 1343 (28) | 4010 (16) | 78 (11) |
| H(21) | 1058 (9) | 1246 (25) | −17 (14) | 63 (9) |
| H(22) | 1424 (10) | 2308 (26) | 392 (14) | 70 (10) |
| H(23) | 1339 (11) | −292 (29) | 954 (16) | 92 (11) |

TABLE 9 (continued)

| Atom | $x/a$ | $y/b$ | $z/c$ | $B$ |
|---|---|---|---|---|
| *Positional parameters ($\times 10^4$) and thermal parameters ($\times 10$)* | | | | |
| H(24) | 1791 (9) | 369 (26) | 593 (14) | 60 (9) |
| H(25) | 2409 (10) | 755 (27) | 1410 (14) | 67 (9) |
| H(26) | 3141 (10) | 1177 (27) | 2370 (14) | 64 (10) |
| H(27) | 3489 (13) | 2081 (34) | 3483 (18) | 114 (13) |
| H(28) | 2931 (12) | 2989 (33) | 4215 (16) | 111 (13) |
| H(29) | 2096 (10) | 2953 (29) | 3648 (15) | 74 (10) |
| H(31) | 180 (9) | 1426 (24) | 398 (13) | 60 (8) |
| H(32) | 537 (10) | 286 (28) | 619 (15) | 86 (11) |
| H(33) | 149 (10) | 2025 (27) | 1677 (14) | 81 (10) |
| H(34) | −19 (8) | 502 (22) | 1427 (12) | 43 (7) |
| H(35) | 334 (8) | −903 (21) | 2191 (11) | 40 (7) |
| H(36) | 684 (9) | −2398 (26) | 3056 (13) | 60 (8) |
| H(37) | 1367 (10) | −3099 (28) | 3968 (14) | 75 (9) |
| H(38) | 2098 (9) | −1859 (26) | 4187 (13) | 67 (8) |
| H(39) | 2109 (9) | 85 (26) | 3510 (13) | 65 (8) |

The population parameters and their estimated standard deviations for the atoms in the $BF_4$ disorder models are:

| | | | |
|---|---|---|---|
| F(11) | 0.863 (7) | F(15) | 0.339 (29) |
| F(12) | 0.896 (9) | F(16) | 0.357 (42) |
| F(13) | 0.374 (38) | F(17) | 0.483 (26) |
| F(14) | 0.357 (53) | F(18) | 0.371 (31) |

Anisotropic thermal parameters are of the form

$$\exp\left(-\tfrac{1}{4}\sum_{i=1}^{3}\sum_{j=1}^{3}B_{ij}h_ih_ja_i^*a_j^*\right)$$

Isotropic thermal parameters are of the form

$$\exp(-B(\sin^2\theta)/\lambda^2)$$

Estimated standard deviations are given in parentheses.

TABLE 10

Final atomic parameters for [Fe(py$_3$tren)](BF$_4$)$_2$, tris(4-(2-pyridyl)-3-aza-3-butenyl)amineiron(II) tetrafluoroborate

| Atom | $x/a$ | $y/b$ | $z/c$ | $B_{11}$ | $B_{22}$ | $B_{33}$ | $B_{12}$ | $B_{13}$ | $B_{23}$ |
|---|---|---|---|---|---|---|---|---|---|
| *Positional parameters ($\times 10^5$) and thermal parameters ($\times 10^2$)* | | | | | | | | | |
| Fe | 20850 (5) | 10836 (3) | 20062 (3) | 397 (2) | 342 (2) | 413 (2) | −15 (2) | 94 (2) | −35 (2) |
| N(11) | 22694 (32) | 22865 (21) | 23037 (19) | 495 (18) | 377 (17) | 535 (19) | −31 (14) | 107 (15) | −80 (14) |
| N(12) | 35070 (27) | 9599 (21) | 28361 (17) | 350 (15) | 473 (18) | 433 (16) | −5 (14) | 86 (12) | −51 (14) |
| N(21) | 5786 (29) | 12525 (19) | 12683 (19) | 449 (17) | 393 (17) | 491 (18) | 32 (13) | 39 (14) | −27 (13) |
| N(22) | 7852 (27) | 9689 (19) | 27292 (17) | 422 (16) | 364 (16) | 483 (16) | −40 (13) | 117 (13) | −66 (13) |
| N(31) | 32918 (27) | 11057 (21) | 12376 (17) | 489 (16) | 331 (15) | 456 (15) | −42 (14) | 150 (12) | −17 (14) |
| N(32) | 20458 (27) | −1430 (19) | 17199 (17) | 399 (15) | 330 (14) | 361 (15) | −9 (12) | 58 (12) | 6 (11) |
| N(7) | 19759 (38) | 26808 (23) | 6168 (21) | 908 (26) | 453 (20) | 732 (23) | 80 (18) | 320 (20) | 20 (17) |
| C(11) | 19390 (70) | 33270 (34) | 12149 (36) | 969 (43) | 398 (27) | 847 (37) | 71 (28) | 228 (32) | 34 (25) |
| C(12) | 14939 (55) | 30109 (32) | 19816 (32) | 725 (32) | 372 (23) | 687 (30) | 39 (22) | 200 (25) | −77 (22) |
| C(13) | 31345 (46) | 24380 (32) | 28667 (30) | 560 (27) | 423 (24) | 665 (29) | −84 (21) | 207 (22) | −168 (22) |
| C(14) | 38658 (38) | 17189 (32) | 31852 (25) | 397 (21) | 602 (26) | 493 (23) | −95 (19) | 120 (18) | −176 (20) |
| C(15) | 48117 (48) | 17471 (44) | 38166 (32) | 487 (27) | 872 (39) | 622 (31) | −126 (27) | 102 (23) | −272 (29) |
| C(16) | 53882 (48) | 10180 (55) | 40847 (32) | 435 (26) | 1308 (55) | 536 (29) | 12 (33) | −30 (22) | −170 (36) |
| C(17) | 50436 (48) | 2492 (46) | 37244 (32) | 522 (28) | 869 (40) | 615 (31) | 122 (27) | −26 (23) | −22 (29) |
| C(18) | 41073 (42) | 2464 (34) | 30974 (25) | 461 (23) | 612 (29) | 485 (25) | 42 (21) | 5 (19) | −56 (22) |
| C(21) | 8217 (65) | 23253 (36) | 2352 (38) | 948 (41) | 560 (31) | 643 (34) | 108 (29) | 112 (30) | 144 (25) |
| C(22) | 5629 (57) | 13898 (31) | 4246 (29) | 699 (31) | 540 (27) | 505 (27) | 71 (23) | −38 (23) | 58 (20) |
| C(23) | −4784 (46) | 11933 (29) | 15564 (31) | 402 (23) | 479 (23) | 725 (30) | 60 (20) | −40 (22) | −90 (21) |
| C(24) | −4203 (38) | 10603 (25) | 23812 (25) | 373 (20) | 428 (20) | 628 (25) | −30 (17) | 115 (18) | −117 (19) |
| C(25) | −14603 (57) | 10080 (36) | 28095 (48) | 457 (28) | 552 (27) | 1049 (46) | −80 (24) | 197 (32) | −168 (30) |
| C(26) | −12707 (63) | 8714 (31) | 35931 (44) | 721 (36) | 566 (29) | 934 (42) | 103 (25) | 457 (34) | 127 (26) |
| C(27) | −752 (65) | 7860 (31) | 39406 (36) | 861 (37) | 537 (27) | 624 (32) | −104 (24) | 367 (29) | −44 (23) |
| C(28) | 9362 (38) | 8375 (25) | 35029 (23) | 581 (22) | 484 (23) | 509 (21) | −36 (17) | 180 (17) | −47 (17) |
| C(31) | 31788 (61) | 24009 (36) | 4077 (36) | 1089 (44) | 429 (27) | 731 (35) | −81 (28) | 436 (32) | 95 (25) |
| C(32) | 39966 (51) | 18628 (32) | 9986 (34) | 662 (30) | 419 (24) | 692 (32) | −125 (22) | 304 (26) | −59 (23) |
| C(33) | 35243 (40) | 3804 (27) | 9371 (25) | 479 (22) | 438 (22) | 442 (22) | −4 (18) | 178 (18) | −9 (17) |
| C(34) | 28012 (34) | −3525 (23) | 11624 (21) | 404 (18) | 360 (19) | 341 (18) | 33 (15) | 64 (15) | −13 (15) |

TABLE 10 (continued)

| Atom | $x/a$ | $y/b$ | $z/c$ | $B_{11}$ | $B_{22}$ | $B_{33}$ | $B_{12}$ | $B_{13}$ | $B_{23}$ |
|---|---|---|---|---|---|---|---|---|---|
| *Positional parameters ($\times 10^5$) and thermal parameters ($\times 10^2$)* | | | | | | | | | |
| C(35) | 28651 (40) | −11710 (27) | 8676 (23) | 560 (23) | 394 (21) | 446 (21) | 38 (18) | 139 (18) | −43 (18) |
| C(36) | 21371 (42) | −18051 (27) | 11424 (25) | 677 (27) | 296 (21) | 537 (25) | 10 (19) | 101 (20) | −33 (18) |
| C(37) | 13723 (46) | −16073 (27) | 17027 (25) | 672 (27) | 357 (23) | 552 (25) | −109 (20) | 162 (20) | 1 (18) |
| C(38) | 13426 (40) | −7809 (27) | 19750 (23) | 554 (23) | 411 (21) | 422 (21) | −38 (17) | 178 (18) | −26 (17) |
| B(1) | 24990 (99) | 83120 (73) | 40855 (54) | 926 (57) | 844 (57) | 674 (45) | −466 (49) | −113 (43) | 231 (49) |
| B(2) | 32204 (61) | 46240 (38) | 37566 (36) | 656 (35) | 485 (30) | 590 (33) | 27 (26) | 56 (27) | −78 (25) |
| F(11) | 27814 (75) | 77045 (44) | 46045 (42) | 2053 (68) | 1090 (40) | 818 (38) | 80 (36) | 103 (36) | 474 (31) |
| F(12) | 36122 (46) | 84382 (42) | 38231 (34) | 1097 (32) | 1326 (38) | 1934 (44) | −284 (31) | 365 (32) | 325 (32) |
| F(13) | 22027 (126) | 90349 (82) | 44337 (67) | 1395 (76) | 949 (63) | 1300 (70) | 326 (60) | −106 (63) | 111 (67) |
| F(14) | 15523 (237) | 80126 (245) | 34931 (105) | 871 (95) | 1719 (229) | 458 (55) | −686 (123) | −352 (63) | 371 (90) |
| F(15) | 19570 (254) | 78516 (174) | 35970 (126) | 1855 (194) | 1404 (138) | 1331 (135) | −542 (115) | 906 (92) | −153 (97) |
| F(16) | 20233 (226) | 82518 (226) | 47866 (94) | 1693 (176) | 2721 (294) | 595 (76) | −912 (172) | 367 (91) | 176 (127) |
| F(17) | 13869 (337) | 86357 (176) | 36654 (174) | 1724 (204) | 1816 (213) | 1558 (195) | −300 (183) | −607 (146) | 742 (161) |
| F(18) | 25241 (457) | 91916 (237) | 40852 (285) | 2139 (272) | 1863 (252) | 3292 (433) | −536 (186) | −405 (251) | 2020 (288) |
| F(21) | 40587 (25) | 40617 (17) | 41491 (15) | 819 (16) | 595 (15) | 758 (15) | 145 (13) | 13 (13) | 21 (12) |
| F(22) | 35250 (34) | 46606 (21) | 30021 (19) | 1453 (26) | 994 (22) | 749 (19) | 119 (18) | 285 (18) | 147 (16) |
| F(23) | 20286 (27) | 43385 (21) | 37259 (21) | 613 (16) | 977 (21) | 1453 (27) | −92 (15) | 117 (16) | −112 (18) |
| F(24) | 33451 (27) | 54157 (17) | 40820 (19) | 941 (19) | 569 (16) | 1186 (22) | 169 (13) | 191 (16) | −322 (15) |
| *Positional parameters ($\times 10^3$) and thermal parameters ($\times 10$)* | | | | | | | | | |
| H(11) | 134 (4) | 380 (3) | 100 (2) | 82 (13) | | | | | |
| H(12) | 278 (4) | 358 (3) | 136 (2) | 70 (14) | | | | | |
| H(13) | 61 (4) | 280 (2) | 189 (2) | 64 (12) | | | | | |
| H(14) | 152 (3) | 351 (2) | 234 (2) | 55 (10) | | | | | |

| | | | | |
|---|---|---|---|---|
| H(15) | 326 (4) | 301 (3) | 303 (2) | 76 (12) |
| H(16) | 499 (4) | 236 (3) | 400 (2) | 66 (12) |
| H(17) | 597 (4) | 98 (2) | 451 (2) | 55 (10) |
| H(18) | 540 (4) | −29 (3) | 388 (2) | 66 (13) |
| H(19) | 380 (3) | −30 (2) | 285 (2) | 48 (10) |
| H(21) | 87 (4) | 235 (3) | −36 (3) | 85 (14) |
| H(22) | 3 (4) | 272 (3) | 35 (3) | 94 (14) |
| H(23) | 123 (4) | 98 (2) | 19 (2) | 66 (11) |
| H(24) | −26 (4) | 123 (2) | 16 (2) | 63 (11) |
| H(25) | −123 (4) | 127 (2) | 125 (2) | 62 (12) |
| H(26) | −208 (4) | 100 (3) | 258 (3) | 73 (18) |
| H(27) | −203 (4) | 83 (3) | 390 (3) | 88 (13) |
| H(28) | 14 (3) | 68 (2) | 446 (2) | 54 (11) |
| H(29) | 174 (3) | 75 (2) | 368 (2) | 52 (8) |
| H(31) | 366 (4) | 289 (3) | 28 (2) | 78 (13) |
| H(32) | 306 (4) | 211 (3) | −10 (2) | 69 (13) |
| H(33) | 427 (3) | 218 (2) | 142 (2) | 49 (11) |
| H(34) | 483 (3) | 169 (2) | 81 (2) | 61 (10) |
| H(35) | 409 (3) | 31 (2) | 58 (2) | 43 (9) |
| H(36) | 339 (3) | −129 (2) | 48 (2) | 37 (8) |
| H(37) | 212 (3) | −235 (2) | 94 (2) | 42 (9) |
| H(38) | 84 (3) | −201 (2) | 188 (2) | 61 (11) |
| H(39) | 86 (3) | −63 (2) | 235 (2) | 36 (8) |

The population parameters and their estimated standard deviations for the atoms in the $BF_4$ disorder models are:

| | | | |
|---|---|---|---|
| F(11) | 0.801 (9) | F(15) | 0.410 (17) |
| F(12) | 0.913 (6) | F(16) | 0.310 (9) |
| F(13) | 0.641 (11) | F(17) | 0.345 (16) |
| F(14) | 0.367 (16) | F(18) | 0.309 (17) |

TABLE 11

Final atomic parameters for $[Co(py_3tren)](BF_4)_2$, tris(4-(2-pyridyl)-3-aza-3-butenyl)amine cobalt(II) tetrafluoroborate

| Atom | $x/a$ | $y/b$ | $z/c$ | $B_{11}$ | $B_{22}$ | $B_{33}$ | $B_{12}$ | $B_{13}$ | $B_{23}$ |
|---|---|---|---|---|---|---|---|---|---|
| *Positional parameters ($\times 10^5$) and thermal parameters ($\times 10^2$)* | | | | | | | | | |
| Co | 13338 (1) | 16808 (4) | 23120 (2) | 372 (2) | 387 (2) | 426 (2) | 18 (2) | 128 (2) | 9 (2) |
| N(11) | 11447 (8) | 35246 (25) | 20020 (12) | 500 (15) | 416 (15) | 460 (15) | 13 (12) | 137 (11) | 43 (13) |
| N(12) | 10780 (8) | 25088 (25) | 32485 (12) | 425 (14) | 452 (17) | 401 (15) | −39 (12) | 124 (11) | −46 (13) |
| N(21) | 17171 (8) | 9541 (25) | 15612 (12) | 396 (14) | 485 (15) | 411 (15) | 53 (13) | 110 (12) | 26 (12) |
| N(22) | 20803 (8) | 21483 (25) | 27552 (17) | 424 (15) | 423 (16) | 451 (15) | −41 (12) | 118 (12) | −24 (12) |
| N(31) | 6648 (8) | 7606 (25) | 20440 (12) | 351 (13) | 420 (15) | 347 (13) | 46 (12) | 65 (10) | 57 (11) |
| N(32) | 14510 (8) | −1126 (21) | 29139 (12) | 323 (13) | 399 (14) | 332 (13) | 19 (12) | 10 (11) | −1 (11) |
| N(7) | 8509 (8) | 19788 (25) | 8433 (12) | 497 (14) | 438 (15) | 439 (13) | 88 (12) | 124 (11) | 83 (11) |
| C(11) | 7826 (17) | 33287 (41) | 7485 (21) | 686 (26) | 538 (23) | 514 (23) | 90 (23) | 86 (20) | 194 (21) |
| C(12) | 11579 (17) | 40194 (41) | 12876 (25) | 646 (28) | 462 (24) | 636 (26) | 9 (21) | 179 (22) | 141 (20) |
| C(13) | 9441 (12) | 41793 (37) | 24232 (21) | 481 (20) | 379 (21) | 679 (25) | 31 (17) | 133 (18) | 38 (19) |
| C(14) | 8948 (12) | 36708 (33) | 31147 (21) | 389 (18) | 440 (21) | 557 (21) | −46 (15) | 174 (15) | −120 (17) |
| C(15) | 6763 (12) | 43264 (41) | 36001 (29) | 496 (22) | 504 (26) | 845 (30) | −42 (20) | 226 (21) | −233 (24) |
| C(16) | 6609 (17) | 37810 (54) | 42541 (29) | 606 (26) | 814 (34) | 722 (30) | −262 (23) | 346 (23) | −430 (28) |
| C(17) | 8572 (17) | 26385 (50) | 44061 (25) | 573 (24) | 820 (30) | 469 (25) | −171 (22) | 180 (19) | −219 (25) |
| C(18) | 10616 (12) | 20293 (37) | 38892 (21) | 469 (20) | 602 (27) | 430 (20) | −32 (18) | 108 (16) | −65 (19) |
| C(21) | 11921 (17) | 14475 (42) | 4375 (21) | 648 (25) | 673 (28) | 363 (20) | 1 (22) | 137 (18) | 20 (20) |
| C(22) | 14882 (17) | 4248 (42) | 8631 (21) | 563 (24) | 588 (25) | 453 (21) | 116 (21) | 148 (19) | −73 (19) |
| C(23) | 21751 (17) | 10479 (33) | 17173 (21) | 514 (22) | 542 (22) | 516 (22) | 55 (19) | 240 (20) | 21 (17) |
| C(24) | 24017 (12) | 16245 (33) | 23956 (17) | 367 (18) | 465 (18) | 549 (20) | −10 (17) | 133 (16) | 86 (18) |
| C(25) | 28970 (17) | 16278 (42) | 26650 (25) | 419 (22) | 646 (25) | 792 (28) | 73 (22) | 147 (22) | 130 (24) |
| C(26) | 30804 (17) | 21484 (42) | 33170 (29) | 420 (25) | 624 (28) | 947 (34) | −95 (20) | −102 (25) | 124 (23) |
| C(27) | 27561 (17) | 26695 (37) | 36917 (25) | 545 (26) | 542 (24) | 706 (30) | −117 (20) | −7 (23) | 39 (21) |
| C(28) | 22672 (12) | 26578 (33) | 33887 (25) | 408 (22) | 421 (20) | 738 (26) | −40 (17) | 153 (20) | 29 (18) |
| C(31) | 4059 (17) | 12550 (41) | 7912 (21) | 503 (22) | 591 (26) | 418 (20) | 49 (19) | −25 (17) | 57 (18) |
| C(32) | 2520 (12) | 12255 (41) | 15150 (21) | 380 (20) | 553 (24) | 461 (20) | 30 (18) | 51 (16) | 60 (17) |
| C(33) | 6342 (12) | −3104 (33) | 23133 (17) | 275 (17) | 485 (21) | 362 (17) | 14 (16) | 90 (14) | −13 (15) |
| C(34) | 10453 (12) | −8154 (29) | 28186 (17) | 405 (17) | 372 (17) | 272 (15) | 12 (15) | 124 (13) | −9 (13) |

| | | | | | | | | | |
|---|---|---|---|---|---|---|---|---|---|
| C(35) | 10135 (12) | −19230 (33) | 31851 (17) | 451 (20) | 459 (22) | 405 (18) | −62 (18) | 98 (16) | 14 (16) |
| C(36) | 14101 (17) | −23221 (37) | 36830 (21) | 739 (27) | 436 (22) | 381 (20) | −18 (20) | 155 (19) | 96 (16) |
| C(37) | 18215 (12) | −16212 (41) | 37870 (17) | 527 (22) | 513 (22) | 381 (18) | 81 (20) | −24 (16) | 53 (18) |
| C(38) | 18313 (12) | −5233 (33) | 33932 (17) | 452 (20) | 394 (20) | 439 (19) | −40 (16) | 31 (16) | 8 (15) |
| B(1) | 29006 (29) | 466 (75) | 1227 (37) | 777 (46) | 601 (43) | 746 (46) | −29 (36) | 274 (34) | −128 (34) |
| B(2) | 47370 (17) | 21226 (46) | 38524 (25) | 599 (28) | 578 (30) | 356 (23) | −37 (23) | 8 (20) | 44 (21) |
| F(11) | 30707 (12) | 1079 (29) | 8599 (17) | 1044 (21) | 943 (21) | 656 (18) | −285 (17) | 142 (15) | −21 (16) |
| F(12) | 24538 (8) | −4632 (29) | −552 (17) | 747 (18) | 1238 (24) | 1039 (19) | −215 (18) | 51 (15) | 171 (17) |
| F(13) | 29441 (29) | 12123 (58) | −1700 (41) | 854 (45) | 837 (39) | 803 (41) | −194 (31) | 155 (31) | 221 (30) |
| F(14) | 32479 (41) | −6424 (149) | −1796 (58) | 719 (52) | 1105 (86) | 775 (58) | 307 (55) | 270 (43) | −308 (54) |
| F(15) | 31008 (54) | −11135 (128) | 1371 (66) | 1401 (89) | 1353 (96) | 1224 (80) | 336 (63) | 385 (54) | 11 (60) |
| F(16) | 33033 (70) | 4007 (306) | −7 (120) | 1317 (124) | 1893 (184) | 1766 (172) | −127 (154) | 1050 (126) | −475 (157) |
| F(17) | 26451 (37) | 9939 (120) | 3099 (58) | 1417 (78) | 1428 (82) | 1104 (71) | 141 (73) | 261 (63) | −571 (62) |
| F(18) | 29029 (54) | 3660 (282) | −5780 (58) | 847 (86) | 2355 (162) | 835 (79) | −100 (105) | 464 (66) | −42 (104) |
| F(21) | 48368 (8) | 11682 (21) | 43217 (12) | 1198 (17) | 808 (15) | 695 (13) | 216 (13) | 155 (12) | 283 (11) |
| F(22) | 47582 (8) | 17692 (25) | 31848 (12) | 1862 (23) | 983 (17) | 461 (11) | 177 (17) | 191 (13) | −103 (12) |
| F(23) | 43105 (8) | 26306 (25) | 38722 (12) | 789 (15) | 1651 (24) | 1547 (21) | 549 (16) | 630 (15) | 822 (18) |
| F(24) | 50718 (8) | 30435 (25) | 40107 (12) | 1037 (17) | 1198 (20) | 1013 (17) | −421 (16) | −6 (13) | 7 (15) |

*Positional parameters ($\times 10^3$) and thermal parameters ($\times 10$)*

| | | | | |
|---|---|---|---|---|
| H(11) | 80 (1) | 361 (3) | 24 (1) | 79 (9) |
| H(12) | 45 (1) | 358 (3) | 84 (1) | 62 (9) |
| H(13) | 148 (1) | 384 (3) | 123 (1) | 47 (9) |
| H(14) | 110 (1) | 497 (3) | 128 (2) | 87 (10) |
| H(15) | 81 (1) | 497 (3) | 225 (1) | 45 (8) |
| H(16) | 54 (1) | 512 (3) | 343 (1) | 49 (9) |
| H(17) | 51 (1) | 424 (3) | 459 (2) | 80 (10) |
| H(18) | 87 (1) | 227 (3) | 490 (2) | 78 (10) |
| H(19) | 122 (1) | 121 (3) | 399 (1) | 59 (9) |
| H(21) | 102 (1) | 113 (2) | −3 (1) | 44 (8) |
| H(22) | 141 (1) | 210 (3) | 34 (2) | 72 (10) |
| H(23) | 126 (1) | −36 (3) | 96 (1) | 62 (9) |
| H(24) | 175 (1) | 14 (3) | 64 (1) | 53 (8) |

TABLE 11 (continued)

| Atom | *x/a* | *y/b* | *z/c* | *B* |
|---|---|---|---|---|
| *Positional parameters ($\times 10^3$) and thermal parameters ($\times 10$)* | | | | |
| H(25) | 236 (1) | 74 (3) | 143 (1) | 64 (10) |
| H(26) | 309 (1) | 123 (3) | 239 (1) | 48 (9) |
| H(27) | 343 (1) | 215 (3) | 355 (1) | 67 (9) |
| H(28) | 286 (1) | 304 (3) | 417 (1) | 70 (10) |
| H(29) | 203 (1) | 298 (3) | 362 (1) | 42 (9) |
| H(31) | 15 (1) | 158 (3) | 44 (1) | 47 (8) |
| H(32) | 48 (1) | 35 (3) | 64 (1) | 65 (9) |
| H(33) | 15 (1) | 212 (3) | 169 (1) | 59 (8) |
| H(34) | −1 (1) | 67 (2) | 149 (1) | 41 (8) |
| H(35) | 35 (1) | −77 (2) | 218 (1) | 32 (7) |
| H(36) | 72 (1) | −233 (2) | 306 (1) | 31 (7) |
| H(37) | 137 (1) | −307 (3) | 395 (1) | 64 (9) |
| H(38) | 212 (1) | −183 (3) | 412 (1) | 48 (7) |
| H(39) | 213 (1) | 4 (2) | 344 (1) | 45 (7) |

The population parameters and their estimated standard deviations for the atoms in the $BF_4$ disorder models are:

| | | | |
|---|---|---|---|
| F(11) | 0.835 (14) | F(15) | 0.435 (19) |
| F(12) | 0.903 (15) | F(16) | 0.247 (25) |
| F(13) | 0.576 (20) | F(17) | 0.354 (19) |
| F(14) | 0.400 (20) | F(18) | 0.285 (19) |

TABLE 12

Final atomic parameters for $[Ni(py_3tren)](BF_4)_2$, tris(4-(2-pyridyl)-3-aza-3-butenyl)amine nickel(II) tetrafluoroborate

| Atom | $x/a$ | $y/b$ | $z/c$ | $B_{11}$ | $B_{22}$ | $B_{33}$ | $B_{12}$ | $B_{13}$ | $B_{23}$ |
|---|---|---|---|---|---|---|---|---|---|
| *Positional parameters ($\times 10^5$) and thermal parameters ($\times 10^2$)* | | | | | | | | | |
| Ni | 13573 (2) | 16422 (6) | 24148 (4) | 365 (3) | 369 (3) | 359 (3) | 12 (3) | 108 (2) | 7 (3) |
| N(11) | 11704 (14) | 34071 (40) | 19789 (21) | 518 (23) | 387 (22) | 463 (21) | 20 (21) | 138 (17) | 32 (20) |
| N(12) | 11031 (13) | 25187 (40) | 32756 (21) | 443 (22) | 398 (24) | 400 (21) | −30 (19) | 155 (17) | −55 (18) |
| N(21) | 16740 (15) | 9158 (35) | 15870 (19) | 402 (21) | 470 (22) | 375 (19) | 44 (18) | 126 (17) | 40 (16) |
| N(22) | 20824 (13) | 20749 (34) | 28001 (20) | 397 (20) | 412 (23) | 454 (20) | −53 (17) | 87 (17) | 1 (17) |
| N(31) | 6763 (12) | 8332 (37) | 20499 (18) | 309 (18) | 444 (22) | 328 (17) | 37 (17) | 70 (14) | 47 (16) |
| N(32) | 14376 (12) | −926 (32) | 29657 (17) | 349 (18) | 363 (20) | 318 (17) | 4 (17) | 37 (14) | 37 (15) |
| N(7) | 8171 (13) | 19481 (35) | 7411 (19) | 526 (22) | 451 (24) | 393 (19) | 106 (18) | 117 (17) | 64 (16) |
| C(11) | 8126 (26) | 32960 (66) | 6885 (34) | 734 (43) | 561 (37) | 489 (32) | 93 (37) | 159 (31) | 193 (31) |
| C(12) | 12069 (28) | 38634 (71) | 12565 (35) | 730 (46) | 465 (41) | 590 (37) | 14 (34) | 154 (33) | 121 (30) |
| C(13) | 9694 (21) | 41031 (58) | 23832 (34) | 512 (32) | 339 (33) | 709 (39) | 41 (27) | 120 (27) | 0 (29) |
| C(14) | 9091 (18) | 36524 (52) | 30960 (29) | 425 (28) | 431 (34) | 547 (30) | −88 (24) | 165 (23) | −111 (25) |
| C(15) | 6719 (22) | 43497 (67) | 35367 (42) | 507 (33) | 532 (41) | 786 (43) | −72 (30) | 260 (32) | −246 (35) |
| C(16) | 6518 (25) | 38799 (81) | 42047 (44) | 543 (38) | 679 (47) | 793 (48) | −206 (34) | 319 (35) | −447 (41) |
| C(17) | 8612 (25) | 27623 (86) | 44113 (36) | 640 (39) | 816 (50) | 445 (35) | −197 (35) | 240 (30) | −218 (37) |
| C(18) | 10817 (20) | 21058 (60) | 39341 (29) | 482 (30) | 581 (38) | 390 (28) | −64 (27) | 104 (24) | −90 (27) |
| C(21) | 11596 (24) | 13082 (60) | 4049 (30) | 642 (36) | 631 (41) | 351 (27) | 11 (30) | 134 (26) | 21 (26) |
| C(22) | 14376 (22) | 3247 (57) | 9046 (29) | 576 (33) | 545 (35) | 401 (28) | 86 (30) | 143 (25) | −57 (26) |
| C(23) | 21305 (21) | 10026 (53) | 17195 (30) | 519 (32) | 538 (32) | 533 (32) | 57 (27) | 275 (28) | −24 (25) |
| C(24) | 23786 (17) | 15768 (49) | 23902 (27) | 372 (25) | 460 (27) | 539 (27) | 35 (25) | 152 (22) | 132 (25) |
| C(25) | 28763 (21) | 16052 (63) | 26157 (39) | 477 (33) | 586 (35) | 813 (41) | 39 (31) | 200 (32) | 114 (34) |
| C(26) | 30857 (25) | 21262 (63) | 32705 (44) | 381 (36) | 636 (41) | 965 (50) | −37 (30) | 12 (35) | 159 (34) |
| C(27) | 27876 (25) | 26044 (58) | 36834 (37) | 520 (37) | 563 (36) | 674 (40) | −156 (29) | −55 (32) | 65 (30) |
| C(28) | 22908 (21) | 25784 (50) | 34366 (31) | 479 (33) | 417 (29) | 592 (34) | −80 (25) | 159 (28) | −6 (25) |
| C(31) | 3715 (21) | 13153 (66) | 7676 (28) | 452 (30) | 714 (45) | 403 (27) | 97 (29) | 0 (23) | 89 (28) |
| C(32) | 2624 (20) | 13361 (58) | 15323 (28) | 404 (28) | 519 (38) | 457 (28) | 55 (26) | 49 (22) | 67 (25) |
| C(33) | 6310 (17) | −2488 (52) | 23109 (24) | 282 (24) | 485 (31) | 355 (23) | −57 (23) | 86 (19) | −46 (22) |
| C(34) | 10321 (17) | −7970 (45) | 28290 (21) | 400 (25) | 378 (26) | 270 (20) | −40 (21) | 103 (18) | −24 (19) |

TABLE 12 (continued)

| Atom | $x/a$ | $y/b$ | $z/c$ | $B_{11}$ | $B_{22}$ | $B_{33}$ | $B_{12}$ | $B_{13}$ | $B_{23}$ |
|---|---|---|---|---|---|---|---|---|---|
| *Positional parameters ($\times 10^5$) and thermal parameters ($\times 10^2$)* | | | | | | | | | |
| C(35) | 9914 (20) | −19181 (49) | 31626 (26) | 454 (28) | 470 (33) | 397 (25) | −36 (25) | 139 (22) | 17 (22) |
| C(36) | 13807 (22) | −23554 (54) | 36666 (28) | 699 (37) | 395 (31) | 419 (27) | −18 (28) | 157 (26) | 87 (24) |
| C(37) | 17930 (20) | −16562 (56) | 38134 (25) | 505 (29) | 480 (30) | 368 (24) | 35 (28) | −22 (21) | 111 (25) |
| C(38) | 18095 (19) | −5421 (50) | 34554 (26) | 410 (28) | 453 (32) | 398 (25) | −49 (25) | 47 (22) | −1 (22) |
| B(1) | 28841 (41) | 365 (111) | 1744 (56) | 590 (66) | 595 (63) | 654 (64) | 54 (53) | 235 (50) | −135 (52) |
| B(2) | 47109 (27) | 20647 (71) | 38339 (34) | 580 (39) | 583 (44) | 364 (31) | −61 (33) | −42 (28) | 52 (29) |
| F(11) | 30011 (130) | 2416 (321) | 8902 (108) | 1091 (120) | 953 (107) | 726 (105) | −349 (94) | 488 (136) | −348 (114) |
| F(12) | 24157 (46) | −3379 (274) | 237 (97) | 527 (75) | 1445 (158) | 976 (74) | −58 (63) | 80 (43) | 388 (102) |
| F(13) | 29300 (83) | 12095 (217) | −1426 (144) | 967 (104) | 831 (102) | 683 (90) | −102 (62) | 222 (61) | 185 (55) |
| F(14) | 31334 (274) | −10427 (1041) | 843 (559) | 961 (182) | 1158 (266) | 1135 (220) | 520 (178) | 105 (165) | −282 (245) |
| F(15) | 32283 (202) | −5694 (907) | −1758 (600) | 748 (201) | 688 (395) | 786 (273) | 170 (212) | 282 (152) | −129 (171) |
| F(16) | 32956 (231) | 4354 (1422) | −52 (356) | 683 (286) | 1572 (906) | 816 (258) | −143 (339) | 209 (208) | 103 (353) |
| F(17) | 25953 (125) | 10538 (326) | 2815 (166) | 1289 (189) | 960 (217) | 921 (158) | 258 (155) | −5 (142) | −187 (119) |
| F(18) | 29336 (146) | 4568 (1010) | −4737 (352) | 765 (165) | 2222 (427) | 1054 (221) | −52 (213) | 638 (152) | 288 (303) |
| F(19) | 25641 (397) | −7724 (671) | −602 (218) | 2324 (696) | 1103 (239) | 1142 (180) | −627 (338) | −83 (253) | −561 (193) |
| F(10) | 31182 (180) | −238 (459) | 8618 (190) | 878 (116) | 935 (145) | 952 (177) | −21 (98) | −500 (155) | 363 (151) |
| F(21) | 48184 (13) | 11709 (31) | 43282 (16) | 1299 (27) | 811 (23) | 697 (18) | 280 (20) | 199 (18) | 295 (17) |
| F(22) | 47603 (16) | 17008 (38) | 31732 (17) | 1948 (37) | 1143 (28) | 543 (18) | 355 (28) | 234 (20) | −68 (20) |
| F(23) | 43005 (14) | 25667 (47) | 38199 (23) | 804 (23) | 2167 (45) | 1657 (34) | 785 (28) | 655 (24) | 1145 (32) |
| F(24) | 50403 (16) | 29842 (42) | 39728 (20) | 1289 (31) | 1278 (34) | 1194 (28) | −502 (27) | −76 (23) | 70 (24) |
| *Positional parameters ($\times 10^5$) and thermal parameters ($\times 10$)* | | | | | | | | | |
| H(11) | 88 (2) | 355 (5) | 21 (3) | 79 (14) | | | | | |
| H(12) | 50 (1) | 364 (4) | 77 (2) | 52 (13) | | | | | |
| H(13) | 154 (2) | 367 (4) | 124 (2) | 63 (15) | | | | | |
| H(14) | 121 (2) | 474 (6) | 126 (3) | 91 (22) | | | | | |

| | | | | |
|---|---|---|---|---|
| H(15) | 85 (1) | 484 (4) | 223 (2) | 29 (11) |
| H(16) | 54 (2) | 517 (5) | 337 (3) | 82 (18) |
| H(17) | 47 (2) | 433 (5) | 449 (3) | 71 (16) |
| H(18) | 85 (2) | 244 (5) | 484 (2) | 69 (17) |
| H(19) | 125 (1) | 127 (4) | 409 (2) | 34 (11) |
| H(21) | 101 (1) | 95 (4) | −2 (2) | 42 (11) |
| H(22) | 141 (1) | 189 (4) | 25 (2) | 59 (12) |
| H(23) | 121 (1) | −32 (4) | 100 (2) | 38 (11) |
| H(24) | 170 (1) | −10 (4) | 66 (2) | 62 (12) |
| H(25) | 229 (1) | 66 (4) | 143 (2) | 43 (12) |
| H(26) | 303 (1) | 125 (4) | 230 (2) | 51 (13) |
| H(27) | 342 (2) | 209 (5) | 342 (3) | 87 (18) |
| H(28) | 289 (1) | 293 (4) | 415 (2) | 38 (11) |
| H(29) | 208 (1) | 288 (4) | 370 (2) | 46 (11) |
| H(31) | 11 (1) | 166 (3) | 43 (2) | 55 (12) |
| H(32) | 41 (2) | 36 (5) | 65 (2) | 70 (16) |
| H(33) | 21 (1) | 221 (4) | 168 (2) | 41 (11) |
| H(34) | −1 (1) | 81 (4) | 157 (2) | 48 (12) |
| H(35) | 34 (1) | −72 (3) | 219 (2) | 29 (9) |
| H(36) | 66 (1) | −230 (4) | 302 (2) | 56 (12) |
| H(37) | 135 (1) | −313 (4) | 391 (2) | 56 (12) |
| H(38) | 207 (1) | −191 (3) | 416 (2) | 38 (10) |
| H(39) | 209 (1) | −8 (4) | 352 (2) | 48 (12) |

The population parameters and their estimated standard deviations for the atoms in the $BF_4$ disorder models are:

| | | | |
|---|---|---|---|
| F(11) | 0.60 (9) | F(16) | 0.167 (47) |
| F(12) | 0.73 (6) | F(17) | 0.245 (19) |
| F(13) | 0.58 (6) | F(18) | 0.336 (55) |
| F(14) | 0.51 (14) | F(19) | 0.310 (62) |
| F(15) | 0.248 (154) | F(10) | 0.392 (88) |

TABLE 13

Final atomic parameters for $[Ni(py_3tren)](PF_6)_2$, tris(4-(2-pyridyl)-3-aza-3-butenyl)aminenickel(II) hexafluorophosphate

| Atom | $x/a$ | $y/b$ | $z/c$ | $B_{11}$ | $B_{22}$ | $B_{33}$ | $B_{12}$ | $B_{13}$ | $B_{23}$ |
|---|---|---|---|---|---|---|---|---|---|
| *Positional parameters ($\times 10^5$) and thermal parameters ($\times 10^2$)* | | | | | | | | | |
| Ni | 22242 (3) | 25919 (5) | 18922 (3) | 299 (3) | 289 (3) | 298 (3) | 8 (3) | 124 (2) | −14 (3) |
| N(11) | 36261 (24) | 19965 (36) | 22984 (19) | 325 (22) | 496 (27) | 366 (22) | 18 (19) | 102 (19) | −9 (20) |
| N(12) | 22917 (24) | 12648 (32) | 11327 (18) | 338 (23) | 317 (22) | 341 (23) | −30 (18) | 127 (19) | −8 (18) |
| N(21) | 23241 (23) | 40584 (34) | 25980 (18) | 354 (22) | 405 (24) | 368 (22) | 43 (18) | 144 (18) | −34 (19) |
| N(22) | 26744 (23) | 40855 (35) | 13881 (19) | 355 (23) | 374 (24) | 361 (23) | 4 (19) | 124 (19) | 23 (20) |
| N(31) | 16266 (26) | 12799 (33) | 23796 (18) | 402 (25) | 330 (23) | 336 (22) | 16 (20) | 110 (19) | 16 (18) |
| N(32) | 7764 (23) | 29588 (32) | 14166 (17) | 369 (22) | 311 (22) | 328 (21) | 2 (18) | 143 (18) | −2 (17) |
| N(7) | 31592 (27) | 20884 (37) | 35740 (19) | 504 (26) | 486 (28) | 389 (23) | 79 (22) | 120 (20) | −44 (21) |
| C(11) | 41093 (38) | 18343 (53) | 35854 (26) | 496 (36) | 747 (43) | 379 (32) | 96 (32) | 14 (26) | −39 (31) |
| C(12) | 43172 (31) | 24178 (52) | 29576 (24) | 345 (26) | 651 (38) | 445 (30) | 27 (31) | 52 (22) | −80 (33) |
| C(13) | 38621 (31) | 12086 (46) | 19105 (25) | 329 (28) | 472 (33) | 458 (32) | 106 (24) | 174 (25) | 45 (27) |
| C(14) | 31574 (32) | 7465 (41) | 12647 (23) | 373 (30) | 332 (27) | 375 (28) | 23 (23) | 181 (24) | 15 (23) |
| C(15) | 33561 (35) | −923 (45) | 8162 (27) | 481 (35) | 413 (33) | 514 (34) | 131 (27) | 250 (30) | 14 (27) |
| C(16) | 26490 (42) | −4665 (45) | 2272 (27) | 700 (42) | 363 (32) | 490 (35) | 110 (30) | 294 (33) | −39 (27) |
| C(17) | 17608 (37) | 209 (46) | 899 (24) | 603 (38) | 463 (35) | 353 (30) | −49 (30) | 151 (27) | −108 (26) |
| C(18) | 16045 (32) | 8953 (43) | 5543 (24) | 402 (30) | 420 (31) | 376 (28) | −23 (24) | 162 (24) | −32 (25) |
| C(21) | 29667 (38) | 32982 (51) | 38231 (24) | 646 (39) | 569 (38) | 312 (28) | 15 (32) | 167 (27) | −77 (27) |
| C(22) | 21515 (35) | 39643 (46) | 32843 (25) | 563 (35) | 479 (34) | 440 (32) | 51 (27) | 257 (27) | −64 (27) |
| C(23) | 25083 (31) | 51163 (44) | 23872 (25) | 364 (30) | 326 (30) | 479 (32) | −7 (23) | 140 (24) | −67 (25) |
| C(24) | 27498 (28) | 51793 (42) | 17353 (23) | 314 (26) | 318 (28) | 417 (28) | −27 (22) | 132 (22) | −2 (24) |
| C(25) | 30489 (34) | 62486 (46) | 15083 (27) | 464 (33) | 378 (32) | 571 (36) | −54 (25) | 178 (28) | −2 (27) |
| C(26) | 33222 (34) | 61948 (53) | 9090 (30) | 416 (33) | 504 (39) | 605 (40) | −86 (28) | 127 (28) | 168 (32) |
| C(27) | 32838 (36) | 50983 (55) | 5668 (25) | 531 (35) | 566 (39) | 396 (32) | −76 (31) | 198 (26) | 80 (30) |
| C(28) | 29425 (33) | 40717 (46) | 8107 (24) | 473 (33) | 461 (34) | 393 (32) | −27 (26) | 174 (26) | 27 (25) |
| C(31) | 25646 (38) | 10368 (52) | 36214 (25) | 642 (38) | 538 (39) | 379 (31) | 90 (31) | 163 (28) | 120 (28) |
| C(32) | 21501 (35) | 3751 (45) | 29157 (26) | 555 (36) | 394 (32) | 487 (34) | 23 (26) | 212 (28) | 53 (26) |
| C(33) | 7361 (35) | 12590 (42) | 21725 (23) | 442 (32) | 344 (30) | 412 (30) | −53 (25) | 211 (25) | −9 (24) |

| | | | | | | | | | |
|---|---|---|---|---|---|---|---|---|---|
| C(34) | 2204 (32) | 21966 (41) | 16582 (22) | 433 (28) | 338 (30) | 356 (26) | −43 (23) | 159 (23) | −95 (22) |
| C(35) | −7586 (32) | 23145 (48) | 14296 (24) | 334 (27) | 523 (36) | 496 (31) | −116 (27) | 151 (24) | −98 (30) |
| C(36) | −11780 (33) | 32153 (52) | 9568 (27) | 327 (30) | 564 (38) | 507 (35) | 40 (27) | 97 (26) | −98 (31) |
| C(37) | −6205 (37) | 40067 (47) | 7246 (24) | 473 (34) | 466 (35) | 417 (32) | 148 (28) | 76 (26) | 54 (26) |
| C(38) | 3434 (34) | 38549 (45) | 9610 (24) | 433 (32) | 434 (33) | 420 (31) | 81 (26) | 173 (25) | 59 (26) |
| P(1) | 57511 (10) | 23764 (15) | 9851 (7) | 465 (8) | 519 (10) | 585 (10) | −45 (8) | 252 (7) | 43 (10) |
| P(2) | −4411 (10) | 27262 (15) | 36878 (7) | 477 (8) | 512 (11) | 567 (10) | −26 (8) | 203 (7) | 44 (8) |
| F(1) | 68536 (23) | 22717 (47) | 12298 (21) | 490 (22) | 2030 (53) | 1272 (35) | −61 (30) | 193 (22) | 632 (38) |
| F(2) | 57154 (32) | 17441 (51) | 2799 (21) | 1271 (40) | 1988 (57) | 907 (33) | 393 (37) | 416 (29) | −418 (35) |
| F(3) | 46593 (21) | 24021 (36) | 7219 (21) | 526 (21) | 1021 (31) | 1493 (36) | 147 (23) | 369 (22) | 345 (30) |
| F(4) | 57825 (43) | 30166 (50) | 16659 (23) | 2442 (69) | 1573 (53) | 964 (34) | −262 (46) | 818 (40) | −584 (36) |
| F(5) | 57789 (33) | 36603 (39) | 6328 (25) | 1508 (46) | 857 (34) | 1530 (43) | −338 (31) | 504 (36) | 437 (32) |
| F(6) | 57199 (25) | 10974 (36) | 13478 (25) | 725 (28) | 852 (52) | 1862 (48) | 82 (22) | 330 (29) | 732 (33) |
| F(7) | 6080 (22) | 22717 (33) | 40879 (19) | 588 (22) | 885 (29) | 1199 (31) | 214 (21) | 177 (20) | 50 (25) |
| F(8) | −14715 (22) | 32014 (35) | 32911 (19) | 498 (21) | 1108 (33) | 1151 (31) | 49 (21) | 118 (20) | 424 (26) |
| F(9) | −1142 (28) | 33644 (38) | 30928 (21) | 1098 (34) | 1142 (36) | 1243 (35) | 50 (28) | 719 (30) | 338 (30) |
| F(10) | −6326 (33) | 14908 (37) | 32178 (22) | 1554 (47) | 800 (32) | 1135 (37) | −221 (30) | 261 (32) | −288 (28) |
| F(11) | −7951 (29) | 19963 (47) | 42120 (21) | 1134 (36) | 1821 (53) | 1135 (35) | 210 (33) | 605 (30) | 879 (36) |
| F(12) | −2432 (29) | 39461 (41) | 41099 (25) | 911 (33) | 1158 (38) | 1822 (49) | 195 (28) | −108 (31) | −1053 (38) |

*Positional parameters ($\times 10^3$) and thermal parameters ($\times 10$)*

| | | | | |
|---|---|---|---|---|
| H(11) | 456 | 218 | 403 | 55 |
| H(12) | 420 | 91 | 357 | 55 |
| H(13) | 429 | 335 | 299 | 47 |
| H(14) | 496 | 216 | 296 | 47 |
| H(15) | 453 | 90 | 205 | 39 |
| H(16) | 401 | −43 | 92 | 44 |
| H(17) | 278 | −109 | −10 | 44 |
| H(18) | 123 | −25 | −34 | 46 |
| H(19) | 96 | 126 | 45 | 38 |
| H(21) | 281 | 318 | 427 | 47 |
| H(22) | 354 | 383 | 392 | 47 |
| H(23) | 156 | 348 | 322 | 44 |

TABLE 13 (continued)

| Atom | $x/a$ | $y/b$ | $z/c$ | $B$ |
|---|---|---|---|---|
| *Positional parameters ($\times 10^3$) and thermal parameters ($\times 10$)* | | | | |
| H(24) | 209 | 482 | 346 | 44 |
| H(25) | 249 | 589 | 266 | 37 |
| H(26) | 307 | 706 | 177 | 45 |
| H(27) | 354 | 697 | 73 | 45 |
| H(28) | 350 | 504 | 14 | 45 |
| H(29) | 289 | 327 | 54 | 41 |
| H(31) | 295 | 42 | 398 | 51 |
| H(32) | 204 | 135 | 378 | 51 |
| H(33) | 267 | 0 | 277 | 44 |
| H(34) | 171 | −30 | 296 | 44 |
| H(35) | 39 | 61 | 236 | 36 |
| H(36) | −115 | 174 | 162 | 41 |
| H(37) | −188 | 330 | 78 | 50 |
| H(38) | −91 | 470 | 38 | 47 |
| H(39) | 74 | 444 | 78 | 42 |

All hydrogen atom parameters were calculated and not refined.

TABLE 14

Final atomic parameters for $[Cu(py_3tren)](BF_4)_2$, tris(4-(2-pyridyl)-3-aza-3-butenyl)aminecopper(II) tetrafluoroborate

| Atom | $x/a$ | $y/b$ | $z/c$ | $B_{11}$ | $B_{22}$ | $B_{33}$ | $B_{12}$ | $B_{13}$ | $B_{23}$ |
|---|---|---|---|---|---|---|---|---|---|
| *Positional parameters ($\times 10^5$) and thermal parameters ($\times 10^2$)* | | | | | | | | | |
| Cu | 13598 (1) | 16187 (3) | 23740 (2) | 388 (1) | 461 (2) | 438 (1) | 24 (1) | 104 (1) | 24 (1) |
| N(11) | 11555 (8) | 34272 (25) | 20052 (12) | 507 (12) | 571 (13) | 565 (13) | −31 (11) | 153 (10) | −68 (13) |
| N(12) | 10999 (8) | 25643 (25) | 33201 (17) | 442 (12) | 482 (14) | 630 (15) | −14 (10) | 140 (11) | −115 (12) |
| N(21) | 16964 (8) | 8605 (21) | 15261 (12) | 446 (12) | 543 (13) | 541 (14) | 67 (11) | 104 (10) | 120 (11) |
| N(22) | 20826 (8) | 20300 (21) | 27452 (12) | 443 (12) | 427 (12) | 570 (13) | −19 (10) | 123 (11) | 57 (11) |
| N(31) | 6889 (8) | 8057 (21) | 20506 (12) | 412 (11) | 433 (12) | 380 (10) | 41 (9) | 102 (8) | 34 (9) |
| N(32) | 14558 (8) | −1184 (21) | 29747 (12) | 410 (11) | 411 (11) | 381 (10) | −23 (9) | 70 (9) | −16 (9) |
| N(7) | 8377 (8) | 19447 (21) | 7675 (12) | 550 (12) | 481 (13) | 427 (11) | 74 (10) | 98 (9) | 85 (9) |
| C(11) | 8079 (12) | 32971 (37) | 7166 (21) | 743 (22) | 622 (21) | 547 (18) | 113 (19) | 153 (17) | 177 (17) |
| C(12) | 11956 (17) | 39009 (41) | 12968 (21) | 728 (24) | 578 (23) | 740 (23) | −33 (19) | 222 (19) | 88 (18) |
| C(13) | 9546 (12) | 41073 (33) | 24052 (21) | 535 (17) | 431 (18) | 761 (22) | 22 (14) | 153 (15) | −58 (17) |
| C(14) | 8966 (8) | 36747 (29) | 31069 (17) | 418 (14) | 445 (17) | 666 (18) | −47 (12) | 136 (13) | −179 (14) |
| C(15) | 6501 (12) | 43666 (37) | 35407 (25) | 483 (17) | 508 (20) | 887 (26) | −57 (15) | 187 (18) | −241 (20) |
| C(16) | 6227 (12) | 39284 (50) | 42023 (25) | 587 (20) | 781 (26) | 778 (26) | −208 (19) | 268 (19) | −367 (23) |
| C(17) | 8374 (12) | 28264 (50) | 44246 (25) | 606 (20) | 862 (28) | 614 (24) | −197 (19) | 162 (18) | −186 (23) |
| C(18) | 10688 (12) | 21745 (41) | 39713 (21) | 528 (17) | 634 (22) | 670 (22) | −37 (16) | 74 (16) | −66 (19) |
| C(21) | 11676 (12) | 13552 (37) | 3834 (17) | 699 (20) | 657 (22) | 425 (16) | 55 (17) | 153 (15) | 12 (16) |
| C(22) | 14581 (12) | 3367 (37) | 8327 (21) | 593 (19) | 669 (21) | 631 (19) | 106 (17) | 173 (15) | −5 (16) |
| C(23) | 21543 (12) | 9697 (33) | 16795 (21) | 513 (18) | 619 (19) | 660 (20) | 93 (15) | 243 (16) | 88 (16) |
| C(24) | 23880 (8) | 15443 (29) | 23592 (17) | 379 (13) | 462 (15) | 661 (18) | 28 (13) | 185 (13) | 146 (15) |
| C(25) | 28859 (12) | 15882 (37) | 26052 (25) | 424 (16) | 627 (20) | 983 (27) | 18 (17) | 207 (18) | 134 (21) |
| C(26) | 30733 (17) | 21204 (37) | 32646 (29) | 403 (19) | 647 (23) | 1115 (33) | −60 (17) | −3 (22) | 167 (21) |
| C(27) | 27672 (17) | 26058 (33) | 36559 (25) | 602 (22) | 543 (20) | 794 (26) | −109 (17) | 23 (19) | 42 (18) |
| C(28) | 22748 (12) | 25456 (33) | 33718 (21) | 536 (19) | 490 (18) | 768 (24) | −32 (15) | 215 (18) | 60 (16) |
| C(31) | 3934 (12) | 12769 (29) | 7776 (17) | 540 (15) | 640 (19) | 444 (15) | 83 (14) | −26 (12) | 71 (13) |
| C(32) | 2772 (8) | 13087 (29) | 15223 (17) | 386 (13) | 595 (18) | 520 (15) | 34 (12) | 46 (11) | 82 (13) |
| C(33) | 6461 (8) | −2589 (29) | 23177 (12) | 375 (13) | 488 (15) | 396 (13) | −31 (11) | 128 (10) | −43 (12) |
| C(34) | 10467 (8) | −8122 (25) | 28402 (12) | 431 (13) | 413 (14) | 305 (11) | −14 (11) | 116 (10) | −27 (11) |

TABLE 14 (continued)

| Atom | $x/a$ | $y/b$ | $z/c$ | $B_{11}$ | $B_{22}$ | $B_{33}$ | $B_{12}$ | $B_{13}$ | $B_{23}$ |
|---|---|---|---|---|---|---|---|---|---|
| *Positional parameters ($\times 10^5$) and thermal parameters ($\times 10^2$)* | | | | | | | | | |
| C(35) | 10011 (8) | −19227 (29) | 31821 (17) | 512 (14) | 496 (16) | 430 (14) | −58 (12) | 144 (12) | 45 (12) |
| C(36) | 13918 (12) | −23530 (29) | 36840 (17) | 752 (19) | 465 (16) | 422 (15) | −8 (15) | 127 (14) | 99 (12) |
| C(37) | 18095 (12) | −16657 (33) | 38264 (12) | 564 (16) | 601 (18) | 391 (13) | 72 (15) | 2 (11) | −5 (14) |
| C(38) | 18286 (8) | −5576 (29) | 34598 (17) | 490 (15) | 486 (16) | 469 (15) | −63 (13) | 37 (12) | −37 (13) |
| B(1) | 28977 (21) | −62 (54) | 1568 (29) | 818 (33) | 615 (31) | 684 (30) | 11 (27) | 253 (25) | −68 (24) |
| B(2) | 47187 (17) | 21224 (42) | 38227 (21) | 648 (24) | 602 (23) | 457 (20) | −21 (19) | 64 (18) | 28 (18) |
| F(11) | 30791 (8) | 302 (21) | 8856 (12) | 999 (15) | 955 (16) | 723 (13) | −188 (13) | 55 (12) | 10 (12) |
| F(12) | 24690 (33) | −6563 (79) | −613 (54) | 1094 (48) | 1030 (49) | 1007 (34) | −315 (38) | 90 (27) | −172 (32) |
| F(13) | 29177 (25) | 12029 (58) | −1357 (33) | 838 (32) | 673 (33) | 792 (32) | −45 (24) | 46 (30) | 95 (24) |
| F(14) | 32354 (33) | −6257 (112) | −1679 (50) | 1051 (44) | 1221 (76) | 1078 (54) | 517 (47) | 446 (37) | 44 (47) |
| F(15) | 30931 (50) | −12061 (108) | 1215 (62) | 1456 (87) | 1007 (74) | 1040 (69) | 316 (54) | 92 (50) | −20 (47) |
| F(17) | 26143 (50) | 10196 (125) | 2796 (58) | 1180 (70) | 1021 (70) | 1067 (66) | 135 (61) | 179 (57) | −324 (56) |
| F(18) | 30506 (42) | 4823 (125) | −3056 (54) | 2718 (99) | 2147 (108) | 2728 (96) | 228 (76) | 2234 (85) | 719 (83) |
| F(19) | 24311 (54) | −1157 (179) | 817 (104) | 347 (47) | 1020 (124) | 736 (79) | 13 (61) | 73 (44) | 137 (79) |
| F(21) | 48150 (8) | 12076 (21) | 43213 (12) | 1302 (17) | 897 (14) | 801 (12) | 329 (12) | 238 (11) | 333 (11) |
| F(22) | 47772 (12) | 17294 (29) | 31633 (12) | 1321 (21) | 1064 (18) | 456 (12) | 254 (17) | 146 (12) | −144 (13) |
| F(23) | 42725 (12) | 26383 (42) | 38051 (21) | 439 (14) | 1313 (27) | 1139 (23) | 256 (17) | 265 (15) | 394 (21) |
| F(24) | 50587 (8) | 30621 (29) | 39963 (17) | 885 (18) | 1243 (22) | 923 (18) | −391 (16) | 20 (13) | −139 (17) |
| *Positional parameters ($\times 10^5$) and thermal parameters ($\times 10$)* | | | | | | | | | |
| F(25) | 501 (1) | 252 (2) | 353 (1) | 56 (4) | | | | | |
| F(26) | 431 (1) | 174 (1) | 331 (1) | 125 (4) | | | | | |
| F(27) | 452 (1) | 307 (1) | 406 (1) | 88 (4) | | | | | |
| H(11) | 85 (1) | 360 (3) | 23 (2) | 67 (8) | | | | | |
| H(12) | 50 (1) | 360 (2) | 81 (1) | 56 (7) | | | | | |
| H(13) | 153 (1) | 367 (3) | 123 (1) | 69 (8) | | | | | |
| H(14) | 116 (1) | 476 (3) | 124 (2) | 74 (10) | | | | | |

| | | | | |
|---|---|---|---|---|
| H(15) | 85 (1) | 486 (3) | 222 (1) | 55 (8) |
| H(16) | 50 (1) | 504 (3) | 329 (1) | 55 (8) |
| H(17) | 44 (1) | 443 (3) | 450 (2) | 89 (10) |
| H(18) | 87 (1) | 249 (3) | 488 (2) | 78 (11) |
| H(19) | 123 (1) | 140 (2) | 413 (1) | 53 (8) |
| H(21) | 99 (1) | 102 (2) | −8 (1) | 62 (6) |
| H(22) | 140 (1) | 201 (2) | 24 (1) | 61 (6) |
| H(23) | 124 (1) | −35 (3) | 96 (1) | 66 (8) |
| H(24) | 169 (1) | 0 (3) | 58 (1) | 67 (8) |
| H(25) | 235 (1) | 66 (2) | 137 (1) | 61 (6) |
| H(26) | 306 (1) | 121 (2) | 231 (1) | 58 (6) |
| H(27) | 338 (1) | 212 (2) | 345 (1) | 68 (7) |
| H(28) | 288 (1) | 296 (2) | 413 (1) | 61 (6) |
| H(29) | 208 (1) | 286 (2) | 361 (1) | 43 (5) |
| H(31) | 15 (1) | 154 (2) | 47 (1) | 44 (5) |
| H(32) | 43 (1) | 37 (2) | 61 (1) | 54 (6) |
| H(33) | 21 (1) | 227 (2) | 168 (1) | 60 (6) |
| H(34) | 0 (1) | 82 (2) | 152 (1) | 37 (5) |
| H(35) | 37 (1) | −73 (2) | 220 (1) | 40 (5) |
| H(36) | 71 (1) | −233 (2) | 308 (1) | 47 (5) |
| H(37) | 136 (1) | −304 (2) | 392 (1) | 47 (5) |
| H(38) | 208 (1) | −190 (2) | 415 (1) | 48 (5) |
| H(39) | 211 (1) | −4 (2) | 354 (1) | 52 (6) |

The population parameters and their estimated standard deviations for the atoms in the $BF_4$ disorder models are:

| | | | |
|---|---|---|---|
| F(11) | 0.910 (4) | F(19) | 0.272 (4) |
| F(12) | 0.681 (5) | F(22) | 0.848 (4) |
| F(13) | 0.490 (4) | F(23) | 0.757 (7) |
| F(14) | 0.448 (4) | F(24) | 0.851 (5) |
| F(15) | 0.377 (5) | F(25) | 0.115 (4) |
| F(17) | 0.302 (4) | F(26) | 0.239 (5) |
| F(18) | 0.561 (6) | F(27) | 0.217 (7) |

TABLE 15

Final atomic parameters for [Zn(py$_3$tren)](BF$_4$)$_2$, tris(4-(2-pyridyl)-3-aza-3-butenyl)aminezinc(II) tetrafluoroborate

| Atom | $x/a$ | $y/b$ | $z/c$ | $B_{11}$ | $B_{22}$ | $B_{33}$ | $B_{12}$ | $B_{13}$ | $B_{23}$ |
|---|---|---|---|---|---|---|---|---|---|
| *Positional parameters ($\times 10^5$) and thermal parameters ($\times 10^2$)* | | | | | | | | | |
| Zn | 13457 (1) | 16814 (3) | 23346 (2) | 351 (1) | 393 (2) | 426 (2) | 16 (2) | 96 (1) | 3 (2) |
| N(11) | 11287 (8) | 35086 (23) | 19773 (12) | 451 (11) | 440 (14) | 497 (12) | 9 (10) | 112 (10) | 16 (11) |
| N(12) | 10946 (8) | 25651 (22) | 32761 (12) | 430 (12) | 457 (13) | 459 (12) | −29 (10) | 106 (10) | −83 (11) |
| N(21) | 17161 (8) | 9572 (23) | 15472 (11) | 408 (11) | 502 (14) | 413 (12) | 58 (10) | 87 (9) | 49 (10) |
| N(22) | 21079 (7) | 20914 (22) | 27720 (12) | 373 (11) | 442 (13) | 507 (13) | −44 (10) | 79 (9) | 21 (10) |
| N(31) | 6666 (8) | 7330 (23) | 20356 (11) | 357 (11) | 407 (13) | 362 (11) | 17 (10) | 50 (9) | 37 (10) |
| N(32) | 14447 (8) | −1182 (23) | 29646 (11) | 396 (11) | 421 (13) | 339 (11) | 18 (10) | 28 (9) | 19 (10) |
| N(7) | 8340 (8) | 19445 (23) | 7996 (11) | 490 (12) | 458 (14) | 411 (12) | 78 (11) | 65 (10) | 93 (10) |
| C(11) | 7654 (15) | 32864 (39) | 7210 (22) | 684 (23) | 554 (21) | 522 (20) | 75 (20) | 50 (18) | 178 (18) |
| C(12) | 11451 (16) | 39789 (39) | 12635 (22) | 696 (25) | 429 (21) | 648 (23) | 5 (19) | 138 (19) | 124 (18) |
| C(13) | 9296 (13) | 41488 (37) | 23981 (23) | 481 (18) | 410 (20) | 739 (24) | 38 (15) | 98 (16) | 26 (18) |
| C(14) | 8901 (10) | 36880 (32) | 31005 (19) | 386 (15) | 479 (19) | 587 (19) | −96 (13) | 130 (14) | −156 (15) |
| C(15) | 6542 (13) | 43505 (42) | 35679 (28) | 476 (19) | 554 (25) | 906 (29) | −76 (18) | 207 (19) | −286 (23) |
| C(16) | 6463 (15) | 38592 (49) | 42259 (27) | 587 (23) | 954 (32) | 699 (28) | −358 (22) | 332 (21) | −478 (27) |
| C(17) | 8613 (14) | 27279 (45) | 44194 (23) | 589 (22) | 789 (27) | 573 (23) | −179 (20) | 162 (18) | −217 (22) |
| C(18) | 10798 (12) | 21284 (38) | 39230 (20) | 534 (18) | 636 (23) | 430 (18) | −81 (17) | 129 (15) | −110 (17) |
| C(21) | 11806 (14) | 14178 (38) | 4150 (19) | 653 (22) | 662 (25) | 381 (17) | 1 (18) | 142 (16) | 46 (17) |
| C(22) | 14847 (14) | 4177 (39) | 8553 (19) | 628 (21) | 616 (23) | 445 (18) | 109 (19) | 169 (16) | −62 (17) |
| C(23) | 21743 (13) | 10196 (33) | 17006 (19) | 534 (19) | 573 (20) | 510 (19) | 86 (16) | 193 (16) | 39 (16) |
| C(24) | 24079 (10) | 15810 (31) | 23825 (17) | 324 (13) | 475 (17) | 616 (18) | 15 (14) | 119 (13) | 121 (16) |
| C(25) | 29074 (13) | 15908 (43) | 26229 (27) | 449 (17) | 705 (25) | 856 (27) | 82 (19) | 159 (19) | 112 (23) |
| C(26) | 30995 (15) | 21061 (43) | 32805 (29) | 399 (21) | 701 (27) | 1005 (34) | −73 (19) | −106 (22) | 204 (23) |
| C(27) | 27957 (15) | 26051 (39) | 36781 (25) | 521 (22) | 614 (23) | 763 (27) | −129 (18) | −54 (20) | 87 (20) |
| C(28) | 23015 (13) | 25901 (33) | 34036 (21) | 511 (19) | 458 (19) | 628 (21) | −63 (15) | 76 (17) | 12 (16) |
| C(31) | 3959 (12) | 12097 (37) | 7752 (19) | 443 (17) | 567 (21) | 449 (18) | 38 (15) | −35 (14) | 46 (16) |
| C(32) | 2516 (11) | 11902 (35) | 15039 (17) | 354 (15) | 534 (20) | 474 (17) | 44 (14) | 2 (13) | 73 (15) |
| C(33) | 6344 (10) | −3254 (32) | 23139 (15) | 347 (14) | 457 (18) | 362 (14) | −22 (13) | 97 (12) | −7 (13) |

| | | | | | | | | | |
|---|---|---|---|---|---|---|---|---|---|
| C(34) | 10407 (10) | −8292 (27) | 28384 (13) | 404 (14) | 393 (15) | 300 (13) | −7 (12) | 93 (11) | −9 (12) |
| C(35) | 10011 (13) | −19428 (31) | 31838 (16) | 518 (17) | 451 (19) | 396 (16) | −59 (15) | 110 (14) | 36 (13) |
| C(36) | 13913 (15) | −23460 (35) | 36884 (19) | 790 (23) | 462 (19) | 390 (17) | −14 (18) | 122 (16) | 103 (15) |
| C(37) | 18055 (13) | −16362 (36) | 38251 (16) | 569 (19) | 509 (19) | 383 (15) | 57 (17) | −30 (14) | 52 (16) |
| C(38) | 18179 (12) | −5440 (33) | 34526 (16) | 478 (17) | 454 (19) | 425 (16) | −38 (15) | 11 (13) | 21 (14) |
| B(1) | 29101 (20) | 121 (56) | 1378 (31) | 615 (26) | 588 (31) | 680 (32) | −74 (25) | 200 (24) | −69 (25) |
| B(2) | 47317 (15) | 21336 (38) | 38519 (21) | 534 (24) | 564 (24) | 381 (19) | −33 (18) | −8 (16) | 43 (17) |
| F(11) | 30784 (9) | 429 (27) | 8758 (13) | 968 (17) | 980 (19) | 703 (15) | −235 (15) | 103 (13) | −30 (14) |
| F(12) | 24607 (10) | −5125 (32) | −255 (14) | 820 (16) | 1389 (25) | 1026 (18) | −245 (17) | 43 (14) | 102 (18) |
| F(13) | 29088 (38) | 12361 (71) | −1083 (45) | 1055 (61) | 591 (37) | 685 (43) | −118 (34) | −16 (40) | 66 (30) |
| F(14) | 32377 (33) | −6357 (115) | −1722 (46) | 807 (46) | 1256 (79) | 643 (46) | 377 (52) | 208 (34) | −222 (45) |
| F(15) | 30884 (50) | −12062 (113) | 1382 (62) | 1381 (90) | 927 (75) | 903 (70) | 321 (58) | 246 (54) | 42 (51) |
| F(16) | 33593 (61) | 3417 (283) | 815 (108) | 688 (93) | 1856 (200) | 1181 (131) | 91 (115) | 195 (86) | −650 (138) |
| F(17) | 26226 (34) | 10026 (104) | 2973 (50) | 1188 (63) | 1128 (65) | 958 (57) | 180 (55) | 266 (49) | −260 (49) |
| F(18) | 29703 (44) | 5507 (153) | −4228 (65) | 1497 (75) | 2785 (145) | 1968 (106) | 104 (96) | 1201 (80) | 885 (93) |
| F(21) | 48184 (8) | 11732 (20) | 43204 (10) | 1091 (16) | 773 (13) | 717 (12) | 158 (12) | 107 (11) | 275 (11) |
| F(22) | 47529 (10) | 17564 (22) | 31831 (10) | 1834 (23) | 884 (15) | 471 (11) | 128 (16) | 111 (12) | −104 (11) |
| F(23) | 43047 (8) | 26683 (25) | 38667 (14) | 664 (13) | 1499 (22) | 1431 (20) | 425 (14) | 451 (13) | 704 (17) |
| F(24) | 50745 (8) | 30311 (23) | 40101 (12) | 887 (14) | 1091 (18) | 1027 (16) | −365 (14) | −14 (12) | −33 (14) |

*Positional parameters ($\times 10^3$) and thermal parameters ($\times 10$)*

| | | | | |
|---|---|---|---|---|
| H(11) | 82 (1) | 350 (3) | 22 (2) | 75 (9) |
| H(12) | 45 (1) | 347 (3) | 83 (2) | 64 (10) |
| H(13) | 150 (1) | 381 (3) | 118 (2) | 67 (9) |
| H(14) | 109 (1) | 485 (3) | 124 (2) | 70 (10) |
| H(15) | 82 (1) | 486 (3) | 225 (2) | 58 (10) |
| H(16) | 51 (1) | 509 (3) | 339 (2) | 59 (11) |
| H(17) | 48 (1) | 423 (3) | 456 (2) | 72 (10) |
| H(18) | 90 (1) | 224 (3) | 496 (2) | 118 (13) |
| H(19) | 123 (1) | 127 (3) | 404 (2) | 67 (9) |
| H(21) | 103 (1) | 105 (3) | −10 (2) | 62 (8) |
| H(22) | 140 (1) | 203 (2) | 30 (1) | 41 (7) |
| H(23) | 127(1) | −29 (3) | 98 (1) | 60 (8) |

TABLE 15 (continued)

| Atom | $x/a$ | $y/b$ | $z/c$ | $B$ |
|---|---|---|---|---|
| *Positional parameters ($\times 10^3$) and thermal parameters ($\times 10$)* | | | | |
| H(24) | 172 (1) | 8 (3) | 61 (2) | 61 (8) |
| H(25) | 236 (1) | 69 (3) | 134 (2) | 65 (8) |
| H(26) | 307 (1) | 119 (3) | 233 (2) | 57 (11) |
| H(27) | 342 (1) | 210 (4) | 348 (2) | 105 (13) |
| H(28) | 292 (1) | 301 (3) | 420 (2) | 83 (10) |
| H(29) | 208 (1) | 292 (3) | 366 (2) | 56 (9) |
| H(31) | 13 (1) | 153 (3) | 44 (1) | 58 (8) |
| H(32) | 48 (1) | 31 (3) | 62 (1) | 56 (8) |
| H(33) | 15 (1) | 205 (3) | 166 (2) | 68 (9) |
| H(34) | −3 (1) | 60 (2) | 149 (1) | 43 (7) |
| H(35) | 34 (1) | −86 (2) | 218 (1) | 48 (7) |
| H(36) | 71 (1) | −235 (3) | 308 (1) | 57 (8) |
| H(37) | 136 (1) | −309 (3) | 395 (1) | 50 (7) |
| H(38) | 208 (1) | −189 (3) | 416 (1) | 55 (8) |
| H(39) | 209 (1) | 0 (3) | 352 (1) | 50 (8) |

The population parameters and their estimated standard deviations for the atoms in the $BF_4$ disorder models are:

| | | | |
|---|---|---|---|
| F(11) | 0.878 (6) | F(15) | 0.337 (32) |
| F(12) | 0.930 (7) | F(16) | 0.190 (20) |
| F(13) | 0.431 (26) | F(17) | 0.353 (15) |
| F(14) | 0.426 (38) | F(18) | 0.525 (27) |

TABLE 16

Atomic parameters for [Cu(py·tren)]$(BF_4)_2$, [(1-(2-pyridyl)-2-azabuten-4-yl)-bis(2-aminoethyl)]aminecopper(II) tetrafluoroborate

| | $x/a$ | $y/b$ | $z/c$ | $B_{11}$ | $B_{22}$ | $B_{33}$ | $B_{12}$ | $B_{13}$ | $B_{23}$ |
|---|---|---|---|---|---|---|---|---|---|
| Cu | 0.2339 (8) | 0.2455 (3) | 0.1193 (6) | 3.5 (4) | 2.0 (3) | 3.5 (3) | −0.1 (3) | 0.8 (2) | −0.2 (3) |
| C(11) | 0.3554 (12) | 0.0713 (7) | 0.0868 (10) | 5.9 (4) | 2.9 (3) | 9.5 (4) | 1.7 (4) | 2.5 (3) | −0.5 (3) |
| C(12) | 0.2965 (13) | 0.1100 (5) | 0.0014 (10) | 7.4 (4) | 3.7 (5) | 8.5 (4) | 0.7 (3) | 3.4 (4) | −2.4 (3) |
| C(13) | 0.3020 (8) | 0.2683 (6) | −0.0379 (7) | 3.6 (4) | 4.9 (3) | 4.6 (4) | −0.1 (3) | 1.4 (4) | −0.3 (3) |
| C(14) | 0.2858 (6) | 0.3625 (4) | −0.0083 (3) | 2.8 (3) | 4.7 (4) | 2.3 (3) | −0.7 (2) | −0.0 (3) | −0.7 (3) |
| C(15) | 0.2946 (9) | 0.4349 (6) | −0.0573 (9) | 5.8 (3) | 6.4 (3) | 5.8 (4) | −1.7 (3) | 0.6 (3) | 3.0 (4) |
| C(16) | 0.2704 (10) | 0.5190 (6) | −0.0270 (6) | 6.9 (4) | 6.2 (5) | 4.9 (5) | −1.1 (3) | −0.9 (4) | 1.8 (4) |
| C(17) | 0.2347 (10) | 0.5278 (4) | 0.0549 (5) | 6.6 (5) | 3.3 (5) | 5.6 (5) | −0.5 (4) | −0.8 (3) | −0.2 (4) |
| C(18) | 0.2225 (12) | 0.4470 (4) | 0.0980 (8) | 7.9 (3) | 2.6 (4) | 6.1 (3) | −0.1 (3) | 1.2 (2) | 0.0 (3) |
| C(21) | 0.3375 (11) | 0.1010 (9) | 0.2255 (8) | 7.2 (6) | 5.2 (5) | 7.5 (6) | 1.6 (5) | −1.0 (4) | 2.7 (5) |
| C(22) | 0.4650 (8) | 0.1739 (10) | 0.2398 (8) | 4.4 (6) | 9.4 (7) | 8.6 (7) | 0.6 (6) | −1.1 (6) | 2.0 (6) |
| C(31) | 0.0661 (9) | 0.0780 (4) | 0.1387 (11) | 4.3 (5) | 3.7 (5) | 10.4 (6) | −1.0 (5) | 2.7 (5) | −0.8 (5) |
| C(32) | −0.0463 (10) | 0.1474 (5) | 0.1793 (12) | 4.4 (5) | 4.0 (6) | 11.6 (7) | −0.7 (5) | 3.4 (6) | 0.9 (5) |
| N(5) | 0.2459 (11) | 0.1124 (5) | 0.1445 (12) | 5.1 (4) | 2.7 (4) | 10.1 (5) | 0.3 (4) | 3.1 (4) | 0.6 (3) |
| N(11) | 0.2881 (9) | 0.2081 (5) | 0.0134 (6) | 4.0 (4) | 4.1 (3) | 4.7 (4) | 0.3 (3) | 1.3 (3) | −1.6 (3) |
| N(12) | 0.2480 (9) | 0.3663 (5) | 0.0676 (8) | 4.2 (4) | 3.2 (4) | 4.3 (3) | −0.3 (4) | 1.5 (4) | 0.5 (4) |
| N(21) | 0.3759 (9) | 0.2644 (7) | 0.2283 (5) | 5.7 (5) | 5.9 (4) | 5.4 (4) | −0.1 (5) | −1.0 (4) | 0.4 (5) |
| N(31) | −0.0253 (9) | 0.2366 (6) | 0.1424 (9) | 3.9 (3) | 3.9 (4) | 7.1 (5) | 0.5 (4) | 2.0 (4) | −0.9 (4) |
| B(1) | 0.7622 (10) | 0.4133 (6) | 0.2508 (8) | 5.9 (4) | 5.2 (5) | 4.7 (5) | −0.5 (4) | 1.4 (5) | 0.3 (5) |
| F(11) | 0.7964 (14) | 0.4658 (8) | 0.3180 (7) | 10.6 (5) | 10.3 (6) | 9.9 (5) | 1.0 (5) | 0.8 (6) | −4.4 (6) |
| F(12) | 0.8949 (13) | 0.4227 (7) | 0.2057 (11) | 8.3 (6) | 9.7 (5) | 8.7 (6) | −1.3 (5) | 3.4 (5) | −0.2 (6) |
| F(13) | 0.6067 (11) | 0.4344 (11) | 0.2108 (9) | 7.4 (6) | 13.8 (7) | 9.1 (6) | −0.5 (6) | −1.0 (5) | 3.6 (6) |
| F(14) | 0.7605 (15) | 0.3254 (8) | 0.2770 (12) | 12.1 (7) | 7.2 (6) | 11.6 (6) | −1.2 (5) | 1.5 (6) | 3.0 (6) |
| B(2) | 0.2550 (14) | 0.2845 (9) | 0.4361 (10) | 10.5 (6) | | | | | |
| F(21) | 0.3425 (18) | 0.3537 (12) | 0.4002 (13) | 17.7 (9) | | | | | |
| F(22) | 0.1955 (17) | 0.3208 (11) | 0.4903 (12) | 15.9 (8) | | | | | |
| F(23) | 0.1507 (15) | 0.2474 (10) | 0.3726 (10) | 11.5 (7) | | | | | |
| F(24) | 0.4007 (15) | 0.2332 (10) | 0.4426 (10) | 11.7 (7) | | | | | |

TABLE 17

| | MnL-$(BF_4)_2$ | CoL-$(BF_4)_2$ | NiL-$(BF_4)_2$ | CuL-$(BF_4)_2$ | ZnL-$(BF_4)_2$ | FeL-$(BF_4)_2$ | NiL-$(PF_6)_2$ |
|---|---|---|---|---|---|---|---|
| $Q(12)$ | 129 | 127 | 127 | 127 | 128 | 119 | 119 |
| $Q(23)$ | 117 | 118 | 117 | 118 | 117 | 120 | 120 |
| $Q(31)$ | 114 | 115 | 116 | 115 | 115 | 122 | 121 |

standard deviations have been underestimated or there are significant systematic differences between the bond distances in different complexes.

Examination of the data shows that the bond distance N(7)–C($J$1) varies systematically from complex to complex, correlated with the bond angles M–N(7) – C($J$1). Therefore this bond distance should be omitted from the half normal probability analysis.

The half normal probability plot for all complexes and all bonds except N(7)–C($J$1) has a slope of 1.36, indicating either additional systematic differences in bond lengths or underestimation of the standard deviations.

Further examination of the data shows that the larger differences tend to appear for the three "different" complexes, $[CuL](BF_4)_2$ (which has very large differences among the metal–nitrogen bond distances), $[FeL](BF_4)_2$ and $[NiL](PF_6)_2$ (which have different crystal structures and considerably differing deviations from 3-fold symmetry compared with the isomorphous set). Therefore, half normal probability plots were prepared using only the complexes $[MnL](BF_4)_2$, $[CoL](BF_4)_2$, $[NiL](BF_4)_2$, and $[ZnL](BF_4)_2$. With all intraligand bonds included, the slope is 1.19. With the N(7)–C($J$1) bond excluded, the slope is 1.08.

Finally, a series of half normal probability plots were prepared comparing various pairs of complexes, omitting the N(7)–C($J$1) bonds in all cases. The slopes for sets composed of 30 bond distances are given in Table 18.

TABLE 18

Slopes of half normal probability plots

| | MnL-$(BF_4)_2$ | CoL-$(BF_4)_2$ | NiL-$(BF_4)_2$ | ZnL-$(BF_4)_2$ | CuL-$(BF_4)_2$ | FeL-$(BF_4)_2$ | NiL-$(PF_6)_2$ |
|---|---|---|---|---|---|---|---|
| $MnL(BF_4)_2$ | – | 1.07 | 1.00 | 0.92 | 1.65 | 1.66 | 1.52 |
| $CoL(BF_4)_2$ | | – | 0.93 | 1.27 | 1.37 | 1.60 | 1.56 |
| $NiL(BF_4)_2$ | | | – | 0.89 | 0.99 | 1.20 | 1.20 |
| $ZnL(BF_4)_2$ | | | | – | 1.28 | 1.54 | 1.38 |
| $CuL(BF_4)_2$ | | | | | – | 1.77 | 1.66 |
| $FeL(BF_4)_2$ | | | | | | – | 1.63 |
| $NiL(PF_6)_2$ | | | | | | | – |

In order to assess the significance of small deviations of the slopes from 1.0 as a function of sample size, we have generated 10 sets of 33 quantities, each set consisting of a random sample from a normal distribution. These 10 sets gave half normal probability plot slopes ranging from 0.82 to 1.14. Thus slopes in this range should not be considered significantly different from 1.0 for samples of this size. Combining these into three sets of 99 quantities each gave slopes of 0.91, 1.06, and 1.06. Finally the entire set of 330 quantities gave a slope of 1.01.

Consideration of all of these results suggests that the standard deviations of the $[MnL](BF_4)_2$, $[CoL](BF_4)_2$, $[NiL](BF_4)_2$, and $[ZnL](BF_4)_2$ structures have been correctly estimated, and we shall therefore assume that those for the other three structures are also valid. We further conclude that the distortion of the coordination polyhedron of $[CuL](BF_4)_2$ and the crystal packing effects have introduced small but significant changes in the bond distances within the ligand.

## ACKNOWLEDGMENTS

The authors wish to acknowledge financial support from the NSF (USA) and the CNR (Italy) for this research. R.M. Kirchner thanks Manhattan College for sabbatical leave, and the ISSECC-CNR (Florence, Italy) for hospitality during the first half of this leave, and the Lab. Kristallographie (Universität Bern, Switzerland) during the second half of this leave. Appreciation is expressed to H.-B. Bürgi (Berne) for helpful discussions, to G. Kolks (New York) for a critical reading of an earlier version of this manuscript, to L. Rose (Seattle) and M. Sabat (Florence) for assistance in preparing Figures, and to T. Ambruster, A. Gutierrez and R. Welch (all Berne) for proof-reading. L.J. Wilson thanks the Robert A. Welch Foundation under Grant C-627.

## REFERENCES

1 P.C. Jain, P. Paoletti, and E.C. Lingafelter, J. Am. Chem. Soc., 90 (1968) 519.
2 P.E. Figgins and D.H. Busch, J. Am. Chem. Soc., 82 (1960) 820.
3 P.J. Krumholz, J. Am. Chem. Soc., 75 (1953) 2163.
4 E.D. McKenzie, Coord. Chem. Rev., 6 (1971) 187–216.
5 Structures of various tris(bipy)metal complexes are described in the following citations, arranged according to metal ion. Fe(II): T. Tada, J. Sci. Hiroshima Univ., Part A, 46 (1982) 73; Fe(III): B.N. Figgis, B.W. Skelton and A.H. White, Aust. J. Chem., 31 (1978) 57; Co(I) and Co(II): D.J. Szalda, C. Creutz, D. Mahajan and N. Sutin, Inorg. Chem., 22 (1983) 2372–2379; Co(II): A. Wada, N. Sakabe and J. Tanaka, Acta Crystallogr., Sect. B, 32 (1976) 1121; Co(III): K. Yanagi, Y. Ohaashi, Y. Sasada, Y. Kaizu and H. Kobayashi, Bull. Chem. Soc. Jpn., 54 (1981) 118; Ni(II): A. Wada, C. Katayama and J.

Tanaka, Acta Crystallogr., Sect. B, 32 (1976) 3194; Cu(II): O.P. Anderson, J. Chem. Soc., Dalton Trans. (1972) 2597; Ru(II): D.P. Rillema, D.S. Jones, H.A. Levy, J. Chem. Soc., Chem. Commun. (1979) 849; and tetrakis(bipy)U(0): G. Del Piero, G. Perego, A. Zazzetta and G. Brandi, Cryst. Struct. Commun., 4 (1975) 521.

6 B.A. Frenz and J.A. Ibers, Inorg. Chem., 11 (1972) 1109–1116.

7 Structures of various tris(phen)metal complexes are described in the following citations, arranged according to metal ion. Fe(II): T. Fujiwara, E. Iwamoto and Y. Yamamoto, Inorg. Chem., 23 (1984) 115; A. Zalkin, D.H. Templeton, T. Ueki, Inorg. Chem., 12 (1973) 1641–1646; W.M. Reiff, E.H. Witten, K. Mottle, T.F. Brennan and A.R. Garafalo, Inorg. Chim. Acta, 77 (1983) L83; H.A. Goodwin, E.S. Kucharski and A.H. White, Aust. J. Chem., 36 (1983) 1115; J.A. Broomhead, J.R. Dilworth, J. Hutchinson, J. Zubieta, Cryst. Struct. Commun., 11 (1982) 1701; L. Johansson, M. Molund and A. Oskarsson, Inorg. Chim. Acta, 31 (1978) 117–123; Fe(III): J. Baker, L.M. Engelhardt, B.N. Figgis and A.H. White, J. Chem. Soc., Dalton Trans., (1975) 530–534; Co(III): E.C. Niederhoffer, A.E. Martell, P. Rudolf and A. Clearfield, Cryst. Struct. Commun., 11 (1982) 1951–1957; Ni(II): G.B. Deacon, C.L. Raston, D. Tunaley and A.H. White, Aust. J. Chem., 32 (1979) 2195; Ref. 6; Cu(II): O.P. Anderson, J. Chem. Soc. Dalton Trans., (1973) 1237–1241.

8 E.I. Steifel and G.F. Brown, Inorg. Chem., 11 (1972) 434.

9 D.L. Kepert, Inorg. Chem., 11 (1972) 1561.

10 E. Larson, G.N. LaMar, B.E. Wagner, J.E. Parks and R.H. Holm, Inorg. Chem., 11 (1972) 2652–2668.

11 A. Avdeef and A.J. Fackler, Jr., Inorg. Chem., 14 (1975) 2002–2006.

12 (a) E.B. Fleischer, A.E. Gebala and P.A. Tasker, J. Am. Chem. Soc., 92 (1970) 6365.

12 (b) E.B. Fleischer, A.E. Gebala, D.R. Swift and P.A. Tasker, Inorg. Chem., 11 (1972) 2775.

13 P.B. Donaldson, P.A. Tasker and N.W. Alcock, J. Chem. Soc. Dalton Trans., (1977) 1160–1165.

14 F. Lions and K.V. Martin, J. Am. Chem. Soc., 79 (1957) 1572.

15 (a) W.O. Gillum, J.C. Huffman, W.E. Strieb and R.A.D. Wentworth, J. Chem. Soc., Chem. Commun., (1969) 843–844.
(b) W.O. Gillum, R.A.D. Wentworth and R.F. Childers, Inorg. Chem., 9 (1970) 1825.

16 R.A.D. Wentworth, P.S. Dahl, C.J. Huffman, W.O. Gillum, W.E. Strieb and J.C. Huffman, Inorg. Chem., 21 (1982) 3060–3063.

17 P.G. Sim and E. Sinn, Inorg. Chem., 17 (1978) 1288–1290; P.G. Sim and E. Sinn, J. Am. Chem. Soc., 103 (1981) 241–243.

18 N.W. Alcock, D.F. Cook, E.D. McKenzie and J.M. Worthington, Inorg. Chim. Acta, 38 (1980) 107–112;

19 D.A. Rudman, J.C. Huffman, R.F. Childers, W.E. Streib and R.A.D. Wentworth, Inorg. Chem., 14 (1975) 747–750.

20 J.E. Parks, B.E. Wagner and R.H. Holm, J. Am. Chem. Soc., 92 (1970) 3500; Inorg. Chem., 10 (1971) 2472.

21 M.R. Churchill and A.H. Reis, Inorg. Chem., 11 (1972) 1811; Inorg. Chem., 11 (1972) 2299; J. Chem. Soc., Dalton Trans., (1973) 1570; Inorg. Chem., 12 (1973) 2280.

22 D.R. Boston and N.J. Rose, J. Am. Chem. Soc., 90 (1968) 6859–6860.

23 G.A. Zakrzewski, C.A. Ghilardi and E.C. Lingafelter, J. Am. Chem. Soc., 93 (1971) 4411.

24 V.L. Goedken and S-M. Peng, J. Chem. Soc., Chem. Commun., (1973) 62.

25 R.A.D. Wentworth, Coord. Chem. Rev., 9 (1972/73) 171–187.

26 I. Gladstone, N.J. Rose and E.C. Lingafelter, Inorg. Chem., 25 (1986) 1516–1518.

27 R. Hoffmann, J.M. Howell and A.R. Rossi, J. Am. Chem. Soc., 98 (1976) 2484–2492.
28 R. Hoffmann, B.F. Beier, E.L. Muetterties and A.R. Rossi, Inorg. Chem., 16 (1977) 511–521.
29 D.L. Kepert, Progr. Inorg. Chem., 23 (1977) 1–65.
30 D.L. Kepert, Progr. Inorg. Chem., 25 (1979) 41–144.
31 M.G.B. Drew, Progr. Inorg. Chem., 23 (1977) 67–210.
32 L.J. Wilson and N.J. Rose, J. Am. Chem. Soc., 90 (1968) 6041–6045.
33 C. Mealli and E.C. Lingafelter, J. Chem. Soc., Chem. Commun., (1970) 885.
34 E.C. Lingafelter, L.C. Andrews, R.M. Kirchner, N.J. Rose and L.J. Wilson, Coord. Chem. Rev., 8 (1972) 55.
35 M.A. Hoselton, L.J. Wilson and R.S. Drago, J. Am. Chem. Soc., 97 (1975) 1722–1729.
36 L.J. Wilson, D. Georges and M.A. Hoselton, Inorg. Chem., 14 (1975) 2968–2975.
37 M.A. Hoselton, R.S. Drago, L.J. Wilson and N. Sutin, J. Am. Chem. Soc., 98 (1976) 6967–6969.
38 E.V. Dose, M.A. Hoselton, N. Sutin, M.F. Tweedle and L.J. Wilson, J. Am. Chem. Soc., 100 (1978) 1141–1147.
39 K.M. Kadish, C.-H. Su, D. Schaeper, C.L. Merrill and L.J. Wilson, Inorg. Chem., 21 (1982) 3433–3437.
40 Private communication by G. Delker and G.D. Stucky.
41 J.E. Huheey, Inorganic Chemistry, 3rd edn., Harper and Row, New York, 1983, pp. 389, 507–508.
42 J.K. Burdett, Molecular Shapes, John Wiley, New York, 1980, pp. 166–167.
43 We have selected what seems to be the most useful descriptive parameters and have assigned their symbols to be consistent with polar coordinates ($r$, $\theta$, and $\phi$) and previous literature notations, as in refs. 8, 15b and 25.
44 Different magnitudes of the value of $\phi$ can be obtained from using different definitions of this twist angle—see K.R. Dymock and G.J. Palenik, Inorg. Chem., 14 (1975) 1220 and M.A. Flandera and E.C. Lingafelter, Inorg. Chem., 15 (1976) 750. We use the twist angle $\phi_{11}'$ as defined by Flandera and Lingafelter.
45 J.C. Slater, Quantum Theory of Matter, 2nd edn., McGraw-Hill, New York, 1968.
46 H.C. Stynes, J.A. Ibers, Inorg. Chem., 10 (1971) 2304, and references therein.
47 The method used is that described in R. Hoffmann, J. Chem. Phys., 39 (1963) 1397–1412; R. Hoffmann and W.N. Lipscomb, ibid., 36 (1962) 2179, 3489; ibid., 37 (1962) 2872.
48 The parameters for Fe(II) are the same as those in R.H. Summerville and R. Hoffmann, J. Am. Chem. Soc., 101 (1979) 3821. The six M–N distances were fixed at 1.95 Å, while C–N and C–C distances have values of 1.30 Å and 1.46 Å, respectively. The N–C–C angle is 115°.
49 The $2e$ level centered on the ligands takes, in an antibonding fashion, a small amount of the character of the lower $1e$ metal orbitals, thus suggesting that some metal-to-ligand $\pi$ bonding is operative when $2e$ is empty. By contrast, $a_2$ does not find any symmetry partner among the metal levels and remains unperturbed. The presence of ligand orbitals at intermediate energies is experimentally confirmed by the electronic spectra of the $[Fe(py_3tren)]^{2+}$ complex, as well as other known low spin tris($\alpha$-diimine)iron(II) complexes, which have intense metal-to-ligand charge transfer bands whose intensities and positions obscure any $d-d$ transitions [36]. The level order shown as **6** persists in calculations on other quasi-experimental TAP tris($\alpha$-diimine)metal(II) models, where metal(II) = cobalt(II) and nickel(II) (the cobalt and nickel atomic parameters were taken from K.I. Goldberg, D.M. Hoffman and R. Hoffmann, Inorg. Chem., 21 (1982) 3863, and the experimentally determined weighted mean values for the Co–N and Ni–N

distances in $[M(py_3tren)]^{2+}$ were used in the respective calculations). However, the energy gap between the $a_2$, $2e$ and $3e$ levels decreases from ca. 3 eV to ca. 1 eV in going from iron to nickel. Also, it should be recalled that the ligand model, shown as **4**, underevaluates the energy of the ligand $\pi$ set by ca. 0.5 eV. Finally, the energy of the $3e$ level ($e_g$ in $O_h$ symmetry) is strongly dependent on the M–N distances used in the calculations since this level has strong $\sigma^*$ character.

50 For electron configurations other than low-spin $d^6$, some electrons normally assigned to the higher-level $3e$ set of the metal might be transferred to ligand orbitals. Populating $\pi$-orbitals of the ligand (such as those shown as **4**) would induce geometrical rearrangements in the ligand, such as a shortening of the C(3)–C(4) distance. As described in Section B(iv)(b), there is some evidence for this shortening in the $[M(py_3tren)]^{2+}$ compounds. On the other hand, the elongation of the M–N bonds for electron counts greater than $d^6$ suggests that the extra electrons effectively populate M–N $\sigma^*$ levels.

51 We have already pointed out [49] the difficulties encountered in a semiempirical MO investigation to establish the relative energy gap between the ligands and the metal higher $d$ level. For the same reasons we conclude that is quite hard to predict, case by case, the precise geometry at which the metal upper levels are stabilized below the ligand levels. It is an oversimplification to use the parameter $\alpha$ to regulate the pathway since the $\alpha$-diimine chelate is not symmetric. The effect of asymmetry between M–N(1) and M–N(2) bonds was not taken into account. Finally, as the size of the metal ion decreases, its orbitals become more contracted, which lowers the energy of the $\sigma^*$ M–L levels. In the latter case the crossing with the $\pi$ levels of the ligands will occur closer to TAP geometry. Perhaps significant in this respect, the nickel atom which has the smallest $M-N_6$ size after iron in this series, also has the most octahedral coordination polyhedron after iron. We are confident that the final effect is still that of maintaining all metal orbital levels below those of the ligand.

52 Although the crystal field stabilization energy (CFSE) is predicted to be zero for both the $d^5$ Mn(II) and $d^{10}$ Zn(II) $py_3tren$ complexes, the molecular orbital stabilization energy (MOSE) is zero only for $d^{10}$ configurations in octahedral complexes, when only $\sigma$ bonding effects are considered (see chapter 10 of ref. 42 for further details). Perhaps significant in this respect, it is $[Mn(py_3tren)]^{2+}$, followed closely by $[Zn(py_3tren)]^{2+}$, that is most distorted from octahedral coordination geometry (in terms of weighted mean values).

53 Values for the van der Waals radii (N = 1.55; Ni = 1.6; Cu = 1.4; Zn = 1.4 Å) are taken from Table 6.1 of ref. 41.

54 The expression $(M-N_6) = 3.5493 - (0.0608)Z + (0.1152)N$, where $Z$ is the atomic number and $N$ is the number of upper $3e$ electrons fits the data with a maximum error of 0.016 Å and a mean error of 0.011 Å.

55 See T.A. Albright, Tetrahedron, 38 (1982) 1339–1388 for the details of the ligand–metal interaction in $O_h$.

56 J. Baker, L.M. Engelhardt, B.N. Figgis and A.H. White, J. Chem. Soc., Dalton Trans., (1975) 530.

57 L. Banci, A. Bencini, C. Benelli, D. Gatteschi and C. Zanchini, Struct. Bonding, 52 (1982) 37.

58 S. Kremer, W. Henke and D. Reinen, Inorg. Chem., 21 (1982) 3013–3022.

59 W. Henke and S. Kremer, Inorg. Chim. Acta, 65 (1982) L115–L117.

60 M. Bacci, C.A. Ghilardi and A. Orlandini, Inorg. Chem., 23 (1984) 2798–2802.

61 J.G. Leipoldt and P. Coppens, Inorg. Chem., 12 (1973) 2269–2274.

62 K. Chandrasekhar and H.-B. Bürgi, Acta Crystallogr., Sect. B, 40 (1984) 387–397.

63 N.N. Greenwood and A. Earnshaw, Chemistry of the Elements, Pergamon Press, Oxford, 1984, p. 1315.
64 M. Di Vaira, J. Chem. Soc., Dalton Trans., (1975) 1575.
65 C.A. Ghilardi, C. Mealli, S. Midollini and A. Orlandini, Inorg. Chem., 24 (1985) 164–168.
66 (a) J.H. Ammeter, H.-B. Bürgi, E. Gamp, V. Mayer-Sandrin and W.P. Jensen, Inorg. Chem., 18 (1979) 733–750, and references therein.
(b) Jahn–Teller radius calculated using eqn. 9 in ref. 66a.
67 G.F. Kokoszka, C.W. Reimann, A.C. Allen, Jr. and G. Gordon, Inorg. Chem., 6 (1967) 1657–1661; B.J. Hathaway, P.G. Hodgson and P.C. Power, Inorg. Chem., 13 (1974) 2009.
68 O.P. Anderson, J. Chem. Soc., Dalton Trans., (1973) 1237–1241; O.P. Anderson, J. Chem. Soc., Dalton Trans., (1972) 2597.
69 P.C. Jain and E.C. Lingafelter, J. Am. Chem. Soc., 89 (1967) 6131.
70 G.D. Andreetti, P.C. Jain and E.C. Lingafelter, J. Am. Chem. Soc., 91 (1969) 4112.
71 P.D. Cradwick and D. Hall, Acta Crystallogr. Sect. B, 26 (1970) 1384.
72 M. DiVaira and P.L. Orioli, Inorg. Chem., 6 (1967) 955.
73 M. DiVaira and P.L. Orioli, Acta Crystallogr. Sect. B, 24 (1968) 595.
74 M. DiVaira and P.L. Orioli, Acta Crystallogr. Sect. B, 24 (1968) 1269.
75 A summary of weighted mean values for the various types of carbon–hydrogen bond angles (degrees) and distances (Å) within the $[M(py_3tren)]^{2+}$ compounds is shown below in Table 19.

| Type | No. of values | Weighted mean | Overall range, $R$ | Sample e.s.d. | E.s.d. of mean | Pooled e.s.d. of mean |
|---|---|---|---|---|---|---|
| C($sp^3$)–H | 72 | 0.994 | 12.3 | 0.056 | 0.007 | 0.004 |
| C($sp^2$)–H | 36 | 0.948 | 9.6 | 0.053 | 0.006 | 0.003 |
| H–C($sp^3$)–H | 36 | 108.0 | 6.1 | 3.8 | 0.6 | 0.4 |
| H–C($sp^3$)–A [a] | 144 | 109.6 | 9.2 | 2.6 | 0.2 | 0.1 |
| H–C($sp^2$)–B [b] | 180 | 119.9 | 11.0 | 3.8 | 0.3 | 0.1 |

[a] $A$ is either C($sp^3$), N(7) or N(1). [b] $B$ is either C($sp^2$) or N(2).

76 Other complexes with a tren or substituted tren (R·tren) ligand are $[Cu(tren)NCS]^+$ [69], $[Zn(tren)NCS]^+$ [70], $[Ni(tren)(NCS)_2]$ [71], $[M(Me_6tren)Br]Br$ (where M(II) = Mn, Fe, Co, Ni, Cu and Zn) [72–74], and dibromo-1-(2-pyridyl-2,5-diaza-5-methyl-hexa-1-enezinc(II) [77]. These have similar values for bond distances, bond angles and torsional angles except when the values involve metal–nitrogen bonds. The latter values differ because in the $py_3tren$ ligand the N(1) atoms are part of a geometrically rigid bidentate $\alpha$-diimine moiety where pyridine donor atoms also influence the metal–nitrogen bonding, while the M–N(7) distances show a considerable variation in geometry, as already described. The structures of all the above M(R·tren) complexes show that the conformation of the tertiary amine is tetrahedral with the lone pair of the amine nitrogen atom directed toward the central metal ion.
77 G. Zakrzewski and E.C. Lingafelter, Inorg. Chim. Acta, 4 (1970) 251.
78 F.A. Cotton and G. Wilkinson, Advanced Inorganic Chemistry, 4th edn., John Wiley, New York, 1980, pp. 119–120.
79 R. Cini, A. Cinquantini, P.L. Orioli, C. Mealli and M. Sabat, Can. J. Chem., 62 (1984) 2908–2913.
80 M.J. Maroney and N.J. Rose, Inorg. Chem., 23 (1984) 2252–2261.

81 M.J. Maroney, J.G. Norman, Jr. and J.H. Osborne, Inorg. Chem., 23 (1984) 2261–2270.
82 E. Bayer and G. Hafelinger, Chem. Ber., 99 (1966) 1689.
83 L. Pauling, The nature of the Chemical Bond, 3rd edn., Cornell University Press, Ithaca, NY, 1960, p. 236.
84 A. Almenningen and O. Bastiansen, Kgl. Norske Vid. Selsk. Skr. No. 4, 1958.
85 A. Almenningen, O. Bastiansen and P.N. Skancke, Acta Chem. Scand., 12 (1958) 1215.
86 W.H. Batschelet and N.J. Rose, Inorg. Chem., 22 (1983) 2083.
87 (a) In 32 cases of a pyridine ring coordinated to a metal ion through its nitrogen atom where there is also an $sp^2$ hybridized atom attached to the ring at position 2, the weighted mean values for the bond distances (in Å) are: N(2)–C(4) = 1.349(1) $R$8.3; N(2)–C(8) = 1.342(1) $R$10.5; C(4)–C(5) = 1.383(1) $R$6.2; C(5)–C(6) = 1.382(1) $R$4.7; C(6)–C(7) = 1.384(1) $R$7.1; C(7)–C(8) = 1.377(1) $R$5.5; where the number in parentheses is the pooled e.s.d., $\sigma = \sum_i 1/(1/\sigma_i^2)$, and $R$ is the normalized range.

(b) When weighted mean bond distance and angle values are compared as a function of metal ion, there are no significant differences observed between comparable values except that N(2)–C(4) is short in $[FeL](BF_4)_2$ due to the unique $\alpha$-diimine interaction found in general for low spin Fe(II) complexes, as described in Section B(iv)(b). But when values are compared as a function of ligand arm there are significant differences between comparable values that form distinct patterns. The arm-by-arm patterns for $[FeL](BF_4)_2$ and $[NiL](PF_6)_2$ are different from each other, and both are different from the pattern found within the isomorphous $[ML]^{2+}$ series. This is not surprising since $[FeL](BF_4)_2$ and $[NiL](PF_6)_2$ have either the space group or the anion, or both of these, different from those of the isomorphous series. Within the isomorphous series ($[ML](BF_4)_2$ where M(II) = Mn, Co, Ni, Cu, and Zn) the values found in different arms are significantly different for bond distances N(2)–C(8) and C(4)–C(5), and for all bond angles not involving hydrogen atoms. For example, arm-by-arm weighted mean values for N(2)–C(8) within the isomorphous $[M(py_3tren)]^{2+}$ series are arm 1: 1.326(2) $R$1.3; arm 2: 1.328(2) $R$3.8; and arm 3: 1.335(2) $R$5.4 (giving a maximum variation between arms of 3.7$\sigma$), whereas for C(4)–C(5) they are arm 1: 1.394(3) $R$2.6; arm 2: 1.384(2) $R$2.7; and arm 3: 1.375(2) $R$3.4 (a maximum variation of 6.5$\sigma$). There is no significant arm-by-arm variation for C(5)–C(6), C(6)–C(7) or C(7)–C(8).
88 In $[CoL]^{2+}$ the distance (in Å) of selected atoms from the pyridine ring least squares plane is given as follows: Co, −0.150( $R$110); N(7), 1.320( $R$95); N(1), −0.166( $R$27); and C(3), −0.061(3).
89 L. Pauling, The Nature of the Chemical Bond, 3rd edn., Cornell University Press, Ithaca, NY, 1960, p. 260.
90 N.L. Howe, M.S. Thesis, University of Washington, Seattle, 1972.
91 L.C. Andrews, Ph.D. Dissertation, University of Washington, Seattle, 1973.
92 R.M. Kirchner, Ph.D. Dissertation, University of Washington, Seattle, 1971.
93 L.P. Torre, Ph.D. Dissertation, University of Washington, Seattle, 1971.
94 B.N. Figgis, R.S. Nyholm, J. Chem. Soc. A, (1958) 4190.
95 B.N. Figgis and J. Lewis, Magnetochemistry, in H.B. Jonassen and A. Weissberger (eds.), Technique of Inorganic Chemistry, Vol. IV, Interscience Publishers, New York, 1965, pp. 142–143.
96 L.E. Alexander and G.S. Smith, Acta Crystallogr., 17 (1964) 1195.
97 H. Tompa, The Absorption Correction in Crystal Structure Analysis, IBM 1620 General Program Library, 8.4.014, 1966.
98 J.M. Stewart, Crystal Structure Calculation System X-Ray-63 for the IBM 709, 7090, 7094. Technical Report TR-64-6, Computer Science Center, University of Maryland, 1964.

99 J.M. Stewart, The X-Ray System of Crystallographic Programs for any Computer having a Pidgen FORTRAN Compiler, Version of July 70, Computer Science Center, University of Maryland, 1970.
100 P.A. Doyle and P.S. Turner, Acta Crystallogr. Sect. A, 24 (1968) 390.
101 D. Cromer and J. Waber, Acta Crystallogr., 18 (1965) 104.
102 R.F. Stewart, E.R. Davidson and W.T. Simpson, J. Chem. Phys., 42 (1965) 3175.
103 D.H. Templeton, International Tables for X-ray Crystallography, Vol. III, Table 3.3.2, Kynoch Press, Birmingham (U.K.), 1962.
104 D.T. Cromer, Acta Crystallogr., 18 (1965) 17.
105 Observed and calculated structure factors may be requested from E.C. Lingafelter.
106 S.C. Abrahams and E.T. Keve, Acta Crystallogr. Sect. A., 27 (1971) 157.